

PERFORMANCE ANALYSIS OF MESH NETWORKS IN INDOOR
AND OUTDOOR WIRELESS TESTBEDS

DAVID LLOYD JOHNSON

PERFORMANCE ANALYSIS OF MESH NETWORKS IN INDOOR
AND OUTDOOR WIRELESS TESTBEDS

By

David Lloyd Johnson

Submitted in partial fulfilment of the requirements for the degree

Master of Engineering (Computer Engineering)

in the

Faculty of Engineering, the Built Environment and Information Technology

at the

UNIVERSITY OF PRETORIA

Advisor: Professor G. Hancke

October 2007

PERFORMANCE ANALYSIS OF MESH NETWORKS IN INDOOR AND OUTDOOR WIRELESS TESTBEDS

By: David Lloyd Johnson

Supervisor: Professor Gerhard Hancke

Department: Electrical, Electronic and Computer Engineering

Degree: MEng (Computer Engineering)

Summary

Physical indoor wireless network testbeds as well as outdoor wireless testbeds have the potential to accelerate the pace of research in the field of wireless ad hoc and mesh networking. They form part of a critical chain of steps needed to develop and test ad hoc networking protocols from concept to eventual uptake by industry. Current research in this area makes use of simulations or mathematical models which oversimplify the physical and Medium Access Control layer.

In Africa specifically, wireless mesh networking has the potential to make a substantial impact on the lack of telecommunications infrastructure across the continent. A combination of good theoretical analysis, indoor test facilities and rural testbeds forms a perfect suite to carry out meaningful research in the field.

A 7x7 wireless grid of closely spaced computers was constructed, making use of highly attenuated 802.11 radios running in ad hoc mode. Modelling and analysis revealed that a suitably attenuated environment was created with variation in signal strength between node pairs following a Gaussian distribution. This emulates a real outdoor network with normal signal propagation issues such as multi-path fading and lack of Fresnel zone clearance.

This testbed was then used to evaluate 3 popular MANET ad hoc routing protocols, namely AODV, DYMO and OLSR. OLSR was tested with the standard hysteresis routing metric as well as the ETX routing metric. OLSR showed the best performance in terms of average throughput and packet loss for a medium size (21 node) and large (49 node) mesh network, with the hysteresis routing metric performing best in large networks and ETX performing best in medium sized networks. DYMO also performed very well, considering its low routing overhead, exhibiting the least amount of delay in a large mesh network (49 nodes). The AODV protocol showed the weakest performance in the grid with close to 60% of possible link pairs achieving no route in a 49-node grid. However, it did present the least amount of routing overhead compared with other routing protocols.

Finally, a medium-sized rural mesh network testbed consisting of 9 nodes was built in a mountainous area of about 15 square kilometers around an AIDS clinic using the OLSR routing protocol with

ETX as the routing metric. The network provided a good service to the satellite-based Internet with throughput rates ranging between 300 kbps for 4 hops and 11000 kbps for 1 hop and an average throughput rate of 2324 kbps. To encourage fair sharing of Internet connectivity, features were installed to limit each user to 40 MB/month of free Internet traffic. A local web server offers cached pages of Wikipedia and Linux repositories to reduce the need for Internet access. VoIP services were also installed between clinic infrastructure to reduce the the need for making expensive GSM calls. It was shown that a mesh network of this size provides a very satisfactory level of broadband service for users accessing a satellite-based Internet facility as well as local VoIP services.

Keywords: ad hoc networking, mesh networking, MANET, wireless testbed, AODV, DYMO, OLSR, rural wireless network.

WERKVERRIGTING ANALISERE VAN GEVLEGDE NETWERKE IN BINNEMUURSE EN BUITEMUURSE DRAADLOSE TOETSPLATFORMS

Deur: David Lloyd Johnson

Opsigter: Professor Gerhard Hancke

Departement: Electrical, Electronic and Computer Engineering

Graad: MEng (Rekenaar Ingenieurswese)

Opsomming

Fisiese binnemuurse draadlose gevlegdenetwerk toetsplatforms asook buitemuurse draadlose toetsplatforms het die potensiaal om die pas van navorsing in die veld van draadlose ad hoc en gevlegde netwerke te versnel. Hulle vorm deel van 'n kritiese ketting van stappe nodig om ad hoc netwerk protokolle te ontwikkel en toets vanaf konsep tot uiteindelijke opname deur nywerheid. Huidige navorsing in hierdie area maak gebruik van simulaties of wiskundige modelle wat die fisiese en medium-toegangsbeheer vlak oorvereenvoudig.

In Afrika het draadlose gevlegde netwerke die potensiaal om 'n wesenlike impak te maak op die tekort aan telekommunikasie infrastruktuur regoor die kontinent. 'n Kombinasie van goeie teoretiese analise, binnemuurse toetsfasiliteite en plattelandse toetsplatforms vorm 'n perfekte samestelling om betekenisvolle navorsing in die veld uit te voer.

'n 7×7 draadlose matriks van naby gespaseerde rekenaars was saamgestel uit 802.11 radios in ad hoc modus waarvan die sein onderdruk was. Met modellering en analise is bepaal dat 'n paslik verswakte omgewing geskep was met verandering in seinsterkte tussen nodepare wat 'n Gaussiese distribusie volg. Hierdie streef na 'n ware buitemuurse netwerk met normale sein voortplanting faktore soos multi-pad verswakking en tekorte aan Fresnelone vrystelling.

Hierdie toetsplatform was gebruik om 3 gewilde MANET ad hoc roete protokolle te evalueer, naamlik AODV, DYMO en OLSR. OLSR was getoets met die standaard histerese roete meting asook die ETX roete meting. OLSR toon die beste werkverrigting met betrekking tot gemiddelde deurvoer en pakkie verlies vir 'n gemiddelde (21 knoop) en groot (49 knoop) gevlegde netwerk, met die histerese roete meting die beste in groot netwerke en ETX die beste in gemiddelde grootte netwerke. DYMO het ook goed gevaar, gegee sy lae roete oorhoofse-belading en die minste totale vertraging in 'n groot gevlegde netwerk (49 knope). Die AODV protokol vertoon die swakste werkverrigting in die matriks met byna 60% van moontlike skakelpare wat geen roete vorm in 'n 49-knoop rooster. In alle gevalle verteenwoordig AODV egter die minste totale roete oorhoofse-belading.

Verder was 'n medium-grootte plattelandse gevlegde netwerk toetsplatform bestaande uit 9 knope in 'n

bergagtige area van omtrent 15 vierkante kilometer rondom 'n VIGS-kliniek gebou. Dit het die OLSR roete protokol, met ETX as die roete meting, gebruik. Die netwerk voorsien 'n goeie diens vanaf die satelliet-gebaseerde Internet met deurvoer tempo's tussen 300 kbps vir 4 hoppe en 11000 kbps vir 1 hop en 'n gemiddeld deurvoer van 2324 kbps. Om redelike verdeling van die Internet konneksie aan te moedig was sagteware geïnstalleer om elke gebruiker te beperk tot 40 mb/maand vrye internet verkeer. 'n Plaaslike webwerf verskaffer bied gestoorde bladsye van Wikipedia en Linux store aan om die noodigheid van interaktiewe internet toegang te verminder. Spraak-oor-Internet-Protokol (SoIP) dienste was ook geïnstalleer tussen die kliniek infrastruktuur om die noodigheid van duur GSM weg te vat. Dit was gewys dat 'n gevlegde netwerk van hierdie grootte 'n baie bevredigende vlak van breedband diens verskaf vir gebruikers van satelliet-gebaseerde Internet fasiliteite asook plaaslike SoIP dienste.

Sleutelwoorde: ad hoc netwerk, gevlegde netwerk, MANET, draadlose toetsplatform, AODV, DYMO, OLSR, plattelandse draadlose netwerk.

ACKNOWLEDGEMENTS

This research was performed in the Wireless Africa Research Group of the Meraka Institute with inputs from Gerhard Hancke, my advisor from the University of Pretoria. The Wireless Africa Research group was created around the time I started working on this thesis and I am grateful to all the members of the team who assisted me with building the research group to where it is today.

I would particularly like to thank:

- My wife, Nula and my two boys, Samuel and Luke, without you and your understanding during this thesis, this whole endeavour would have been impossible
- Kobus Roux, my manager at the CSIR, who has supported my work and created the space and time for this research to be possible. Without this, it would have been impossible to balance work responsibilities and the time needed to complete this thesis.
- John Hay whose knowledge of operating systems and networking was invaluable in building the indoor wireless grid.
- Albert Lysko for his many useful inputs on the electromagnetic behaviour of the lab.
- The ACTS clinic staff who were so supportive while constructing the mesh network in the rural area of Peebles Valley and allowed us to share some of their VSAT bandwidth with other users in the mesh network.
- The International Development Research Centre (IDRC) for providing the funding for the Peebles Valley mesh project as part of the First Mile First Inch project which was successfully concluded in 2007.

LIST OF COMMONLY USED ABBREVIATIONS

AODV	Ad hoc On-demand Distance Vector routing
DYMO	Dynamic MANET On-demand routing
ETX	Expected Transmission Count
IETF	Internet Engineering Task Force
MANET	Mobile Ad hoc Network
NIC	Network Interface Card
ns2	Network Simulator 2
OLSR	Optimized Link State Routing Protocol
OLSR-ETX	Optimized Link State Routing Protocol using the ETX routing metric
OLSR-RFC	Optimized Link State Routing Protocol using standard hysteresis routing metric
RIP	Routing Information Protocol
VoIP	Voice over Internet Protocol
WMN	Wireless Mesh Network
WNIC	Wireless Network Interface Card

TABLE OF CONTENTS

CHAPTER ONE - INTRODUCTION	1
1.1 Scope	1
1.2 Motivation	2
1.3 Objectives	3
1.4 Contribution	3
1.5 Research methodology	4
1.6 Overview of thesis	4
CHAPTER TWO - BACKGROUND	6
2.1 Introduction	6
2.2 Ad hoc networking	6
2.3 Development of Ad hoc networking	7
2.3.1 Research prior to 1990	7
2.3.2 Research in the 90's	8
2.3.3 Latest developments	9
2.4 Ad hoc routing protocols	10
2.4.1 AODV	10
2.4.2 DSR	12
2.4.3 OLSR	13
2.4.3.1 Hysteresis routing metric	13
2.4.3.2 ETX routing metric	15
2.4.4 DYMO	16
2.5 Linux implementations of ad hoc routing protocols	18
2.5.1 OLSR	18
2.5.2 AODV	18
2.5.3 DYMO	18
2.6 Testbeds	19
2.6.1 Network emulators	19
2.6.2 Live network testbeds	20
2.7 Previous work on comparison of routing protocols	21

2.8	Limitations of simulation and mathematical modelling	23
2.8.1	Mathematical modelling	23
2.8.2	Network simulations	23
 CHAPTER THREE - CONSTRUCTION OF THE MESH TESTBED		25
3.1	Introduction	25
3.2	Physical construction of the 7x7 grid	25
3.3	Challenges to establishing a functional testbed	26
3.4	Measurement process	29
 CHAPTER FOUR - MODELLING THE MESH TESTBED		32
4.1	Introduction	32
4.2	Electromagnetic modelling	32
4.2.1	Electromagnetic properties	33
4.2.1.1	Link budget related properties	33
4.2.1.2	Coupling between antennas	35
4.2.1.3	Near and far field	36
4.2.1.4	Fresnel zone clearance	37
4.2.2	Signal strength measurements	38
4.2.2.1	Measurement Process	38
4.2.2.2	Measurement results	38
4.3	Creating a multi-hop base line	40
4.4	Route complexity	42
 CHAPTER FIVE - PERFORMANCE ANALYSIS		47
5.1	Introduction	47
5.2	Hop count distribution	47
5.3	Routing traffic overhead	50
5.4	Throughput, packet loss, route flapping and delay measurements	54
5.4.1	Results for a string of pearls 7 nodes long	55
5.4.2	Results for 3x7 grid (21 nodes)	55
5.4.3	Results for full 7x7 grid (49 nodes)	57
5.5	Comparison of throughput results against baseline	60
5.6	A challenge to the ETX metric	60
 CHAPTER SIX - CASE STUDY OF A RURAL MESH NETWORK PILOT		64
6.1	Introduction	64

6.2	Peebles valley mesh design	65
6.2.1	Hardware	65
6.2.2	Software	66
6.2.3	Gateway	67
6.2.4	Services	67
6.2.5	Configuration	69
6.2.5.1	Addressing	69
6.2.5.2	802.11 and OLSR Settings	69
6.3	Evaluation	69
6.3.1	Throughput and delay performance	70
6.3.2	Internet usage patterns	72
6.3.3	Behavioural patterns of users	75
6.3.4	Environmental observations	75
6.4	Conclusion	76
6.5	Future considerations	77
CHAPTER SEVEN - CONCLUSIONS		78
7.1	Summary of contribution	78
7.2	Future work	80
7.2.1	Improvements to the indoor testbed lab conditions	80
7.2.2	Refinement of experimental parameters	81
7.2.3	Refinement of ad hoc routing protocols	82
7.3	Conclusion	82
REFERENCES		83
APPENDIX A - PATH SEARCH CODE TO FIND ROUTES THROUGH GRID		87
APPENDIX B - LOG-NORMAL SHADOWING MODEL		89
APPENDIX C - LARGE FORMAT DIAGRAMS FOR PERFORMANCE ANALYSIS IN 3X7 GRID		90
APPENDIX D - LARGE FORMAT DIAGRAMS FOR PERFORMANCE ANALYSIS IN 7X7 GRID		95

CHAPTER ONE

INTRODUCTION

An invasion of armies can be resisted, but not an idea whose time has come

Victor Hugo, *Histoire d'un crime*, 1852

1.1 SCOPE

In developing regions of the world, low penetration of basic ICT infrastructure such as telephony and Internet, as well as insufficient distribution of electricity, is isolating Africa from the global information society. Although cellular networks are showing fairly impressive growth in Africa, the penetration of broadband access requires new paradigms and thinking to create significant breakthroughs due to challenges such as electricity distribution, affordability and literacy.

Basic access to communication and information services remains an obstacle in the economic development of rural (low-density) communities throughout Africa. This access depends on an established telecommunications network backbone and connectivity technology which connects the customer premises to the backbone, which will be referred to as “First Mile” technology.

For telecommunications providers the risks involved in “First Mile” connectivity are often too high in developing regions due to the issues such as affordability, theft and lack of easy access. Exploring alternative connectivity solutions for higher risk rural areas and aggregating this connectivity to a backbone network presents a far lower risk solution to network operators.

“First mile” connectivity solutions include a wide array of technologies, including wired Ethernet, power line communication, optical fibre, Wi-Fi, Community GSM and network topologies such as mesh networks. The typical applications that run over these “First mile” networks are basic Internet access and email, but also include VoIP telephony and audio and video streaming.

Unfortunately in most developing countries there is a monopoly over fixed line networks which hinders innovative rural access provision for poor communities. Innovation in these areas requires a different mindset, an approach that focuses on communities, empowers communities and instills a sense of ownership and control of communications infrastructure in communities. There are numerous examples of this around the world, for example ICT Liberationist, Onno Purbo, has created a networked community [1] that is now expanding and creating new demand for ICTs on shoestring budgets but with strong support and motivation at the community level .

Many of the “first mile” technologies are cutting edge and not yet supported by telecommunication providers who are committed to older technologies servicing mass markets, yet another reason why their existing business models have not worked for the rural poor. Mesh networking is one such “first mile” technology which makes use of simple low-cost wireless routers that are installed on houses to build a community based wireless network without the need for any fixed existing infrastructure. This work focuses on the performance analysis of mesh networking on testbed networks as a solution to the issue of connecting rural communities to each other and the rest of the world.

Carrying out research on mesh networking solutions for rural communities cannot simply be done via mathematical modelling or simulations due to their inability to accurately model the physical world. As a consequence indoor and outdoor testbed networks become vital tools in the hands of a researcher exposing the shortcomings of theoretical work done on simulations.

Indoor testbed networks provide a controlled environment for the researcher to carry out experiments before deploying mesh networks in an outdoor environment and assist in understanding performance measures such as scalability, delay and throughput. An outdoor testbed, providing broadband connectivity to users, is the most realistic test environment which will be affected by environmental effects on signal propagation and realistic application traffic load on the network. These networks also help expose important social issues such as finding key community leaders and institutions that will be good stewards of the wireless mesh routers, once they are installed. They also help expose a researcher to the practical challenges, which are often more critical to the success of community based networks than some of the technical challenges that are present.

This research will mainly focus on the creation and modelling on an indoor 7 by 7 mesh testbed followed by the performance analysis, on this testbed, of mainstream ad hoc networking protocols that are defined by the IETF MANET working group. This is followed by a section which describes a case study of an outdoor mesh network in a rural community making use of the best performing ad hoc routing protocol in the indoor testbed.

1.2 MOTIVATION

Mesh networking is a relatively new technology originating out of ad hoc networking research from the early 90's. As a consequence, it is still replete with many research challenges such as limited scalability, difficulty in choosing an appropriate routing protocol and lack of suitability to real time media traffic.

Traditionally ad hoc and mesh networking research has mostly been carried out using simulation tools but many recent studies have revealed the inherent limitations these have in modelling the physical layer and aspects of the MAC layer. Researchers should acknowledge that the results from a simulation tool only give a rough estimate of performance. There is also a lack of consistency between the results of the same protocol being run on different simulation packages which makes it difficult to know which simulation package to believe.

There is also very little mathematical modelling work available for ad hoc networks but what is available can only be used as a basic “rule of thumb” when it comes to understanding ad hoc networking performance.

The core of this thesis is dedicated to building suitable testbeds to carry out mesh networking experiments which will try to provide researchers with more realistic results on mesh networking performance. Hopefully these testbeds and their associated results will stimulate further improvements to mesh networking protocols which adapt to realistic network conditions.

1.3 OBJECTIVES

This thesis will mostly concern itself with the construction, modelling and performance of an indoor wireless grid testbed and will conclude with a case study of a deployed outdoor rural wireless mesh testbed. The aim of this thesis is to analyse the performance of mesh networking protocols on live testbed networks. There are three goals in this thesis:

- Build an indoor network testbed based on a grid structure that models real multi-hop outdoor networks satisfactorily.
- Analyse and compare the performance of well established MANET protocols in this testbed.
- Analyse the performance of a live rural mesh network case study and report on user experiences.

1.4 CONTRIBUTION

There is currently very little published material based on the performance analysis of mesh networking in real network testbeds. There are also very few indoor grid-based wireless networks deployed world wide; as of this publication date there were two other known established indoor testbeds based on a grid structure [2, 3]. This work will contribute the following:

- Summarize the current status of ad hoc standards-based networking protocols and report on significant testbed networks that have been established internationally.
- Help other researchers understand the process and challenges in constructing an indoor wireless grid for carrying out mesh networking experiments

- Contribute a set of comparative results for MANET routing protocols run on a physical wireless testbed as opposed to the majority of work which was done using simulations.
- Contribute to the understanding of the performance of rural mesh networks as well as some of the social and practical challenges associated with building these networks.

1.5 RESEARCH METHODOLOGY

This work follows a standard scientific as opposed to Socratic method in which a set of theories or hypotheses are tested via physical experiments. The scientific community and standards bodies have selected a set of advised routing protocols for various scenarios from a vast set of competing protocols. There are a set of existing theories based on mathematical modelling and simulation on the performance of these protocols which lead to a set of hypotheses.

By constructing a physical testbed network and running these protocols in the testbed, some of the previously held theories on protocol performance will be challenged.

Following a hypothetico-deductive cycle [4], this work tests the predictions of these hypotheses using a novel testbed, which leads to new observations and ultimately to the original hypothesis being adjusted or redefined.

The literature survey followed a process whereby the most cited or seminal works were uncovered and referenced works in these publications were recursively examined until the earliest works were traced. The literature was organized chronologically to understand how the field has evolved over the past few decades from the early 70's until now.

1.6 OVERVIEW OF THESIS

The thesis is structured as follows:

- In Chapter 2, the background information with regard to the development of mesh networking and testbed networks is described.
- In Chapter 3, the construction of the indoor mesh testbed is described together with key challenges encountered when constructing such a lab. The measurement process used to carry out experiments is also described and this testbed together with a set of measurement processes forms the bases of subsequent chapters which make use of this testbed environment
- In Chapter 4, the testbed is modelled to help understand its properties and establish its suitability to mesh networking experiments. Electromagnetic as well as networking characteristics are modelled and defined.
- In Chapter 5, A detailed analysis of 3 MANET routing protocols, namely OLSR, AODV and DYMO is carried out. It specifically compares hop count, routing traffic overhead, throughput, delay, route flapping and packet loss for these protocols running on the 7x7 wireless grid.

- In Chapter 6, a case study of a rural mesh network is presented which outlines its performance as well as the usage of the network by the community.
- In chapter 7, a summary of the contribution of this thesis is presented together with conclusions and future work.

CHAPTER TWO

BACKGROUND

Science alone of all the subjects contains within itself the lesson of the danger of belief in the infallibility of the greatest teachers in the preceding generation. As a matter of fact, I can also define science another way: Science is the belief in the ignorance of experts.

Richard Feynman, *The Pleasure of Finding Things Out*

2.1 INTRODUCTION

In order to understand the results presented in this work a number of aspects of mesh networking need to be covered. Mesh networks make use of ad hoc networking protocols but these terms are often used interchangeably. Some definitions will be offered to clear up the differences between an ad hoc network and a mesh network. Some background is given on ad hoc networking and its development over the past few decades; this is followed by a description of the specific ad hoc routing protocols that will be discussed in this work. Other testbeds that have been constructed around the globe are described in order to compare their approach to the testbed that was built as part of this research. As the testbed will be used to make comparisons of ad hoc routing protocols, some previous work in this regards is described. Finally, a summary of arguments that have been provided for the necessity of testbeds is given to help understand the motivation behind this work.

2.2 AD HOC NETWORKING

An ad hoc network is the cooperative engagement of a collection of wireless nodes without the required intervention of any centralized access point or existing infrastructure. Ad hoc networks have the key features of being self-forming, self-healing and do not rely on the centralized services of any

particular node. There is often confusion about the difference between a wireless ad hoc network and a wireless mesh network (WMN).

A wireless ad hoc network is a network in which client devices such as laptops, PDAs or sensors perform a routing function to forward data from themselves or for other nodes to form an arbitrary network topology. When these devices are mobile, they form a class of networks known as a mobile ad hoc network (MANET), where the wireless topology may change rapidly and unpredictably. Wireless sensor networks are a good example of a wireless ad hoc network.

A wireless mesh network is characterized by dedicated wireless routers which carry out the function of routing packets through the network. These routers are static or quasi-static nodes and client devices which connect to the wireless routers normally do not have any routing functionality. Broadband community wireless networks or municipal wireless networks are good examples of wireless mesh networks.

There are no protocols in the IETF which have assumed the term mesh networking protocol and this standards body only uses the term ad hoc networking protocol. Only the IEEE 802.11s standard has used the term mesh networking protocol to describe the behaviour of this standard. In the rest of this thesis the term ad hoc networking protocol will still often be used, even in the context of a mesh network.

2.3 DEVELOPMENT OF AD HOC NETWORKING

2.3.1 RESEARCH PRIOR TO 1990

Mathematicians were already thinking about the basic problems of finding the shortest path through a connected graph as early as the 1950's. American mathematician Richard Bellman wanted to calculate the shortest path between cities with a specific number of roads and together with mathematician Lester R. Ford Jr came up with the Bellman-Ford algorithm in 1956 [5]. This computes a single-source shortest path in a weighted digraph, which is a graph in which some of the edge weights can be negative. Dutch mathematician Edsger Dijkstra developed an algorithm named after himself which solves the single-source shortest path problem for a directed graph with non-negative edge weights in 1959 [6].

However the first routing protocol implemented in a live network was in 1969 on the Advanced Research Projects Agency Network (ARPANET) of the U.S. Department of Defense (DoD) [7]. This was the world's first operational packet switching network making use of an early version of the Routing Information Protocol (RIP) based on the Bellman-Ford algorithm. It was capable of routing between a small number links connecting DoD and Universities over 64 kbps digital leased lines, and is the precursor of the global Internet.

When a packet was sent to a node, the path was not known in advance; instead an Interface Message Processor (IMP) individually decided which line to use in transmitting a packet addressed to another destination using a simple lookup table procedure. A network delay table was also maintained

by the IMP which gave an estimate of the delay it expected a packet to encounter in reaching every possible destination. This basic routing system was sufficient for the purposes of the small ARPANET network but it would have failed to handle the complexity of massive interconnected networks we find today in the Internet or a large mesh network.

The 80's saw the birth of TCP/IP networking and wireless networking in the form of packet radio. Afek *et al.* [8] described a full reversal method and the partial reversal method for handling packet radio networks with frequently changing topology. Afek was trying to solve some of the problems that packet radios were experiencing such as collisions due to flooding when a route goes down, routing loops, and a lack of redundant routes. In the Full Reversal Method, when a link breaks, each node other than the destination that has no outgoing link reverses the directions of all its incoming links at each iteration. In the Partial Reversal Method, every node other than the destination keeps a list of its neighboring nodes that have reversed the direction of the corresponding links. At each iteration, where links are reversed, each node that has no outgoing link reverses the directions of the links which do not appear on its list of previously reversed links, and empties the list. The Partial Reversal Method, especially, helps limit flooding throughout the network and both ensure that there are no routing loops.

2.3.2 RESEARCH IN THE 90'S

The Internet was truly born in the 90's and the Internet Engineering Task Force (IETF) had already improved their Internet routing protocol by introducing a link state algorithm called Open Shortest Path First (OSPF) in the late 80's which allowed routers to dynamically determine the shortest path between any two networks [9]. The term ad hoc networking was developed in the 90's and major research in this field began during this decade.

It was during this decade that the IETF Mobile ad hoc Networks (MANET) [10] working group was formed. Its purpose is to standardize IP routing protocol functionality suitable for wireless routing within both static and dynamic topologies. The fundamental design issues are that the wireless link interfaces have some unique routing interface characteristics and that node topologies, within a wireless routing region, may experience increased dynamics, due to motion or other environmental factors.

The group has been focused on exploring a broad range of MANET problems, performance issues, and related candidate protocols which were submitted as experimental Request For Comments (RFCs). In 2004 they devised a revised charter in which the WG will operate under a reduced scope by targeting the promotion of a number of core routing protocol specifications to experimental RFC status. Some maturity of understanding and implementation exists with each of these protocols, yet more operational experimentation experience is seen as desirable. Overall, these protocols provide a basic set of MANET capabilities covering both reactive and proactive design spaces.

With this experimental protocol base established, the WG will move on to design and develop MANET common group engineered routing specifications and introduce these to the Internet Stan-

dards track.

2.3.3 LATEST DEVELOPMENTS

Figure 2.1 shows the evolution of standards over the past few decades. The arrows show how various routing protocols have evolved out of previously developed protocols. Starting with Bellman-Ford and Dijkstra in the early 50’s to the first IETF Internet protocols, RIP, OSPF and the Border Gateway Protocol (BGP), developed in the 80’s. The IETF MANET group was formed in 1997 and the protocols developed there, which will be discussed in section 2.4, mostly evolved from earlier work by the IETF for wired networks.

There is now a very strong drive by the IEEE to standardize mesh networking at layer 2 and to this end they have created the 802.11s working group [11]. Devices in an 802.11s mesh network are called Mesh Points (MP) and they form a layer 2 mesh with one another over which mesh paths can be established using a routing protocol. These MPs can provide standard “hot spot” access as well as form an inter-“hot spot” mesh backbone.

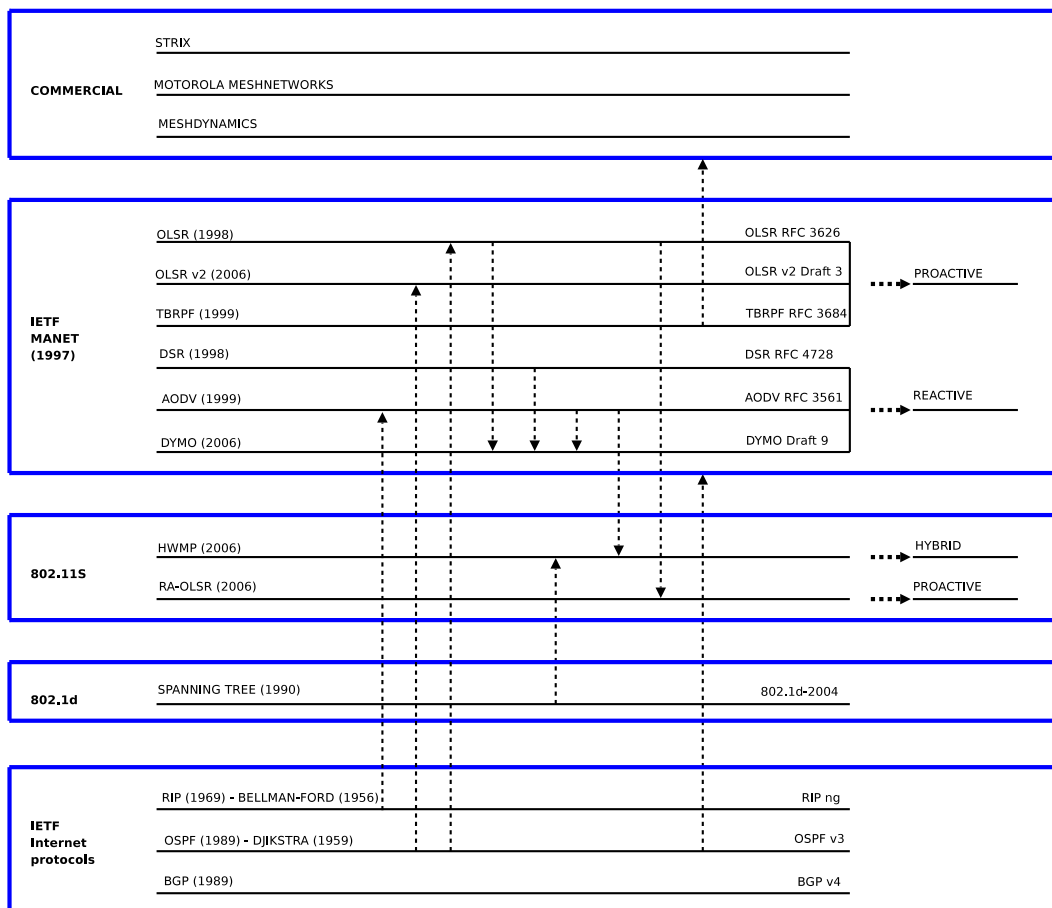


Figure 2.1: Evolution of ad hoc networking over the past few decades.

The standard defines a default mandatory routing protocol called the Hybrid Wireless Mesh Protocol (HWMP), but does allow vendors to operate using alternate protocols. One of these, described

in the draft, is called Radio Aware Optimized Link State Routing (RA-OLSR). HWMP is a hybrid routing protocol inspired by a combination of Ad hoc On-demand Distance Vector (AODV) routing and the spanning tree algorithm embedded in the 802.1d standard. RA-OLSR is a proactive protocol based on Optimized Link State Routing (OLSR) with a radio aware routing metric.

There are also many commercial mesh networking groups that have formed, some of which are also outlined in Figure 2.1. These companies often make bold statements about the impressive performance of their protocols with respect to scaling and delay but it is very difficult to verify these claims as none of the algorithms or source code is available to carry out any tests.

2.4 AD HOC ROUTING PROTOCOLS

Three main categories of ad hoc routing protocols have surfaced over the past decade. These are reactive routing protocols, proactive routing protocols and hybrid routing protocols. This work only concerns itself with reactive and proactive routing.

Reactive or on-demand protocols find routes on demand by flooding the network with Route Request packets. As a result, only the routes that the network needs are entered into a routing table. The disadvantage of this method is that there will be a startup delay when data needs to be sent to a destination to allow the protocol to discover a route. The two reactive protocols that will be investigated in this paper are Ad hoc On-demand Distance Vector (AODV) [12] routing and its recent successor called Dynamic Manet On-demand routing (DYMO) [13].

Pro-active or table-driven routing protocols maintain fresh lists of destinations and their routes by distributing routing tables in the network periodically. The advantage of these protocols is that a route is immediately available when data needs to be sent to a particular destination. The disadvantage of this method is that unnecessary routing traffic is generated for routes that may never be used. The Proactive routing protocol that will be investigated on the testbed is called Optimized Link State Routing (OLSR) [14].

2.4.1 AODV

AODV is a reactive routing protocol which only stores next-hop information corresponding to each flow for a data packet transmission. Route discovery is carried out using a Route Request (RREQ) message when a node lacks a route to a destination. The RREQ message also includes a last-known sequence number for the destination node as well as a unique RREQ id which is incremented each time a node forwards a RREQ. A RREQ is flooded through the network in a controlled way. For example a node only forwards a RREQ if it has not done so before and this is done by checking the RREQ id for duplicates. Each node that forwards the RREQ creates a reverse route back to the originating node, by entering the previous hop as the next hop entry to the originating node.

When the RREQ reaches the destination node, a Route Reply (RREP) is sent back along the reverse path used by the RREQ. A RREQ can also reach a node which already has a path to the

destination and a RREP can be sent back from this node. The sequence number is used to check how fresh a route is that is cached at any particular node. If the destination sequence number stored at the intermediate node is greater than or equal to the sequence number contained in the RREQ it will send a RREP and the RREQ is discarded. All nodes with knowledge of routes to a destination store a destination sequence number for each route to a destination. A node may also optionally send a gratuitous RREP to the destination node to prevent any future route discovery being initiated by the destination node.

Route maintenance is used to respond to changes in topology. Nodes continuously try to detect link failures by listening to RREQ and RREP messages and using HELLO messages if a RREQ or RREP are not sent within a set number of seconds. When a node detects a link break or receives a data packet it has no route for, a Route Error (RERR) packet is sent to inform other nodes about the error. The RERR contains a list of unreachable destinations and this is propagated back to all nodes in the routing table that make use of the route through the unreachable destination.

To find a new route, the source node initiates a new route discovery for the unreachable destination, or a node upstream may also try to locally repair the route by initiating a route discovery from there. Figure 2.2 shows AODV discovering a route from node 1 to node 10 using Route Requests (RREQ) and Route Replies (RREP) sent back over the shortest route back to node 1. All other RREQs arriving at node 10 other than the one taking route 1-3-5-10 will contain RREQ id's that are greater than the one contained in this route and will be rejected.

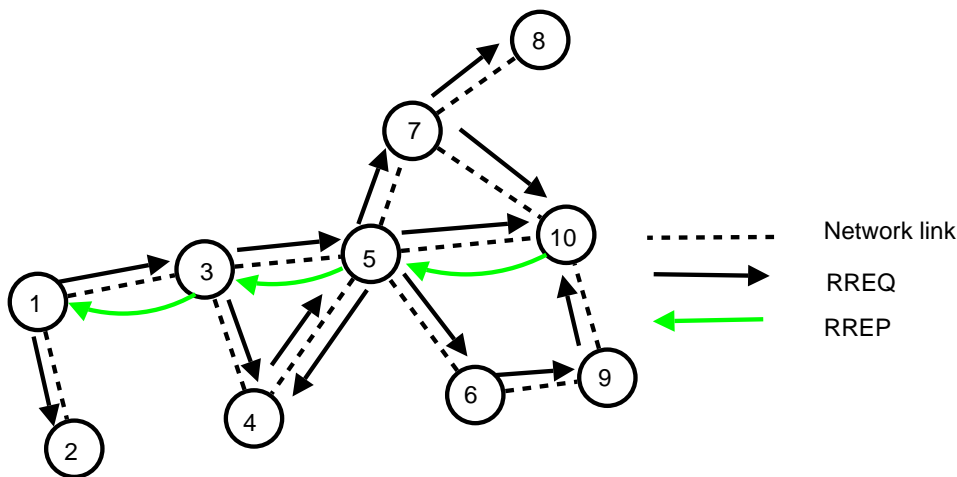


Figure 2.2: AODV routing protocol showing the route discovery process.

2.4.2 DSR

Although DSR is not specifically evaluated in this work, it needs to be discussed as it forms one of the building blocks of the DYMO routing protocol which is evaluated.

The Dynamic Source Routing protocol (DSR) [15], as the name suggests, is a source-based routing protocol which dynamically discovers a source route to any destination in the network. Source routes place routing path information in the packet and the path used is predetermined by the source node. DSR guarantees loop-free operation as intermediate nodes don't keep any routing information; it is also beacon-less and does not require the exchange of periodic HELLO messages.

Figure 2.3 shows how DSR creates the a route from node 1 to node 8 by flooding a Route Request (RREQ) in the network. The full path back to node 1 is contained in the routing packet as the RREQ is forwarded towards the destination, node 10. A node will only forward a RREQ if the node is not the target, it has not forwarded the packet previously and it does not find its own address in the route record. To simplify the diagram, Figure 2.3 does not show forwarded RREQs that would be discarded by the receiver.

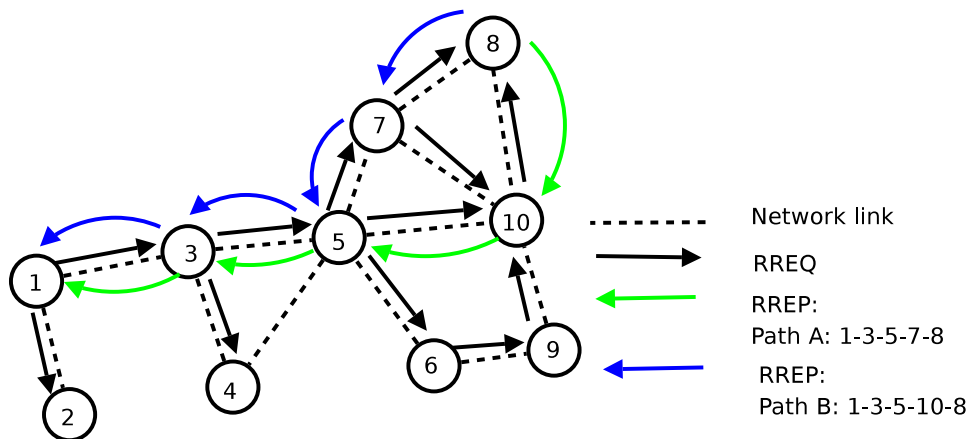


Figure 2.3: Route discovery process for DSR showing how a route is discovered from node 1 to node 8. Only optimal routes are shown to simplify the diagram.

DSR allows for a number of mechanisms to send a Route Reply (RREP) back to the initiator. It can be sent back using a route in its route cache, it can perform a route discovery itself with the RREP piggybacked in this route discovery or, as shown in Figure 2.3, it can be sent back along the accumulated RREQ path and in this case there are two possible paths that will finally be stored in the initiator nodes route cache for redundancy. In the first two cases, links for sending and receiving can be asymmetrical, while for the accumulated path case, routes will always be symmetrical.

Each node that transmits a packet is responsible for ensuring that the next hop neighbour receives

the packet. When a link break is detected, while forwarding a packet, a Route Error (RRER) is sent to the node originating the packet, stating the link that is currently broken. The initiating node will then either use another route in its cache or initiate a new route discovery.

2.4.3 OLSR

OLSR is a pro-active protocol and maintains its topological information by regularly sending link state messages between nodes to learn about new nodes in the network and nodes that have left the network. OLSR reduces the overhead of flooding link state information by requiring fewer nodes to forward the information. A broadcast from node X is only forwarded by its multipoint relays. Multipoint relays of node X are its neighbours such that each two-hop neighbour of X is a one-hop neighbour of at least one multipoint relay of X. Each node transmits its neighbour list in periodic beacons, so that all nodes can know their 2-hop neighbours in order to choose the multipoint relays (MPRs).

To obtain the topology information, for a node to be able to select its MPR set, it is first necessary to get information about its one-hop and two-hop neighbours. In addition to this information, nodes that have selected a specific node as an MPR, known as the MPR selector set, need to be maintained. All this information is obtained by periodically sending HELLO messages in which a node exchanges information about its neighbours, the link state and the type of neighbours it has. When a message is initially sent from node A to node B, an empty HELLO message is sent and node B then returns a HELLO message with node A's address contained in it. Node A then sends a HELLO message back to node B announcing node B as a symmetric neighbour.

As these HELLO messages contain a list of neighbours of the sending node, a node receiving the message can maintain its two-hop neighbour set based on this list. All symmetric neighbours advertised in the HELLO packet, but not including the node itself, are added to the receiver's two-hop neighbour set. For each advertised neighbour in a HELLO message, a flag indicates if the sending node has chosen this neighbour as an MPR. Upon receiving a HELLO packet, a node checks the list of neighbours and compares this with its own address. If a match is found, the sender of the HELLO message is added to the MPR selector set of the receiver.

Figure 2.4 illustrates how the OLSR routing protocol will disseminate routing messages from node 3 through the network via selected MPRs 1, 5 and 10.

2.4.3.1 HYSTERESIS ROUTING METRIC

The RFC for OLSR makes use of hysteresis to calculate the link quality between nodes. The purpose of this hysteresis is to try and stabilize the network in the presence of many alternative routes. Link hysteresis is calculated using an iterative process. If q_n is the link quality after n packets and h is the hysteresis scaling constant between 0 and 1, then the received link quality for each consecutive successful packet is defined by Equation 2.1 :

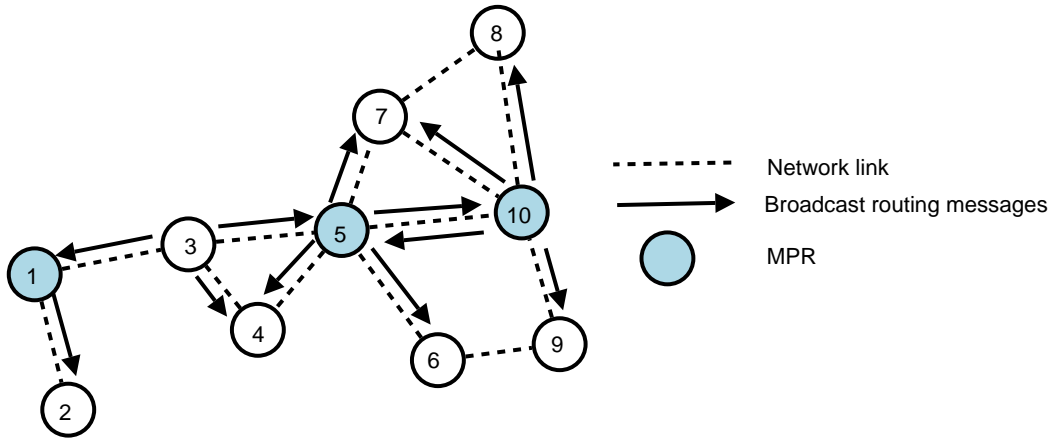


Figure 2.4: OLSR routing protocol showing selection of MPRs.

$$q_n = (1 - h)q_{(n-1)} + h \quad (2.1)$$

For each consecutive unsuccessful packet the link quality is defined by Equation 2.2 :

$$q_n = (1 - h)q_{(n-1)} \quad (2.2)$$

When the link quality exceeds a certain high hysteresis threshold, q_{high} , the link is considered as established and when the link quality falls below a certain low hysteresis threshold, q_{low} , the link is dropped.

To develop a mathematical prediction for the link quality for n consecutive successful packets a geometric series is employed. The solution to n consecutive successful packets for a starting condition set to q_0 is given in Equation 2.7

$$q_1 = (1 - h)q_0 + h \quad (2.3)$$

$$q_n = (1 - h)^n q_0 + h[(1 - h)^{n-1} + (1 - h)^{n-2} + \dots + 1] \quad (2.4)$$

$$q_n = (1 - h)^n q_0 + h \left[\frac{1 - (1 - h)^n}{1 - (1 - h)} \right] \quad (2.5)$$

$$q_n = (1 - h)^n q_0 + 1 - (1 - h)^n \quad (2.6)$$

$$q_n = (q_0 - 1)(1 - h)^n + 1 \quad (2.7)$$

The derivation for link quality for n consecutive unsuccessful packets is trivial. The solution to n consecutive unsuccessful packets for a starting condition set to q_0 is given in Equation 2.9.

$$q_1 = (1 - h)q_0 \quad (2.8)$$

$$q_n = (1 - h)^n q_0 \quad (2.9)$$

Figure 2.5 shows a graph for 7 consecutive successful packets followed by 7 unsuccessful packets with $h = 0.5$, $q_{high} = 0.8$ and $q_{low} = 0.3$, based on these equations.

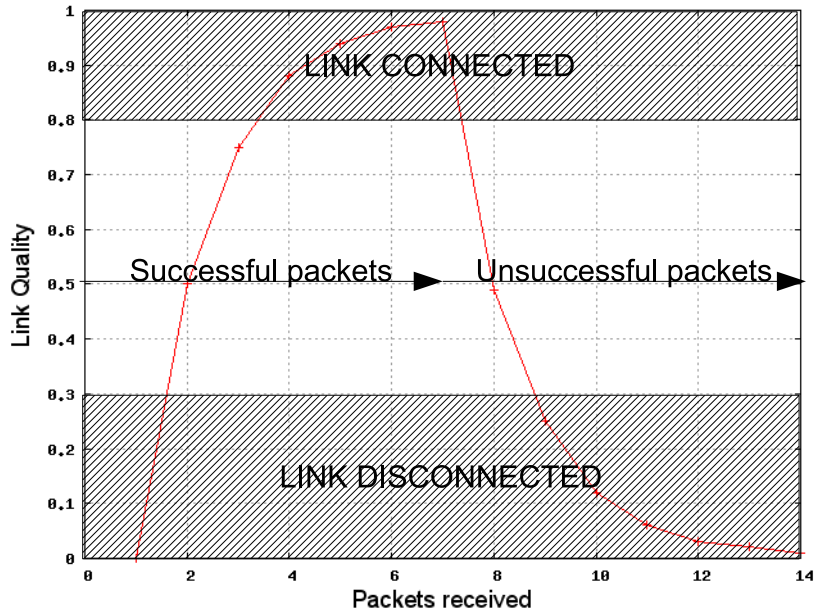


Figure 2.5: Link Hysteresis in the OLSR routing protocol.

Hysteresis produces an exponentially smoothed moving average of the transmission success rate and the condition for considering a link established is stricter than the condition for dropping a link.

2.4.3.2 ETX ROUTING METRIC

A new improved routing metric, called Expected Transmission Count (ETX) [16] proposed by MIT, has also been incorporated into the source code for OLSR but it is not officially part of the RFC. All the MANET RFCs prefer to use hop count as a routing metric for the sake of simplicity.

The alternative ETX metric calculates the expected number of retransmissions that are required for a packet to travel to and from a destination. The link quality, LQ , is the fraction of successful packets that were received by us from a neighbor within a window period. The neighbor link quality, NLQ , is the fraction of successful packets that were received by a neighbor node from us within a window period. Based on this, the ETX is calculated as follows:

$$ETX = \frac{1}{LQ \times NLQ} \quad (2.10)$$

In a multi-hop link the ETX values of each hop are added together to calculate the ETX for the complete link including all the hops.

Figure 2.6 shows the ETX values for 7 consecutive successful packets followed by 7 consecutive unsuccessful packets assuming a perfectly symmetrical link and a link quality window size of 7.

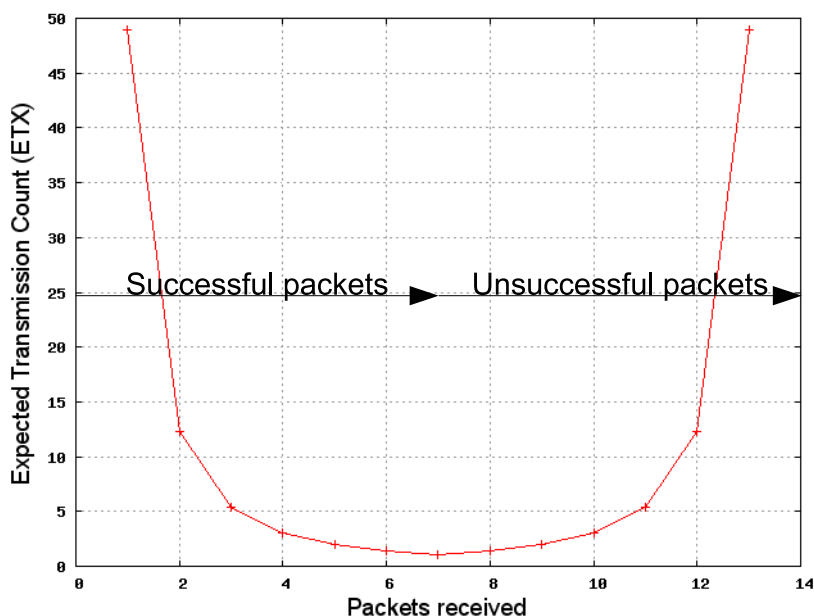


Figure 2.6: *ETX path metric values for successive successful and unsuccessful packets.*

A perfect link is achieved when ETX is equal to 1. ETX has the added advantage of being able to account for asymmetry in a link as it calculates the quality of the link in both directions. Unlike hysteresis, ETX improves and degrades at the same rate when successful and unsuccessful packets are received respectively. Routes are always chosen such that the sum of all the ETX values of adjacent node pairs is minimized.

2.4.4 DYMO

DYMO is the most recent ad hoc networking protocol proposed by the MANET working group. It seeks to combine advantages of reactive protocols, AODV and DSR, together with some link state features of OLSR. It makes use of the path accumulation feature of Dynamic Source Routing (DSR) by adding the accumulated route, back to the source, to the Route Request (RREQ) packet. As the RREQ progresses from the source to the destination, DYMO also adds routes back to the source. It retains the destination sequence number feature of AODV to check if a node has forwarded a message before and to check for stale routes but HELLO packets are an optional feature and are normally left out by default.

DYMO only has an option to send a Route Reply (RREP) on the reverse path of the RREQ and as a consequence DYMO does not support asymmetric links. If a node in the network is acting as a gateway, this information is also embedded in the RREQ or RREP messages to enable other nodes to

learn routes to a default gateway.

Route maintenance is carried out by continuously monitoring active links and updating timeout fields for entries in the routing table when receiving and sending packets. When a node receives a data packet for a destination it does not have a valid route for, it responds to the source with a Route Error (RERR) message. Other routes that are effected by the route failure are also added to the RERR message. When a node receives a RERR, it compares the list of nodes contained in the RERR to the corresponding entries in its routing table. If a route table entry for a node from the RERR exists, it is invalidated if the next hop node is the same as the node the RERR was received from and the sequence number of the entry is greater than or equal to the sequence number found in the RERR.

Detecting link failures can be done with HELLO messages, link layer feedback, route timeouts or using the MANET Neighborhood Discovery Protocol (NHDP) [17]. NHDP is directly derived from the link quality measurement techniques used in OLSR-like link hysteresis. When a link is broken a RERR is disseminated to notify other nodes about the broken link and the process is identical to the one described above.

When a node receives a RERR for a destination, the node can initiate a route discovery to find a route to the destination by sending a RREQ message.

Figure 2.7 shows how DYMO creates the full path back to node 1 in the routing packet as the RREQ is forwarded towards the destination node 10. The RREP is sent back along this accumulated path.

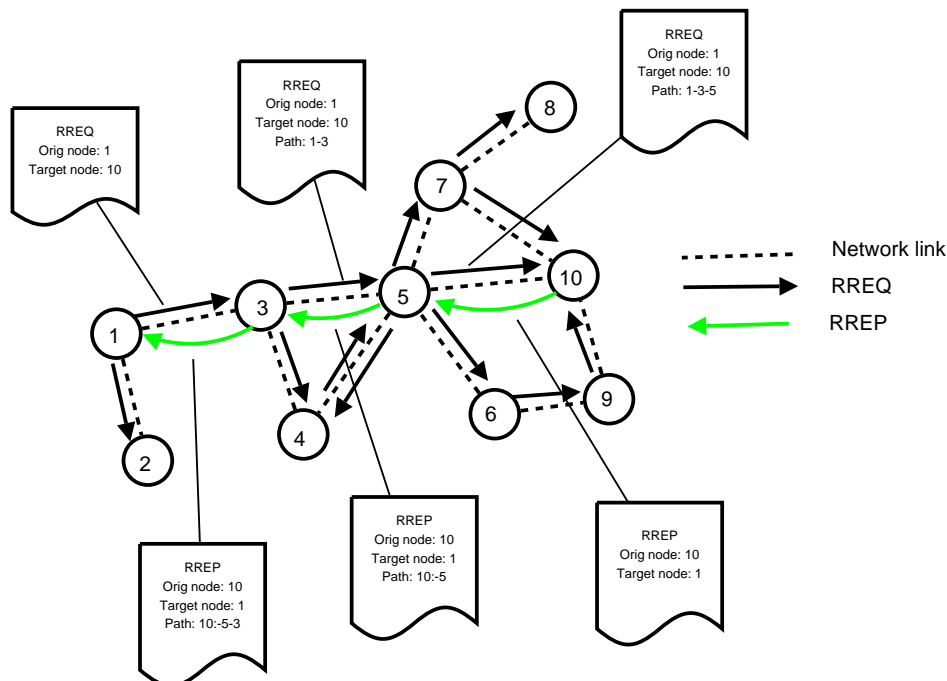


Figure 2.7: DYMO route discovery process showing how path accumulation is used to discover a route from node 1 to node 10.

2.5 LINUX IMPLEMENTATIONS OF AD HOC ROUTING PROTOCOLS

A crucial part of comparing different ad hoc networking protocols on a real testbed is finding implementations of the protocol that are well written and are as close as possible to the original published RFC.

Currently there are approximately 110 known ad hoc routing protocols that are widely known and of these only approximately 14 have an implementation which can run on a physical network. There are, however, many more which have implementations which can run in a simulation environment such as ns2. All the MANET protocols have been implemented on a UNIX platform. AODV has 10 implementations, OLSR has 7, DSR has 4, DYMO has 2 and TBRPF has 1.

The choice between a multitude of implementations of the same protocol was based on whether the particular implementation claimed to be RFC compliant, and if there was a strong developer community supporting the code base. Preference was also given to cases where the same code base was used for simulations and running the code on a physical network, as this would make future comparisons of simulations and live network results very simple.

Only the three routing protocols that were used on the testbed, namely OLSR, AODV and DYMO, are highlighted here.

2.5.1 OLSR

For OLSR, the implementation developed by Tonnesen [18] was used. This implementation is commonly called olsr.org and is now part of the largest open source ad hoc networking development initiative. Version 0.4.10, which is RFC3626 compliant, is used and is capable of using the standard RFC link hysteresis metric or the new ETX metric for calculating optimal routes. All parameters mentioned in the RFC are implemented and can be modified through a configuration file.

2.5.2 AODV

For AODV, the implementation by Nordstrom was used [19]. This implementation is designated AODV-UU and the current version used in the testbed is 0.9.3. The code is compliant with the AODV RFC3561 standard. This code base also supports the use of the same C code to run ns2 simulations. All parameters mentioned in the RFC are implemented and can be modified by changing the source code.

2.5.3 DYMO

For DYMO, the implementation by Ros [20] was used. This implementation is named DYMOUM and was developed out of the AODV-UU code base. The current version being used in the testbed is 0.3 and the code is compliant with Internet draft version 5 of DYMO. All parameters mentioned in the Internet draft are implemented and can be modified by changing the source code.

All the implemented routing protocols were used with their default RFC suggested configuration parameters.

2.6 TESTBEDS

A recent network testbeds workshop report [21] highlighted the importance of wireless testbed facilities for the research community in view of the limitations of available simulation methodologies. It was concluded that these testbeds enable a critical stage in the process of understanding the relationship between research and reality and help clarify which simplifications in theoretical work are valid. Indoor testbeds provide a controlled environment for the researcher to carry out experiments and ensure that router firmware is stable before deploying the mesh network in an outdoor environment. An outdoor testbed, providing broadband connectivity to users, is the most realistic test environment which will be effected by distances between nodes, environmental effects on signal propagation and realistic application traffic load on the network.

Two testbed environments traditionally support network and distributed systems research: network emulators and live networks. Emulation testbeds give users great control over the host and network environments and offer easy reproducibility but only offer artificial network conditions. Live network testbeds provide real network conditions, but are not easily repeatable environments and provide less control over the experiment.

2.6.1 NETWORK EMULATORS

One of the most well established large-scale open emulation environments for networking research is Emulab [22]. Emulab features 160 end nodes and 40 core nodes connected with about 4 km of cabling. It allows users to completely customize link parameters such as delay, bandwidth and packet loss using dedicated emulation nodes which act as Ethernet bridges. Emulab integrates with the ns2 simulation environment via ns2's emulation facility. This means you can write standard ns2 simulation scripts and run them on a real emulated network.

Emulab have also piloted some wireless networking using a grid of closely spaced PCs with wireless NICs on a rack. The PCs connect to each other in a vertical plane which makes it different from the normal wireless testbeds which place PCs or robots on a horizontal floor. There is no attempt, however, to attenuate the signal and this is used mainly to study the interference characteristics of 802.11.

A recent project at Emulab is mobile Emulab [23] which extends the emulab network testbed software to provide a remotely accessible mobile wireless and sensor testbed using robots. Robots make use of low-power wireless sensor network devices (motes) and single-board computers which allow users to position the robots, control the network interfaces on the computers and run programs and log data. Richard Feynman

Some labs have also looked at emulating the physical air interface layer, for example work being

done at Carnegie Mellon University [24] makes use of an FPGA-based DSP, which emulates the physical layer and is controlled by an emulation controller. The emulation controller is driven by scripts which specify a node's movements and physical layer characteristics; it then calculates the dynamic multipath fading and attenuation characteristics for each signal path and sends this to the FPGA-based DSP. This was tested with a simple experiment using 4 laptops with 12 possible signal paths but the DSP could handle up to 50 nodes.

2.6.2 LIVE NETWORK TESTBEDS

There are numerous Universities and research institutions such as Microsoft Research [25] which have constructed indoor live testbeds, which link together computers with wireless interface cards placed in offices around a building. Although these might be useful for the institutions to carry out ad hoc networking tests for the own internal environment, they don't create a repeatable research platform for others to carry out the same experiments and make comparisons.

The EWANT project [26] is a small-scale testbed which makes use of laptops equipped with wireless cards connected via RF cable to a shielded metal table which has multiple holes in which you can clamp down antennas. The wireless cards connect to multiple antennas through an attenuator and a RF multiplexer and by switching the signal through to different antennas, mobility is emulated. The concept was only demonstrated for 4 nodes.

Some full-scale testbeds are constructed to satisfy specific project requirements. For example, the Carnegie Mellon University (CMU) testbed [27] was built to evaluate the Dynamic Source Routing (DSR) protocol for ad hoc wireless networks. They used 5 mobile nodes implemented with rented cars carrying laptops and 2 static nodes spread over an area of 300m by 700m. No flexible experimental control was necessary as it addressed a specific application need.

Another well known testbed is the Ad hoc Protocol Evaluation (APE) testbed [28] which was used to compare different ad hoc routing protocols. Manual node placement was carried out in a large physical space and mobility was managed by choreographing the movement of volunteers carrying laptops. However, using humans to generate movement in a lab setup is a very unreliable mechanism considering the length of time often required to carry out an experiment.

MINT, a miniaturized network testbed for mobile wireless research [29], makes use of low-gain external antennas mounted on mobile robots connected through RF attenuators to a number of core nodes. A central controller oversees the operation of all the core nodes and makes use of ns2 scripts to configure an experiment similar to the mechanism used in Emulab. One limitation of MINT is that mobility of the robots is restricted to a set area to avoid RF cables from getting entangled.

The ORBIT testbed [3] at Rutgers University and the Kansei testbed [2] at Ohio state University are two large scaled-down indoor wireless network testbeds that are the most comparable in design to the indoor testbed that was constructed as part of this work.

The open access research testbed for next-generation wireless networks (ORBIT) testbed consists of a 20 by 20 grid of wireless nodes spaced 1 m apart making use of noise injection to decrease the

transmission range between nodes. The key issue in the testbed was that of repeatability and a large amount of work went into periodic calibration of the equipment to ensure that results were reliable. Injection of noise at each corner of the grid to decrease the Signal To Noise Ratio (SNR) appeared to have the sufficient desired effect of limiting range. However, it still created an artificial signal path which had localised weaker areas closer to the noise source.

The Kansei testbed consists of a 15 by 14 grid with nodes spaced 900 mm apart making use of 20 dB fixed attenuators to decrease the transmission range between the nodes. A log-normal shadowing model was used to understand the conditions necessary for equivalence between an outdoor network and a scaled indoor network. The following conditions were given for equivalence: (a) linear relationship between mean power and log-distance, (b) distribution of signal strength values around the mean value has to be independent of distance and (c) the two networks must have the same path loss exponents found in the log-normal shadowing model. This research showed that all these conditions are met in the scaled testbed. The log-normal shadowing model is described in Appendix B.

One of the most successful outdoor academic mesh network testbeds is the Roofnet project at MIT [30]. This testbed network has over 100 nodes spread across rooftops of volunteers in Cambridge who use it for broadband access. It is mainly used for studying the behaviour of wireless mesh networks and does not provide any experimental configuration flexibility to the researcher.

The Digital Gangetic Plains (DGP) project [31] is a good example of a live rural wireless network testbed that is used for broadband access by communities and also used as a research vehicle for students at the Indian Institute of Technology in Kanpur. It is an extensive testbed in a rural setting consisting of about 13 multi-hop directional 802.11 links spanning up to 80 km. This work has exposed several research and operational issues around setting up a mesh network in a rural area.

2.7 PREVIOUS WORK ON COMPARISON OF ROUTING PROTOCOLS

There is currently very little published work on ad hoc networking protocol performance comparisons and most of the work that has been done has been carried out on network simulators. Another critical issue with performance comparisons is the objectivity of the work, as many of the benchmarks involve the authors of the protocol itself. Reports on the comparison of routing protocols on static mesh network testbeds are essentially non-existent at the moment.

One of the most referenced pieces of work on comparative performance was done by Broch, Maltz and Johnson, the author of the DSR protocol, in 1998 [32]. At the time, the main contending ad hoc networking protocols were DSR, AODV, Destination Sequence Distance Vector (DSDV) and the Temporally-Ordered Routing Algorithm (TORA) and these were the focus of the comparison. An ns2 simulation was built for 50 mobile nodes moving about and communicating with each other with a range of mobility rates and movement speeds.

It was found that each of the protocols studied performed well in some cases yet had certain drawbacks in others. DSDV performed quite predictably, delivering virtually all data packets when node mobility rate and movement speed are low but failed to converge as node mobility increased.

TORA had the highest routing packet overhead and after 30 sources dropped a significant fraction of the data packets. DSR performed well at all mobility rates and movement speeds although the routing overhead was higher than the rest due to its use of source routing. AODV performed almost as well as DSR at all mobility rates and movement speeds with lower routing overhead at low mobility but the highest routing overhead with high rates of node mobility.

A subsequent performance comparison of AODV and DSR was carried out in 2000 by Das, Royer and Perkins, the author of AODV [33]. This comparison used an improved version of AODV and concluded that DSR outperforms AODV in less stressful situations i.e. smaller networks with lower load and mobility, whereas AODV outperforms DSR as these network stresses increase. However DSR does consistently generate less routing overhead than AODV.

A more recent comparison of OLSR and AODV in 2004 [34] was based on a collection of works which looked at the performance of these two protocols. It found that the AODV protocol will perform better in the networks with static traffic, where the number of source and destination pairs is relatively small for each host. However, it does use less bandwidth to maintain routes with the routing table being kept small and, as a result, is well suited to resource constrained environments. OLSR on the other hand performs better in high-density networks with highly sporadic traffic between a large number of hosts. OLSR, however, does need continuous available bandwidth in order to receive topology updates. Scalability is limited in both: in AODV the flooding overhead becomes high in high mobility networks and in OLSR the size of the routing table and topology update messages grows quickly as the network size increases.

Comparing routing protocols on live testbeds has been scarce and this could be because certain institutions would prefer to focus on testing and improving a routing protocol that they have developed or have a vested interest in. For example, MIT roofnet mentioned in Section 2.6.2 only runs the Srcr routing protocol that they have developed on their testbed. Most of the more general testbeds, mentioned in Section 2.6, do not have any detailed comparative results yet.

In 2002 some early comparisons of AODV and OLSR were carried out on the APE testbed. They were based on early implementations of these protocols, OLSR-inria and Mad-hoc-AODV, which have since been dramatically improved. The experiment was choreographed amongst 37 people carrying laptops so that two clusters would move in and out of range of each other. What they did find is that Mad-hoc-AODV failed in detecting link breakages and setting up new multi-hop routes in mobile scenarios. OLSR on the other hand was more resilient to these breakages and could set up new stable multi-hop routes. Both protocols showed a similar number of fluctuating links and the authors concluded that a direct comparison of the performance was not yet possible due to the different levels of maturity of the protocol implementations.

The defence industry has always been very interested in ad hoc networking as an option for creating spontaneous networks between soldiers on the battlefield. The U.S. Army carried out an exercise in which AODV, DSR, OLSR, OSPFv2 and the Zone Routing Protocol (ZRP) was evaluated under the Qualnet simulator using live traffic logs of an actual military exercise [35]. Successfully

delivered packets were measured under various traffic conditions.

DSR showed the best performance at low data rates but AODV performed most efficiently at high data rates which agrees with the work carried out by Das *et al.* [33]. AODV's delay vs Packet Delivery Ratio (PDR) characteristics showed the best performance but DSR began to catch up as the delay increased due to network size which suggests it may eventually surpass AODV in a large network. OLSR generally performed second best with the Zone Routing Protocol (ZRP) in 3rd place with regard to percentage of successfully delivered packets. It was suspected, however, that a different network scenario with a mix of mobile and static nodes could favour ZRP given its hybrid proactive and reactive algorithm.

2.8 LIMITATIONS OF SIMULATION AND MATHEMATICAL MODELLING

In order to understand the need for mesh network testbeds, it is useful to look at the strengths and weaknesses of all the tools that are used to help characterize wireless networks.

2.8.1 MATHEMATICAL MODELLING

Deriving mathematical formulae which characterize the behaviour of wireless networks is an extremely useful tool to generate estimations for generalized problems. They can also be useful for understanding theoretical upper or lower bounds to problems. A good example of this is the Shannon-Hartley theorem which establishes the channel capacity or the maximum amount of error-free digital data that can be transmitted over a communication link with a specific bandwidth in the presence of noise. Another good example of this, and one which will be frequently discussed in this work, is Gupta and Kumar's recent equation which models the best and worst case data rate in a network with shared channel access, as the number of hops increases [36].

"Rules of thumb" are another area where mathematically derived answers become useful when constructing wireless networks. For example Kleinrock's derivation of optimum transmission radii for packet radio networks [37] resulted in a "rule of thumb" which states that a node should see no more than six other nodes in order to optimize throughput in the network.

However, when the performance of a specific network topology or routing algorithm is required, the complexity required to mathematically model these situations becomes vast and arriving at a tractable solution becomes increasingly difficult. There is, however, still scope for mathematical modelling research to derive laws for mesh networks similar to ones which Shannon developed to understand channel capacity.

2.8.2 NETWORK SIMULATIONS

When mathematical modelling isn't applicable, simulation has proven to be a valuable tool to analyse system performance prior to the physical construction of a network. The key advantage of simulation is that routing algorithms can be accurately modelled in code together with the network topology

on which they will run. With the advent of easily available high speed computers, rapid results can be obtained within hours for complex network systems and routing algorithms by adjusting a few parameters, rerunning a simulation and comparing differences in performance.

Network simulation on popular tools like GloMoSim, Opnet and ns2 make up the bulk of published networking research today, but an evaluation by Andel *et al.* [38] of 114 peer reviewed research papers in the field of mobile ad hoc networks revealed some serious challenges to the credibility of simulations. These are some of the key findings:

1. There is a lack of consistency between the results of the same protocol being run on different simulation packages. This is largely due to differences in the way each model the physical world for example:
 - Simulators have different physical layer models available which significantly affect results. GloMoSim has two-ray path loss, Rayleigh and Ricean models available, ns2 only has a two-ray path loss model and Opnet only has a free-space path loss model.
 - Opnet bases signal reception on bit error rate (BER), ns2 uses signal-to-noise ratio threshold (SNRT) and GloMoSim had both options.
2. Researchers don't follow good scientific rigor - here are some highlighted issues:
 - Results are not independently repeatable due to simulator versions, distances between nodes, mobility models and traffic types not being specified. Documentation is not released with results which contains simulation code and experimental set-ups highlighting parameters used.
 - Results are not statistically valid due to no confidence intervals being stated and number of simulation runs not being given

Until simulation packages have improved physical layer models and certain aspects of the MAC layer, the researcher should acknowledge that the results from a simulation give a rough estimate of performance. Published work based on simulations should also be very explicit with regard to exact simulation parameters and statistical assumptions being used.

CHAPTER THREE

CONSTRUCTION OF THE MESH TESTBED

Construction and destruction are part of the creative process

3.1 INTRODUCTION

This section describes the construction of the indoor mesh testbed in order to help other researchers to construct a similar facility. There were many challenges that needed to be overcome before reliable experiments could be carried out and these are also highlighted in this section. Finally, a description is given of the measurement processes used to carry out the various experiments which help characterize the performance of a routing protocol.

3.2 PHYSICAL CONSTRUCTION OF THE 7X7 GRID

The mesh testbed consists of a wireless 7x7 grid of 49 nodes, which was built in a 6x12 m room as shown in Figure 3.1. A grid was chosen as the logical topology of the wireless testbed due to its ability to create a fully connected dense mesh network and the possibility of creating a large variety of other topologies by selectively switching on particular nodes as shown in Figure 3.2.

Each node in the mesh consists of a VIA 800 C3 800MHz motherboard with 128MB of RAM and a Wistron CM9 mini PCI Atheros 5213 based Wi-Fi card with 802.11 a/b/g capability. For future mobility measurements, a Lego Mindstorms robot with a battery powered Soekris motherboard containing an 802.11a (5.8 GHz) WNIC and an 802.11 b/g (2.4 GHz) WNIC shown in Figure 3.1 can be used.

Every node was connected to a 100 Mbps back-haul Ethernet network through a switch to a central server, as shown in Figure 3.3. This allows nodes to use a combination of a Pre-boot Execution

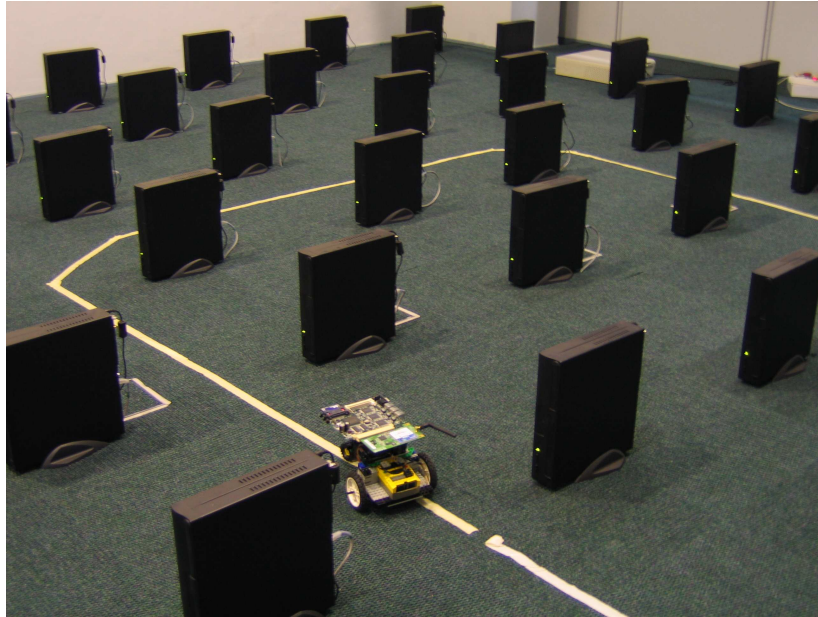


Figure 3.1: *Layout of the 7x7 grid of Wi-Fi enabled computers. The optional line-following robot will be explored in the future to test mobility in a mesh network.*

Environment (PXE), built into most BIOS firmware, to boot the kernel and a Network File System (NFS) to load the file system.

The physical constraints of the room, with the shortest length being 6 m, means that the grid spacing needs to be about 800 mm to comfortably fit all the PCs within the room dimensions.

At each node, an antenna with 5 dBi gain is connected to the wireless network adapter via a 30 dB attenuator. This introduces a path loss of 60 dB between the sending node and the receiving node. Reducing the radio signal to force a multi-hop environment, is the core to the success of this wireless grid and this is discussed later in section 4.2.

The wireless NICs that are used in this grid have a wide range of options that can be configured:

- *Power level range:* The output power level can be set from 0 dBm up to 19 dBm.
- *Protocol modes:* 802.11g and 802.11b modes are available in the 2.4 GHz range and 802.11a modes are available in the 5 GHz range
- *Sending rates:* 802.11b allows the sending rate to be set between 1 Mbps and 11 Mbps and 802.11g allows between 6 Mbps and 54 Mbps

This network was operated at 2.4 GHz due to the availability of antennas and attenuators at that frequency, but in future the laboratory will be migrated to the 5 GHz range, which has many more available channels with a far lower probability of being affected by interference.

3.3 CHALLENGES TO ESTABLISHING A FUNCTIONAL TESTBED

The following issues need to be considered carefully when constructing a testbed:

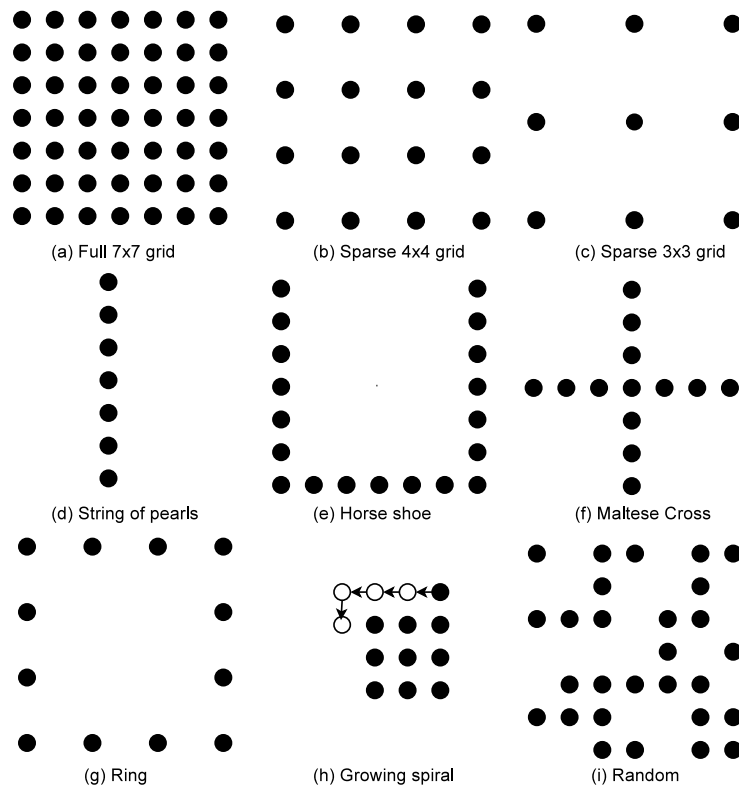


Figure 3.2: Various topologies that can be tested on the 7x7 grid: topology (a) to (c) demonstrate various levels of density in a grid, topology (d) represents the simplest topology, topology (e) is used to create a long chain to force routing protocols to use the longest multi-hop route, topology (f) is used to test congestion through a critical node, topology (g) is used to test route optimization, diagram (h) shows how to evolve to a full grid topology using a spiral and topology (i) is used run tests with a random distribution of nodes.

1. *Communication Grey zones:* Communication grey zones [39] occur because a node can hear broadcast packets sent at very low data rates, but no data communication can occur back to the source node sent at a higher data rate. Figure 3.4 shows how a RREQ can be broadcast to the edge of the communication grey zone but the RREP cannot get back to the source node. This problem was solved by locking the broadcast or multi cast rate to the data rate.
2. *Complexity and density of the grid:* The mesh grid forms a highly connected dense graph, which creates a difficult optimization problem for a routing algorithm. In a full 7x7 grid, the routing algorithms are presented with thousands of equivalent hop length routes; OLSR using ETX will constantly be receiving new routes with changing ETX values. This is discussed further in Section 4.4.
3. *Hardware issues:*

There are many physical hardware problems that have to be dealt with, such as faulty wireless NICs and drifting received signal strength as the WNICs heat up. These have been character-

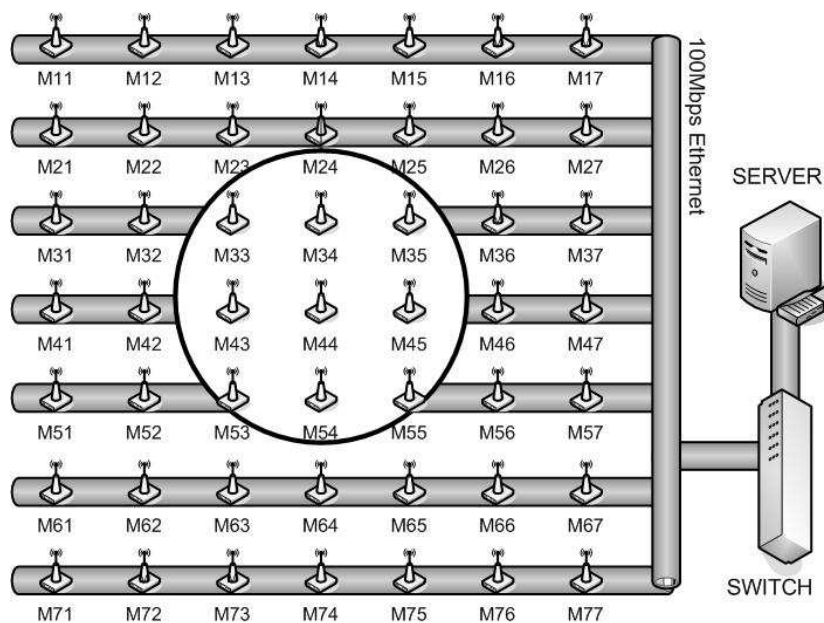


Figure 3.3: *The architecture of the mesh lab. Ethernet is used as a back channel to connect all the nodes to a central server through a switch. Each node is also equipped with an 802.11 network interface card.*

ized in the Section 4.2 which deals with electromagnetic modelling.

4. Routing protocol bugs:

Both AODV and DYMO gave kernel errors when the network size was greater than approximately 20 nodes. This caused the routing algorithms to freeze and not allow any packets to enter or exit the wireless interface. The particular error complained that the maximum list length had been reached. This constant was increased in the source code and subsequently the problem disappeared, but it did confirm the fact that these protocols had not been tested on networks as large as this testbed.

5. Antenna dual diversity:

Dual diversity is a mechanism employed by many new WNICs, which has two antenna ports to allow the radio to receive the stronger of two signals on each of these ports. This is especially applicable in indoor environments where there is a large degree of multipath present. It was found that when dual diversity was switched on, the nodes became very erratic. The throughput would vary as much as 50% within the space of 1 minute. As a result, dual diversity was turned off for the experiments.

6. Wide choice of wireless card parameters:

Finding the best combination of communication mode, data rate and transmit power was not a simple process. Receive sensitivity is increased by switching the radio to a lower data rate and transmit power can be varied between 0 and 20 dBm. Figure 4.1 shows which combinations of

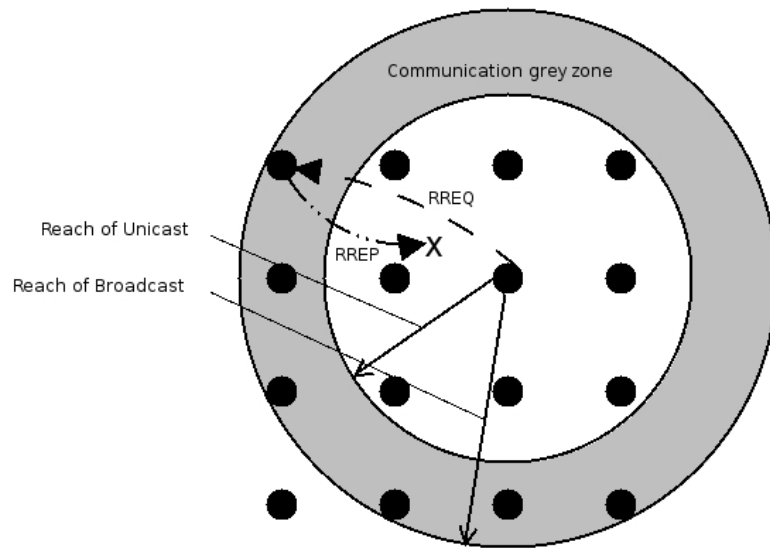


Figure 3.4: *Communication grey zones.*

these establish connectivity for various distances between nodes. However only trial and error eventually helped converge the settings to using 802.11b mode with a data rate of 11 Mbps and a power level ranging from 0 to 8 dBm.

7. *Time-consuming experiments:*

Experiments were very time consuming. Testing the throughput and delay for all permutation pairs of 49 nodes in the grid for 4 routing protocols using a 20-second test time takes approximately 52 hours.

8. *Interference:*

Finding a channel in the 2.4 GHz band, which is relatively free from interference, is not easy. The building, where the experiments were conducted, has an extensive in-building wireless network operating on 2.4 GHz. Even relatively weak signals close to -90 dBm are a problem when you are using a highly attenuated lab. In the future the lab will be migrated to 5.8 GHz, which has far more available channels.

3.4 MEASUREMENT PROCESS

All measurements other than throughput tests were carried out using standard Unix tools available to users as part of the operating system. The measurement values were sent back to the server via the Ethernet ports of the nodes and therefore had no influence on the experiments that were being run on the wireless interface.

It was found that the lab provides the best multi-hop characteristics, delay and throughput trade off when the radios are configured with the following settings:

- Channel = 6
- Mode = 802.11b
- Data rate = 11Mbps
- TX power <8dBm

The following processes were used for each of the metrics being measured:

1. *Delay*: Standard 84-byte ping packets were sent for a period of 10 seconds. The ping reports the round trip time as well as the standard deviation.
2. *Packet loss*: The ping tool also reports the amount of packet loss that occurred over the duration of the ping test.
3. *Static number of hops for a route to a destination*: The routing table reports the number of hops as a routing metric.
4. *Round trip route taken by a specific packet*: The ping tool has an option to record the round trip route taken by an ICMP packet but unfortunately the IP header is only large enough for nine routes. This sufficed for most of the tests that were done but occasionally there were some routes which exceeded 9 round trip hops, and no knowledge of the full routing path could be extracted in these instances. However, this was large enough to always record the forward route taken by a packet.
5. *Route flapping*: Using the ping tool with the option highlighted above makes it possible to record the complete route taken by a packet every second. It is then a simple process to detect how many route changes occurred during a set period of time by looking for changes in the route reports.
6. *Throughput*: The tool Iperf [16] was used for throughput measurements. It uses a client server model to determine the maximum bandwidth available in a link using a TCP throughput test but can also support UDP tests with packet loss and jitter. For these experiments an 8K read-write buffer size was used and throughput tests were performed using TCP for 10 seconds. UDP could be considered a better choice as it measures the raw throughput of the link without the extra complexity of contention windows in TCP. This does make the measurement more complex, however, as no prior knowledge exists for the link and the decision on the test transmission speed is done through trial and error.

7. *Routing traffic overhead:* In order to observe routing traffic overhead, the standard Unix packet sniffing tool, tcpdump, was used. A filter was used on the specific port that was being used by the routing protocol to only capture these packets. The measurement time could be varied by the measurement script, but 20 seconds was the default that was mostly used. The tool made it possible to see the number of routing packets leaving and entering the nodes as well as the size of these routing packets.

To force dynamic routing protocols such as AODV and DYMO to generate traffic while establishing a route, a ping was always carried out between the furthest two points in the network.

8. *Growing network size:* When tests are done which compare a specific feature to the growing number of nodes in the network, a growing spiral topology, shown in Figure 3.5, starting from the center of the grid, is used. This helps to create a balanced growth pattern in terms of distances to the edge walls and grid edges, which may have an electromagnetic effect on the nodes.

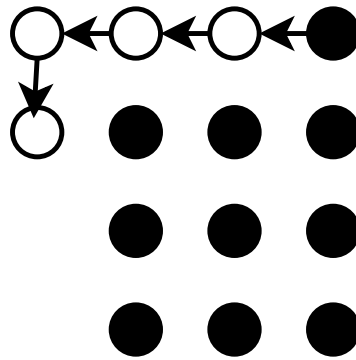


Figure 3.5: *Growing spiral topology for tests which compares a metric against a growing network size.*

9. *Testing all node pairs in the network:* When throughput and delay tests were carried out on a fixed size topology, all possible combinations of nodes were tested. If the full 7x7 grid was used this equates to 2352 (49×48) combinations.
10. *RTS/CTS tuned off:* All tests are done with RTS/CTS disabled as this did not improve the performance of the mesh. Other researchers have reported similar findings [40].

CHAPTER FOUR

MODELLING THE MESH TESTBED

It is a mathematical fact that the casting of this pebble from my hand alters the centre of gravity of the universe

Thomas Carlyle, *Sartor Resartus III*

4.1 INTRODUCTION

Before experiments are carried out on the testbed, its characteristics need to be well understood in order to ensure that results are reliable. This section will look at a number of aspects in the testbed: (a) the electromagnetic properties will be measured and compared against some developed theory; (b) a base line will be generated for the grid in terms of throughput and delay in a loss-less scenario; (c) the route complexity of the grid will be modelled to understand the total number of possible routes through the grid and the number of equivalent length routes through the grid between the two furthest apart nodes on a diagonal.

4.2 ELECTROMAGNETIC MODELLING

In order to understand the stochastic behavior of the wireless nodes in the grid, the underlying electromagnetic properties need to be understood. Once these properties are understood from the background theory, some measurements will be made to see how closely these match real measurements. The results obtained on a testbed can also be scaled to a larger network, if the following necessary conditions are satisfied [2]: (a) there is a linear relationship between mean power and log-distance, (b) distribution of signal strength values around the mean is independent of distance, (c) the networks are in similar environments with the same path loss exponents contained in the log normal shadowing model. See Appendix B for an explanation of the log normal shadowing model.

4.2.1 ELECTROMAGNETIC PROPERTIES

The following is a list of properties, in the wireless grid, which will affect the signal reported by the wireless NICs:

- Link budget related properties
 - Transmitted power level of the wireless NICs.
 - Receive sensitivity of the radio which in turn depends on its radio mode (802.11a/b/g) and the data rate being used.
 - Attenuation due to cable losses, insertion losses or the placement of intentional attenuators between the wireless NIC and antenna.
 - Antenna gain.
 - Free space loss due to distances between nodes.
- Coupling between antennas due to their close proximity to each other.
- Placement in the near or far field of the antenna.
- Limited Fresnel zone clearance due to insufficient antenna height.

Each of these will be dealt with in turn.

4.2.1.1 LINK BUDGET RELATED PROPERTIES

As discussed in section 3.2, the testbed makes use of 5 dBi antennas connected via 30 dB attenuators. The purpose of the attenuators is to decrease the communication range. The transmit power level of the NICs can be set between 0 dBm and 20 dBm and the following derivation is used to calculate the theoretical range of the nodes without taking into account antenna coupling or Fresnel zone clearance.

The link budget equation for a line of sight radio system is given in Equation 4.1:

$$P_{RX} = P_{TX} + G_{TX} - L_{TX} - L_{FS} - L_M + G_{RX} - L_{RX} \quad (4.1)$$

where P_{RX} = received power (dBm), P_{TX} = transmitter output power (dBm), G_{TX} = transmitter antenna gain (dBi), L_{TX} = transmitter losses from cables and connectors (dB), L_{FS} = free space loss or path loss (dB), L_M = miscellaneous losses from fading margin, body losses, polarization mismatch and other losses (dB), G_{RX} = receiver antenna gain (dBi) and L_{RX} = receiver losses from cables and connectors (dB).

For this system we will set the following parameters:

- $L_M = 0$: miscellaneous losses can be ignored for this approximation.

- $L_{TX} = L_{RX} = L_{ATT}$: Losses at TX and RX are both equal to the value of the attenuator.
- $G_{TX} = G_{RX}$: All the antennas are the same.

In order to find the maximum distance that this system can handle we need to know what free space loss was experienced when we set the received signal to the receiver sensitivity.

So we can rewrite this as Equation 4.2:

$$L_{FS} = P_{TX} - P_{RX} - 2L_{ATT} + 2G_{TX} \quad (4.2)$$

The free space loss is given by equation 4.3. It is important to note that the free space loss equation is an approximation which prescribes that the transmitting and receiving antennas be placed many orders of magnitude of the wavelength away from one another and the space surrounding the antennas should be free from any obstacles.

$$L = 20 \log \frac{4\pi D}{\lambda} \quad (4.3)$$

Where D = distance between transmitting nodes (m), λ = signal wavelength (m), L = power loss (dBm)

So the final solution to calculate the maximum distance possible is given by Equation 4.5:

$$20 \log \frac{4\pi D}{\lambda} = P_{TX} - P_{RX} - 2L_{ATT} + 2G_{TX} \quad (4.4)$$

$$D = \lambda \frac{10^{\frac{P_{TX} - P_{RX} - 2L_{ATT} + 2G_{TX}}{20}}}{4\pi} \quad (4.5)$$

The following parameters are used for the lab :

- Antenna gain (G_{TX}) = 5 dBi
- Attenuation used (L_{ATT}) = 30 dB
- Wavelength used (λ) = 0.122 (for $f = 2.45$ GHz)

The receive sensitivity of the radio, which is the level above which it is able to successfully decode a transmission, depends on the mode and rate being set. The faster the rate, the lower the receive sensitivity threshold.

Figure 4.1 shows free space loss curves for all possible scenarios over the distance of the grid to illustrate what the received signal will be at any particular node. This figure also shows the receive sensitivity of the radio at various modes and data rates. In theory, where the curve line rises above the

horizontal lines, there will be connectivity but as will be seen later, there are factors other than free space loss which affect signal propagation.

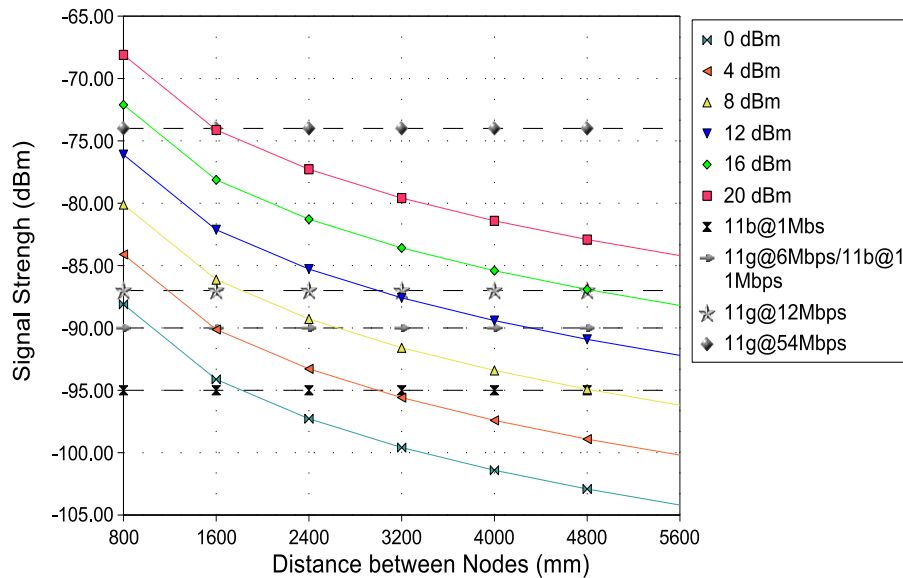


Figure 4.1: Received signal strength vs. distance between nodes in the grid spaced 800 mm apart. The horizontal lines show the receive sensitivity of the Atheros 5213 wireless network card. If the received signal strength curve is above this line, there will be connectivity between the nodes.

Table 4.1 shows the maximum range of a node for a few possible radio parameters and transmit power levels. The minimum possible range is 0.15 m and the maximum range is 17.26 m. These radio ranges suit the 6×12 m room dimensions and the 800mm node spacing very well. It is clear, from the table, that it is possible to limit the range from zero connectivity between nodes to full connectivity between all nodes as well as any possibility in between.

4.2.1.2 COUPLING BETWEEN ANTENNAS

When antennas are placed in close proximity to each other they form a complex propagation path as each antenna re-transmits some of the received signal. These antennas form an array, which effectively changes the effective radiation pattern of the transmitter from the point of view of the receiver. The antenna gain pattern is calculated as a product of the antennas own pattern and an array factor which is determined by the geometry of the array. In order to model this, a program for numerical electromagnetic modelling, based on the method of moments is used [41]. A discussion of this model is out of the scope of this thesis but the results revealed that maximum variation in received signal strength, due to coupling, can be high as 7 dB with a standard deviation of 2.6 dB when PC cases are not taken into account.

Parasitic coupling between nodes has also been noticed as nodes can communicate to one another even when antennas are not present or when the antennas are replaced with a load terminator.

Table 4.1: Possible radio range of a node when configured with various radio parameters.

Power level (dBm)	radio mode	data rate (Mbps)	Receive sensitivity (dBm)	Range (m)
0	802.11g	54	-74.00	0.15
0	802.11g	36	-79.00	0.27
0	802.11g	24	-82.00	0.39
0	802.11g	12	-87.00	0.69
0	802.11g	6	-90.00	0.97
0	802.11b	11	-90.00	0.97
0	802.11b	5.5	-92.00	1.22
0	802.11b	2	-94.00	1.54
0	802.11b	1	-95.00	1.73
20	802.11g	36	-79.00	2.74
20	802.11g	6	-90.00	9.71
20	802.11b	1	-95.00	17.26

Communication was only possible over a distance of approximately 1m but this is still significant in the scale of this testbed. Early experiments in the lab were actually conducted using nodes without antennas as it achieved similar goals to installing attenuators together with properly characterized antennas. However, as could be expected, the results were very unpredictable with some nodes having good connectivity and some not being able to connect at all.

This parasitic coupling depends on the effectiveness of the screening on the wireless NIC, quality of RF connections, and the geometry and quality of the PC case. The PC cases being used, have a front panel made of plastic which is transparent to RF energy and the rear panel has multiple ventilation holes, which also allows for RF leakage. Creating well screened PC cases should eliminate this problem.

4.2.1.3 NEAR AND FAR FIELD

The simple free space loss formula is based on the assumption of $1/r$ decay for the electrical and magnetic fields. This, however, is only the case when the distance from an antenna to an observer, r , is much greater than wavelength, λ .

Communicating in the near field should be avoided as this would mean that the testbed will not accurately represent the behaviour of a normal large-scale wireless network.

When the distance satisfies this requirement, also known as the far field zone, the antenna's radiation pattern is considered to be independent of distance. For antennas whose size is comparable or greater than the wavelength, λ , an additional criterion needs to be introduced which is given by Equation 4.6

$$r > \frac{2D^2}{\lambda} \quad (4.6)$$

where D is the maximum dimension of the antenna. This condition is derived from an established standard in electromagnetics where the phase error (in the electrical field wave) should be less than 22.5 degrees. The smaller this phase error, the closer the wave is to a plane wave, and the smaller the error in the measured field strength.

The inter-node spacing in the testbed is 0.8 m along the axis parallel to the edge. Using Equation 4.6 this node spacing will be satisfactory for antennas up to 0.22 m long. The 5 dBi dipole antennas being used in the grid are currently 0.154m and therefore satisfy the requirements of being in the far field.

4.2.1.4 FRESNEL ZONE CLEARANCE

Another property which effects propagation losses is obstructions. Fresnel zones are used to characterize an infinite number of concentric ellipsoids of revolution which define volumes in a radiation pattern. The n th Fresnel zone in metres, at a given observation point, is given by Equation 4.7. When objects lie within these Fresnel zones they cause additional attenuation, but decrease in severity with each nth Fresnel zone iteration.

$$F_n = \sqrt{n\lambda \frac{d_1 d_2}{d_1 + d_2}} \quad (4.7)$$

Where λ is the wavelength (m) and d_1 and d_2 are the distances (m) from the 1st and 2nd antennas to an observation point on the line of sight path.

In the testbed, the inter-node spacing is 0.8 m. At the wavelength of 0.122 m (derived from the frequency of 2.45 GHz), one can produce the plots of the 1st Fresnel zone, shown in Figure 4.2, for various pairs of nodes. From this figure it is clear that a clearance of at least 0.5 m above the metal cases is needed for the 1st Fresnel zone to be clear of obstructions.

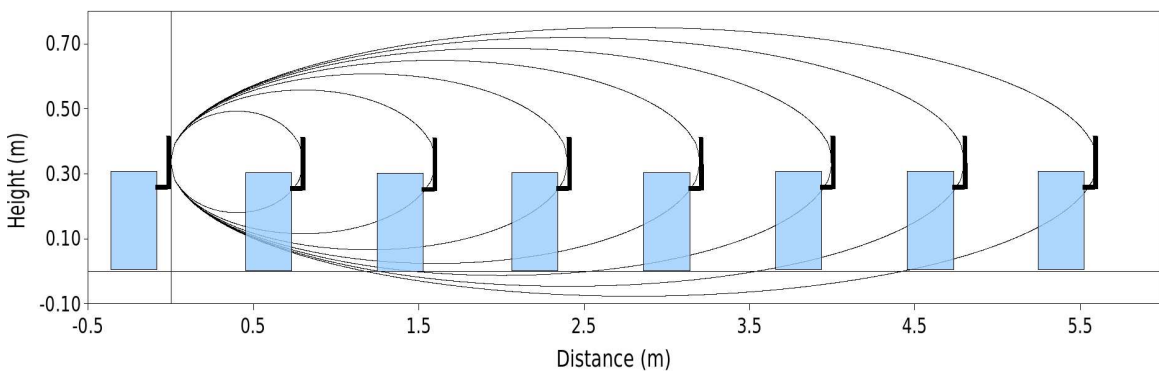


Figure 4.2: 1st Fresnel zone obstruction between column of 7 PCs.

From this diagram you can see that the further a receiving node is from the transmitted node the more the PC will obstruct the Fresnel zone which will lead to further attenuation.

4.2.2 SIGNAL STRENGTH MEASUREMENTS

In order to see how these electromagnetic properties were affecting the testbed some real signal strength measurements were made and analysed.

4.2.2.1 MEASUREMENT PROCESS

Most 802.11 compatible wireless cards measure the received signal in Received Signal Strength Indicator units or RSSI. RSSI is a measurement of the strength (not necessarily the quality) of the received signal strength in a wireless environment, in arbitrary units. RSSI is used internally in a wireless networking card to determine when the signal is below a certain threshold at which point the network card is clear to send (CTS).

RSSI measurements result in a one byte integer value, varying from 0 to 255 depending on the vendor. A value of 1 will indicate the minimum signal strength detectable by the wireless card, while 0 indicates no signal. For example, Cisco Systems cards return a RSSI of 0 to 100, reporting 101 distinct power levels. In the case of the testbed under consideration, the Wi-Fi chipset used for the measurements is made by Atheros and this card returns a RSSI value from 0 to 60.

Atheros uses this simple formula to convert from RSSI to dBm: power level (dBm) = $RSSI - 95$. This gives a dBm range of -35 dBm at 100% and -95 dBm at 0%.

RSSI is measured on a Wireless Network Interface Card (WNIC) every time a beacon is broadcast from another node containing the Service Set Identifier (SSID). According to the 802.11 standard, RF energy from the antenna is measured from the beginning of the Start Frame Delimiter (SFD) and the end of the Physical Layer Convergence Procedure (PLCP) Header Error Check (HEC). This happens periodically, at an interval specified by the user with the default being 100 ms.

Signal strength measurements were carried out by only turning on 2 nodes (1 pair) during each individual measurement. All other nodes in the grid were off and not radiating any RF energy. It is possible to accelerate running the tests by turning all the nodes on, and reading the signal strength between specific node pairs. However, analysis showed that the RSSI values, recorded in this way, were up to 6dB higher. At the same time, the signal quality (SQ) indicator read out of the WNICs was lower, typically by as much as 20 units which meant that there was a much higher noise floor present. On these grounds, this test acceleration method was not considered any further.

In order to avoid any time dependency of the measured results due to certain transmitters working continuously for a period of time, which is shown to be a valid assumption in Figure 4.3, a random approach was used for the selection of nodes for the test pair.

4.2.2.2 MEASUREMENT RESULTS

Time dependency of the signal was checked by turning on 2 nodes and recording the RSSI values whilst the nodes kept exchanging beacons. A continuous sequence of 200 measurements which lasted approximately 30 seconds was made for 100 random combinations of nodes. The results of the

difference between the mean and the recorded value was then averaged for each of the 200 time intervals. The plot of the outcomes is shown in Figure 4.3. This shows a slight increase in the signal strength which is within 1 dB and can be considered negligible.

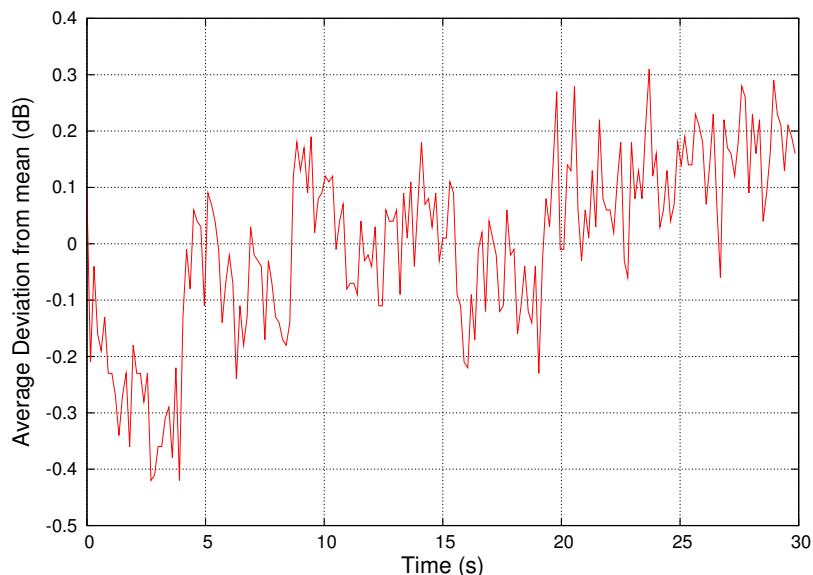


Figure 4.3: *RSSI deviation from the mean versus time, measured over a period of 30 seconds, starting from nodes being off. After 30 seconds, the change in RSSI was found to be negligible.*

The results of the signal measurements between 10584 random node pairs in the 7x7 grid is now reported. A histogram of the recorded RSSI values is shown in Figure 4.4. This graph shows a clear Gaussian distribution of data which one would expect from a set of measurements representing signal strength measurements. This confirms the second condition for obtaining the same results if the testbed were scaled up [2], namely that the distribution of signal strength values around the mean is independent of distance.

The same set of measurements is now used to compare measured versus predicted free space loss signal strength versus distance in Figure 4.5. The discrete distances that are apparent for the measured signal are due to the finite number of possible distances in a 7x7 grid for all possible links between each node.

There is a general trend for the measured signal strength to become weaker than the predicted free space loss signal strength as the distance increases. This is most likely due to the effect of Fresnel zone interference discussed in Section 4.2.1.4. The large 10dB standard deviation for measurements made with the same distance is due to multipath fading and other issues that have been raised in Section 4.2 such as antenna coupling. Overall the result shows a decay pattern which matches the predicted free space loss decay fairly well. This confirms the first condition for obtaining the same results if the testbed were scaled up [2], namely that there is a linear relationship between mean power and log-distance.

Exponents of the log shadowing model will be very specific to the room conditions and won't be easy to duplicate unless microwave absorbing materials are placed on the walls to create an anechoic

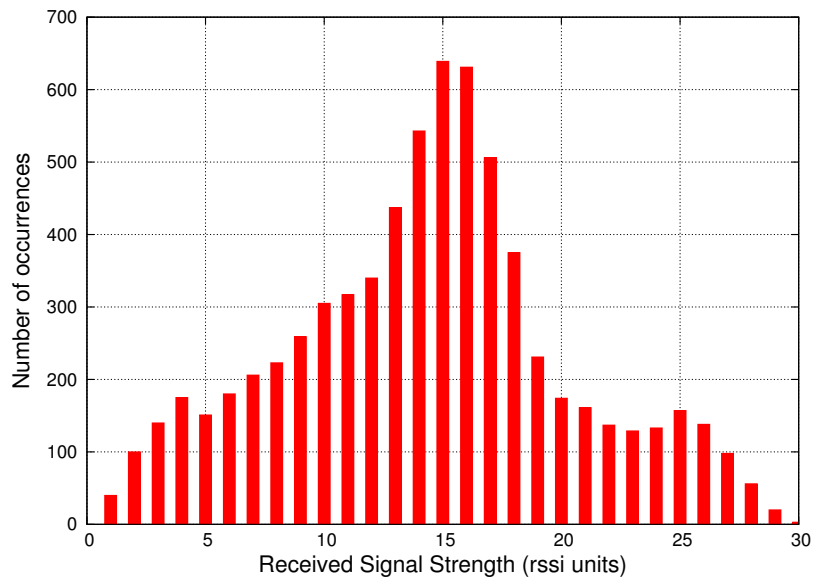


Figure 4.4: RSSI distribution based on 10584 recordings of signal strength from random node pairs on the 7x7 testbed.

chamber.

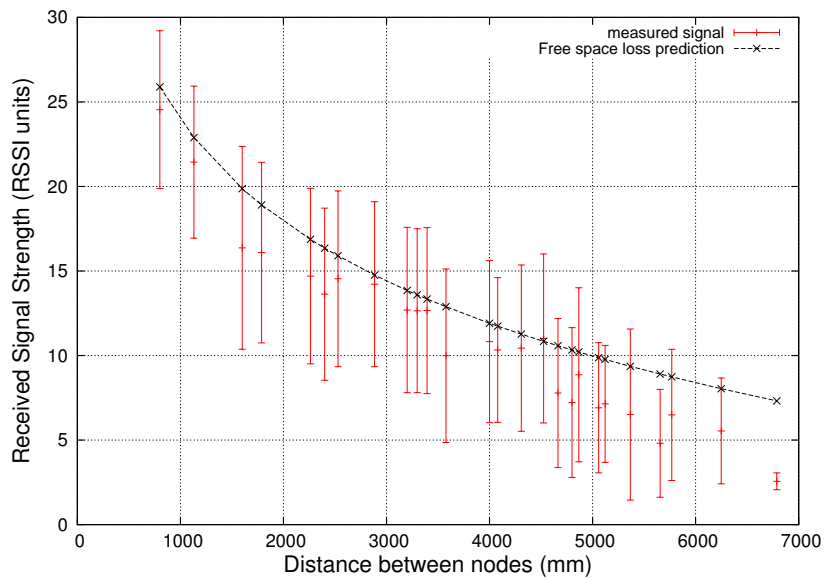


Figure 4.5: Comparison between measured and predicted free-space loss for received signal strength.

4.3 CREATING A MULTI-HOP BASE LINE

In order to establish the baseline for performance of the wireless nodes in the grid, it is useful to remove any effects of routing and establish the best possible multi-hop throughput and delay between the nodes. Figure 4.6 shows a string of pearls 49 nodes long built by creating a zigzag topology in the grid, using manually configured static routes.

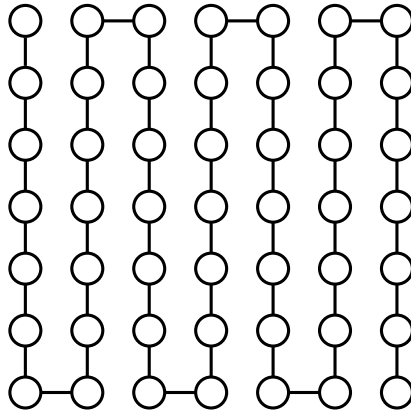


Figure 4.6: Creation of a string of pearls topology 49 nodes long using the 7x7 grid.

All the radios were set to their maximum power (20 dBm), using 802.11b mode with a data rate of 11 Mbps to avoid any packet loss. Throughput degradation due to hop count in packet-based networks with single radios has been well studied by Gupta *et al.* [36]. The theoretical best case and worst case throughput in an asymptotic sense is given by Equations 4.8 and 4.9.

$$\lambda_{WORST}(n) = \frac{W}{\sqrt{n \log(n)}} \quad (4.8)$$

$$\lambda_{BEST}(n) = \frac{W}{\sqrt{n}} \quad (4.9)$$

where W = Bandwidth of first hop and n = number of hops.

These equations do not take into account effects of the 802.11 MAC layer protocol or signal propagation and, as such, present an idealistic case only valid in an asymptotic sense. A recent study [42] by Gupta and Kumar using laptops equipped with 802.11 based radios placed in offices revealed, using a least-squares fit, that the actual data rate versus the number of hops is given by Equation 4.9.

$$\lambda_{LMS-GUPTA}(n) = \frac{W}{n^{1.68}} \quad (4.10)$$

This represents a dramatic difference in throughput after a multiple number of hops for 802.11 compared to the theoretical predictions. After 10 hops the measured results were as little as 10% of the theoretical worst-case prediction.

Throughput and delay measurements were now carried out on the 7x7 grid using the mechanisms highlighted in Section 3.4.

Figure 4.7 shows the results of these multi-hop throughput measurements and compares them

to theoretical and previously measured results. The measurements revealed a less pessimistic result but one which was still less than the worst-case theoretical predictions. The asymptotic validity of Gupta's theoretical predictions is clearly shown for small hop counts where after 2 hops, the worst case prediction is actually higher than the best case prediction.

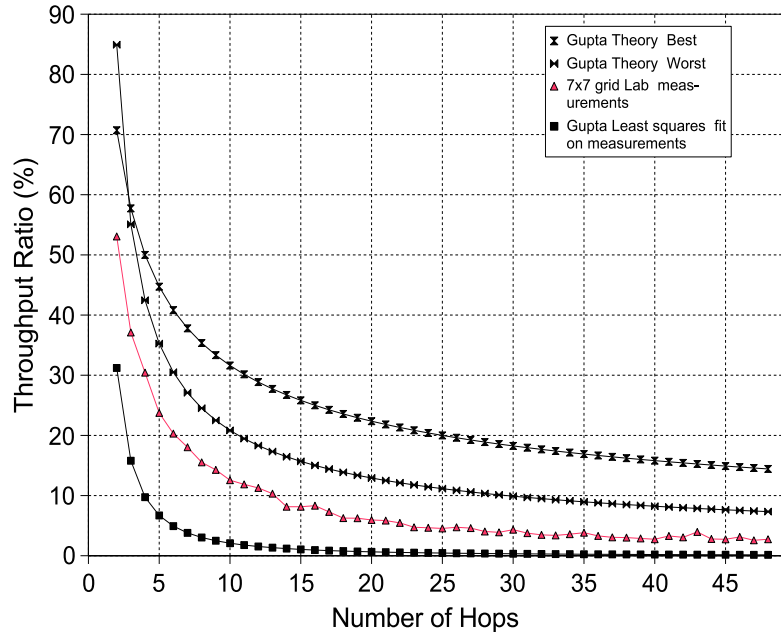


Figure 4.7: Comparison of 7x7 grid multi hop throughput to theoretical and other measured results.

Figure 4.8 shows a least squares fit on the log of both the x and y axes for throughput results obtained with the testbed. This reveals the following function for TCP throughput under ideal conditions for the grid:

$$\lambda_{LMS-GRID}(n) = \frac{W}{n^{0.98}} \quad (4.11)$$

The delay between node pairs with increasing number of hops between them is shown in Figure 4.9. The unloaded network delay follows a simple linear progression with increasing standard deviation due to a larger collection of nodes with non-uniform NICs involved in the link.

4.4 ROUTE COMPLEXITY

The higher the degree of connectivity between nodes in the grid, the more complex the routing decision becomes for an ad hoc routing algorithm. The number of edges leaving or entering a vertex gives a good indication of the complexity within a graph. If the signal strength is higher, the degree of connectivity within the grid will increase. Although this will potentially decrease the hop count

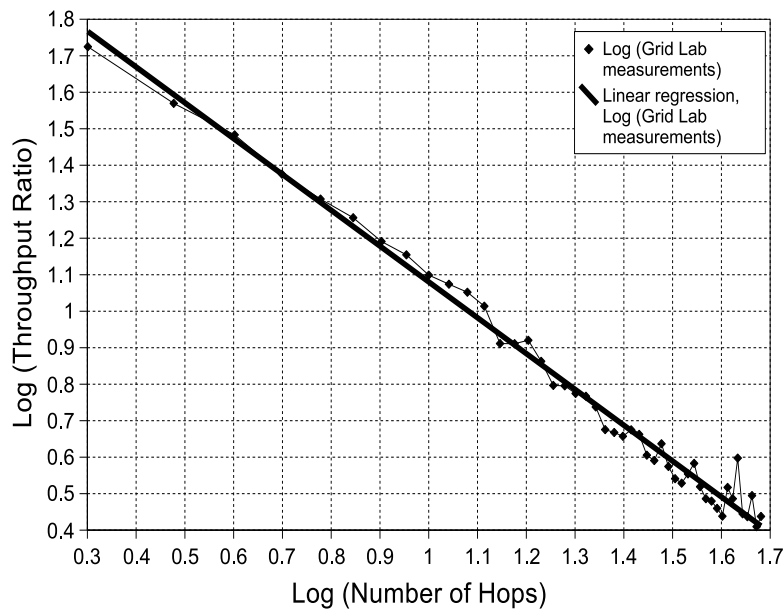


Figure 4.8: *Linear regression of log of the throughput vs the log of the hop count for a 49-node-long chain in the 7x7 grid.*

across the grid, it has many other negative outcomes. Firstly it increases the convergence time of the routing protocol, secondly it causes more interference amongst nodes in the grid and thirdly it has the potential to cause more route flapping between pairs of communicating nodes with certain routing protocols [43].

To illustrate this, Figure 4.10 shows all the possible connections between nodes for a 7x7 grid if the signal radius is greater than or equal to $\sqrt{2}$ and less than 2 in a unit-spaced grid where a path is sought from A1 to G7. Some boundary conditions were set which specify that a directed edge to a vertex can only be created if the vertex is closer to the destination than the previous vertex.

An algorithm which is illustrated in Appendix A was developed to calculate all possible routes through the grid. The total number of routes possible in this graph is 170277 and the number of paths through the grid with equivalent hop count is shown in Table 4.2

Table 4.2: *Distribution of equivalent hop counts in the 7x7 grid with a radius greater than or equal to $\sqrt{2}$ and less than 2 in a unit-spaced grid.*

Hops	1-5	6	7	8	9	10	11	12	13	14	15	16	17
Routes	0	1	42	490	2814	9722	22320	35742	40746	32892	18176	6276	1056

To understand how the complexity of the grid changes as the coverage radius increases, the number of equivalent hop routes is plotted in Figure 4.11 up to a total of 4 hops for a radius increasing from unit length up to the length of a diagonal between the furthest two points on the grid which is $6\sqrt{2}$. The depth of the search was limited to 5 hops due to the search space being too large for even

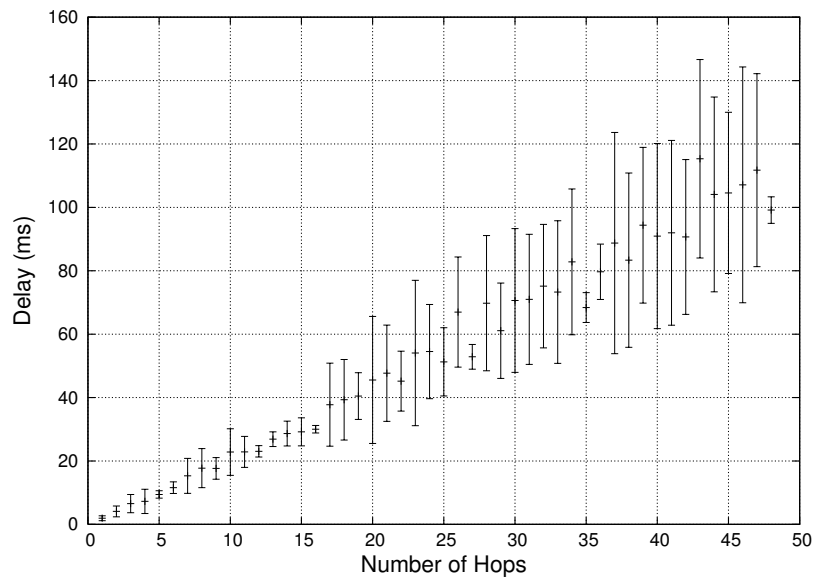


Figure 4.9: *Delay versus hop count for a 49-node-long chain in the 7x7 grid.*

a days computation time. For clarity, the smallest hop count category, which is 2 hops, is shown as the radius increases in Figure 4.12. All these graphs follow a sigmoid curve with increasing signal radius.

The larger the number of equivalent hop routes in a network, the harder it is for a hop-count-based routing algorithm to settle on optimum routes. If some damping isn't employed the algorithm will tend to flap between routes. A special case in point is where the radius is greater than or equal to 1 and less than $\sqrt{2}$ where there is only one hop count category of 12 hops with a total of 924 possible routes. This is the worst case scenario in terms of the number of shortest path routes to the destination.

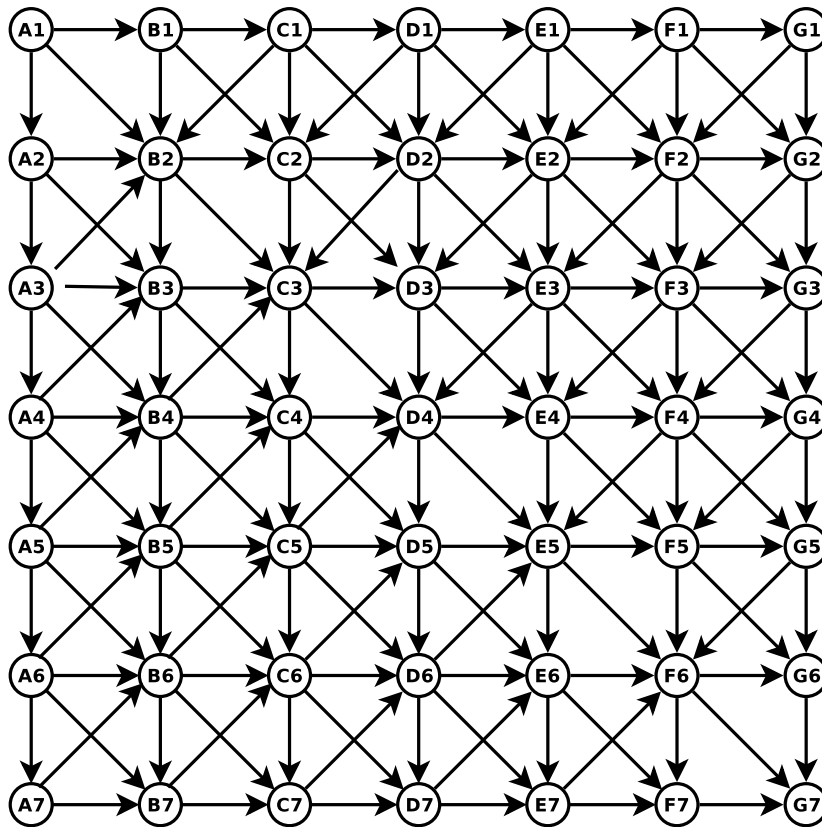


Figure 4.10: All possible connections between nodes if signal radius is greater than or equal to $\sqrt{2}$ and less than 2 in a unit-spaced grid and all vertices in a path decrease the distance to the destination.

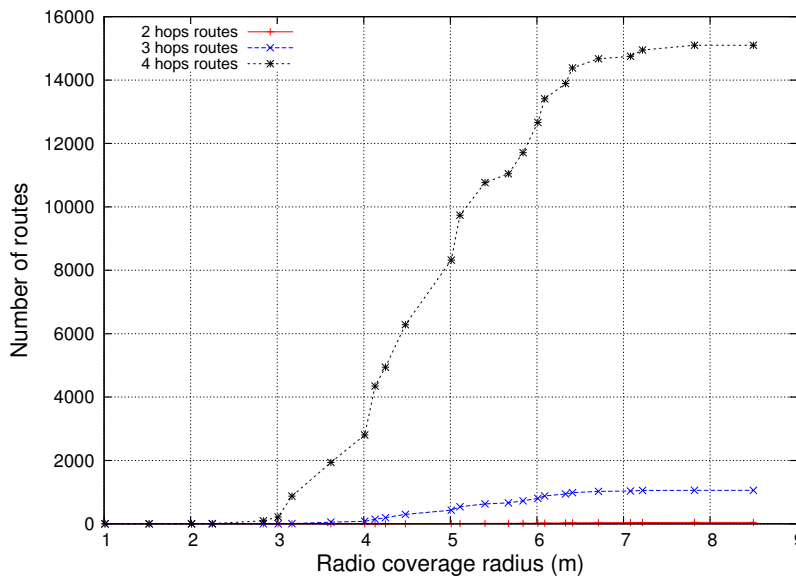


Figure 4.11: Number of equivalent hop routes through a 7x7 unit-spaced grid for a radius range of 1 to $6\sqrt{2}$.

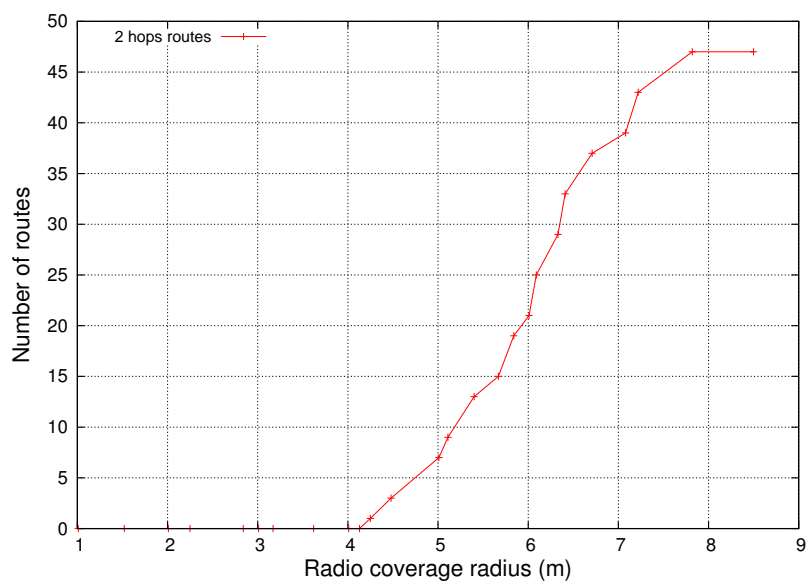


Figure 4.12: Number of 2-hop routes through a 7x7 unit-spaced grid for a radius range of 1 to $6\sqrt{2}$.

CHAPTER FIVE

PERFORMANCE ANALYSIS

Performance is your reality. Forget everything else.

Harold Genee

5.1 INTRODUCTION

Performance analysis of the indoor testbed itself as well as various MANET routing protocols in the testbed is now carried out. A number of characteristics of each routing protocol were tested; these are : (a) hop count distribution, (b) routing traffic overhead, (c) throughput, (d) packet loss, (e) route flapping and (f) delay. These are well established performance measures to understand how a routing protocol optimizes routing paths through a network. The following settings were used in the testbed for all the following measurements:

- Channel = 6
- Mode = 802.11b
- Data rate = 11 Mbps
- TX power = 0 dBm

5.2 HOP COUNT DISTRIBUTION

The ability to create a multi-hop network in the mesh testbed is a key measure of the ability of the lab to emulate a real world wireless mesh network. From signal strength measurements in Section

4.2.2.2 it was clear that the range of the signal can be limited to just under a metre. This section will now verify this from the perspective of the routing protocol creating a multi-hop topology.

Before a comparative study of hop count is carried out between the chosen set of routing protocols, an initial test with OLSR was carried out using ETX as a routing metric. This routing protocol and metric was chosen as it has a built in “graphical topology representation” feature, which makes it easy to visually inspect how effectively the lab creates a multi-hop environment. In addition to this, OLSR is a well established routing protocol for static wireless mesh networks.

In order to evaluate how the multi-hop environment evolves as the network grows, a growing spiral topology, as described in Section 3.4, was used. A node was added to the spiral every 10 seconds and the wireless NICs were configured to 802.11b mode, 11 Mbps data rate and a power level of 0 dBm. Figure 5.1 shows the total number of routes in specific hop categories versus a growing number of nodes in the grid. Up to 5 hop links were achieved with 2 hop links forming the dominant category after 16 nodes. This shows that a good spread of multi-hop links has been achieved in the grid.

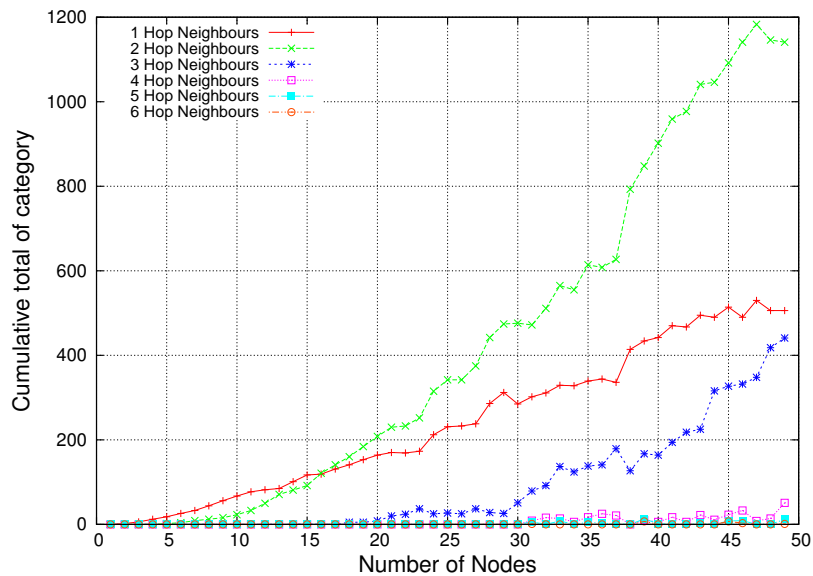


Figure 5.1: Total number of routes in specific hop categories versus a growing number of nodes in the grid.

Once all 49 nodes were added to the network, a topology depicted in Figure 5.2 was created. The values in the graph are the ETX values for each node pair within radio range of each other. It is clear from this diagram that there is a lack of uniformity in links formed between equivalent distance node pairs. This is due to the variation in electromagnetic properties that were highlighted in Section 4.2.

Now that it has been established that a multi-hop environment is possible, a comparison between AODV, DYMO, OLSR-RFC and OLSR-ETX was carried out. To start with, a very simple string of 3 nodes was configured and all 4 routing protocols were run on this topology. This helped to reveal the routing strategy taken by each of these protocols and whether these were optimal or not by showing the delay and throughput characteristics. From the results shown in Figure 5.3 one can quickly see that AODV’s “minimizing hop count” strategy resulted in very poor throughput whereas OLSR’s

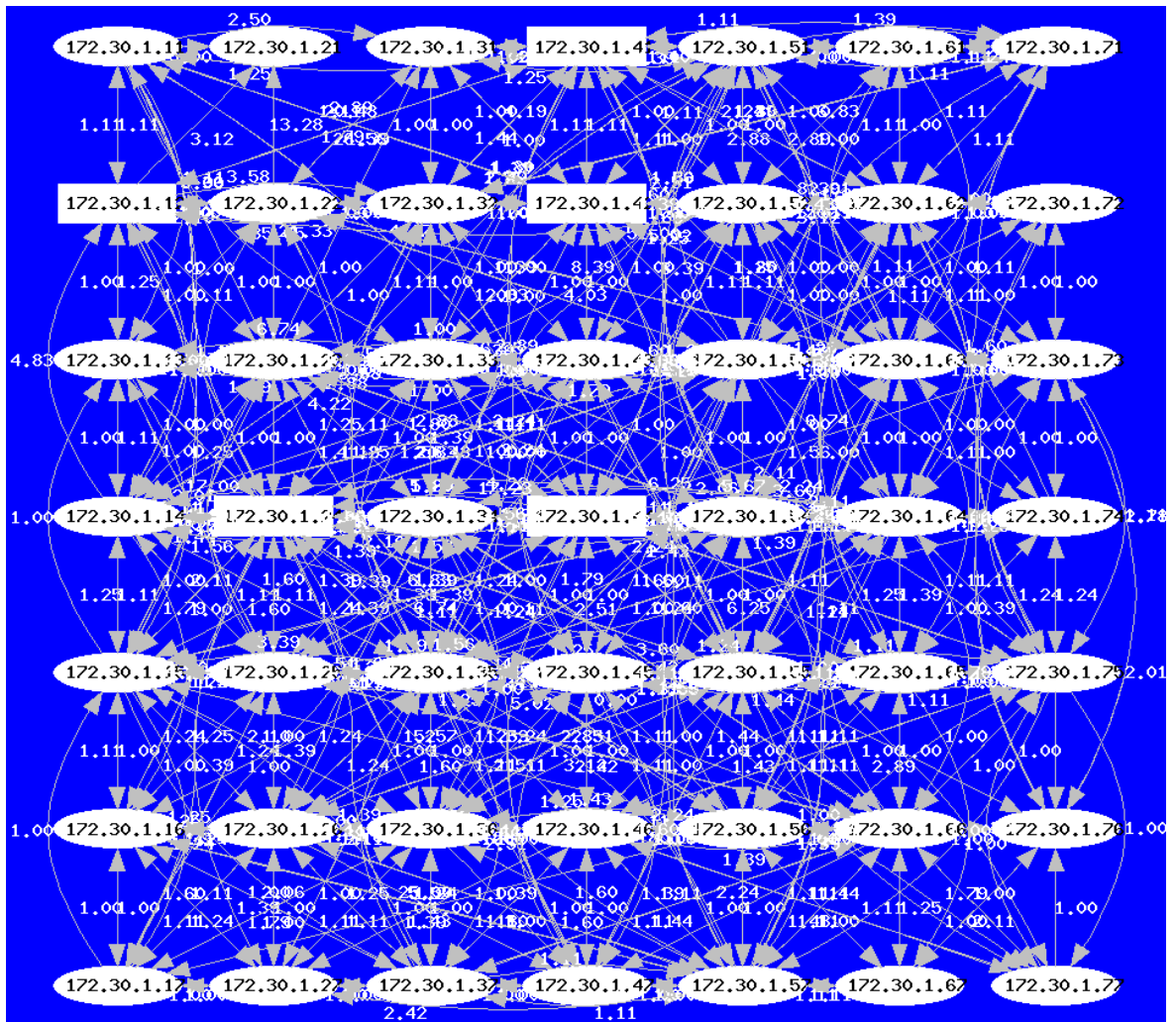


Figure 5.2: OLSR topology using the ETX metric showing good multi-hop characteristics. The wireless NICs were configured to 802.11b mode, 11 Mbps data rate and power level set to 0 dBm.

“minimizing packet loss” strategy resulted in the best throughput even with a higher hop count. It is also clear that OLSR supports asymmetrical links.

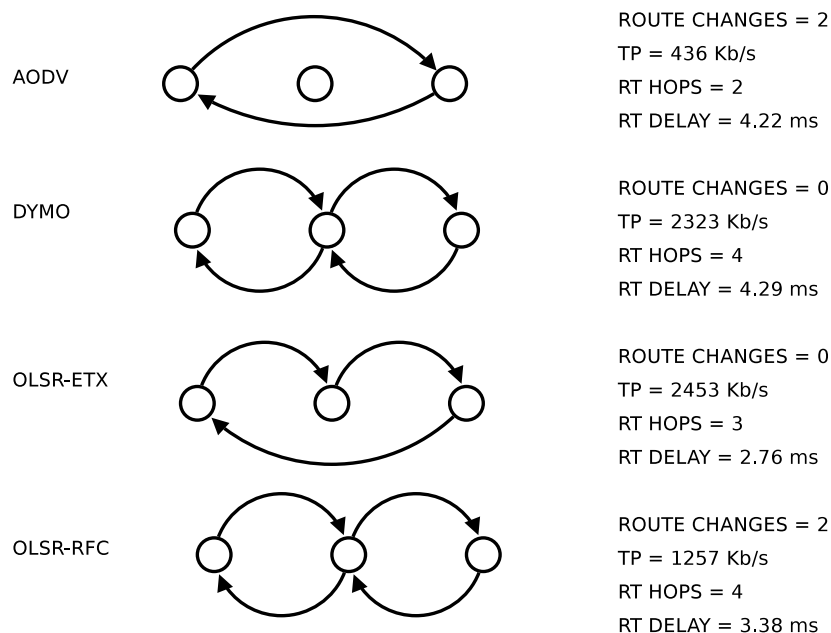


Figure 5.3: Topology created by each MANET routing protocol for a simple string of pearls 3 nodes long.

Finally Figure 5.4 shows a comparison of all 4 routing protocols in terms of average hop count versus distance. This experiment used the full 7x7 grid with hop tests between every possible pair of nodes in the grid. The set of all possible pairs is equal to 2352 (49x48).

It is clear from this graph that AODV is again trying to minimize hop count. OLSR-RFC tends to use more hops as links with long distances between them tend to be penalized by its steep downward hysteresis curve when packets are dropped (see Section 2.4.3). DYMO picks the first possible route it can obtain and doesn't try to continuously optimize for shorter hop links. OLSR-ETX has decided that shorter hops than those used by OLSR-RFC are better in terms of minimizing packet loss.

5.3 ROUTING TRAFFIC OVERHEAD

The ability of a routing protocol to scale to large networks is highly dependent on its ability to control routing traffic overhead. Routing traffic contains messages that a routing protocol needs to establish new routes through a network, maintain routes or repair broken routes. These can be simple HELLO messages, which are sent periodically to allow neighbouring nodes to learn about the presence of

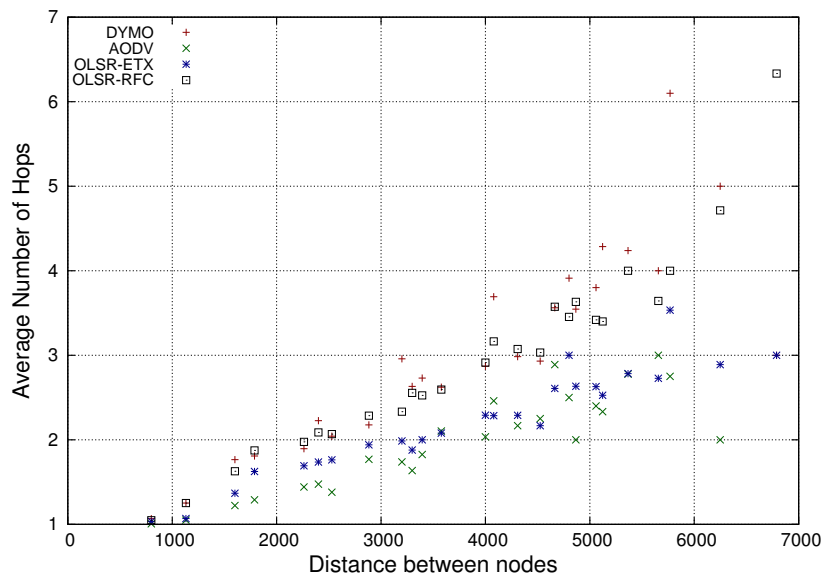


Figure 5.4: Average number of hops versus distance for full 7x7 grid between all 2352 possible pairs.

fellow nodes, or they can be topology messages containing routing tables.

The amount of inbound and outbound routing traffic as well as the packet size of routing packets was measured as the network size grows in a spiral fashion. The measurement process was described in Section 3.4. Once this data was collected for each node in the network, the traffic was averaged across all the nodes in the network and normalized to the amount of traffic per second.

Figure 5.5 shows the inbound traffic for all 4 routing protocols and Figure 5.6 shows the outbound traffic. As expected, OLSR, being a proactive routing protocol, showed the highest degree of routing overhead. OLSR traffic rapidly increases but then begins to level off after about 25 nodes due to the Multipoint Relays (MPRs) limiting router traffic forwarding. OLSR-ETX had slightly more routing traffic than OLSR-RFC as it made use of less hops, as shown in the previous Section 5.2. When a routing protocol has less hops, the coverage of a single node's routing broadcast traffic is wider and adjacent nodes will be receiving and forwarding more routing traffic.

AODV showed the highest degree of routing overhead, in terms of number of routing packets, for small networks under 14 nodes but quickly levelled off with OLSR overtaking AODV for larger networks above 14 nodes. This AODV traffic is a combination of route discovery and route maintenance over the 20-second period. The levelling off could be seen as artificial as a route was only discovered between the two furthest points in the network as the spiral grew. This meant that some nodes on the periphery of this link might not have been involved in the route establishment due to their hop distance from nodes involved in the route discovery. However, the comparison still holds if comparing routing traffic to establish a single link between two nodes in a network. Clearly a reactive protocol like OLSR will have the advantage that the routing traffic, although higher, enables it to establish a link between any pair of nodes in the network.

DYMO shows the least amount of routing traffic due to its lack of HELLO packets. This is also

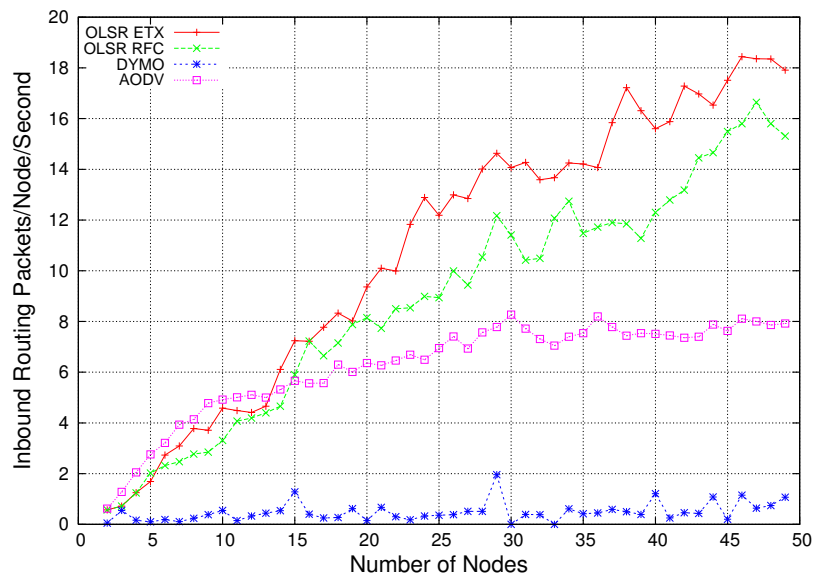


Figure 5.5: *Inbound routing packets per node per second versus increasing number of nodes using a growing spiral.*

due to no further routing packets being transmitted once it has found a route to a destination. The occasional spikes in the routing traffic are for cases where it took longer to establish a route due to possible poor link quality between the nodes involved.

Figure 5.6 shows that the outbound traffic is less than the inbound traffic as the routing algorithm makes a decision to rebroadcast the packet or not. Each protocol has its own mechanism to control the rebroadcasting of routing traffic, OLSR makes use of MPRs and AODV, for example, makes use of destination sequence numbers to check if the routing information is new.

Figure 5.7 shows how routing packet lengths grow as the number of nodes increase. This is another important characteristic to analyze if a routing protocol is to scale to large networks. As the network grows, OLSR needs to send the entire route topology in Topology Control (TC) update messages, which helps explain this steady linear increase with the number of nodes. OLSR with the ETX extension uses a longer packet length due to the extra overhead of carrying link quality metrics.

AODV does not carry any route topology information in its packets, which explains its extremely small packet length which stays constant. DYMO makes use of path accumulation which explains its steady increase in size relative to the number of hops between the two furthest points on the network.

True routing overhead, in terms of the number of bytes/node/second, is calculated by multiplying the routing protocol by the router packet length. Based on this, AODV will have the lowest routing overhead and OLSR-ETX will have the highest.

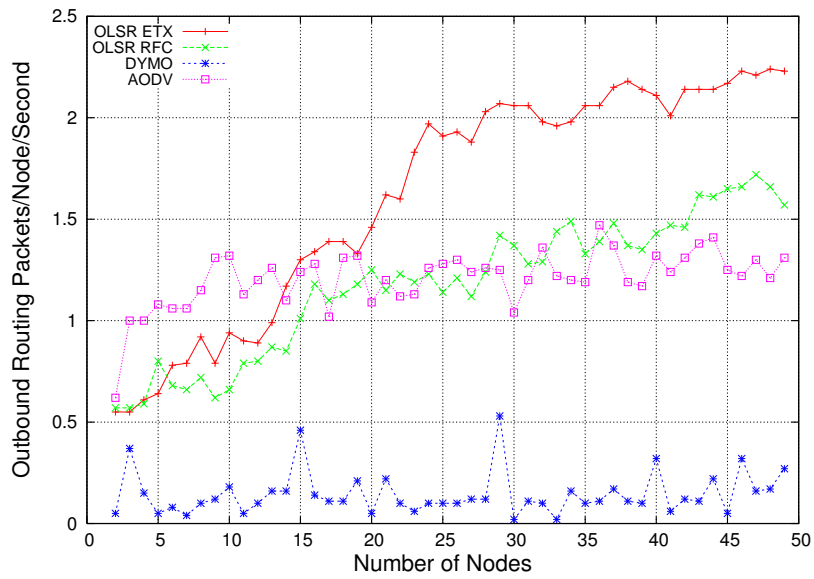


Figure 5.6: Outbound routing packets per node per second versus increasing number of nodes using a growing spiral.

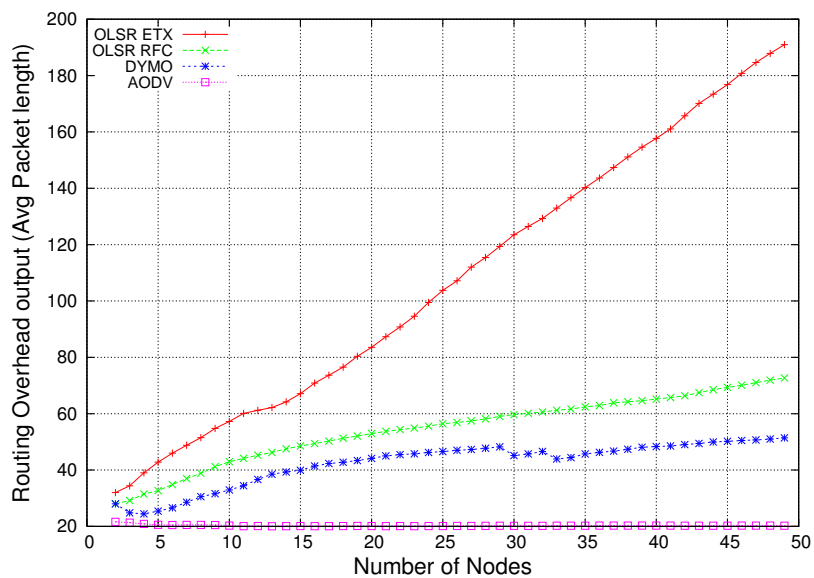


Figure 5.7: Average routing packet length growth versus increasing number of nodes.

5.4 THROUGHPUT, PACKET LOSS, ROUTE FLAPPING AND DELAY MEASUREMENTS

The ability of a routing algorithm to find an optimal route in the grid will be exposed by its throughput, packet loss and delay measurements. Route flapping, which is an established phenomenon in wireless mesh networks [43], can also have an effect on the performance of the network. Throughput, packet loss, route flapping and delay measurements were grouped together in order to check for causal relationships between these measurements, for example one can check if route flapping tends to have an effect on throughput.

In order to evaluate their performance, a series of tests were done with increasing complexity. To start with, a simple case was constructed using a 7-node string of pearls to test routing performance. This was followed by three adjacent 7-node columns of 21 nodes and finally the full 7x7 grid of 49 nodes. Each of these cases will now be presented in turn.

The results will be presented in tables and each of the table headings is now discussed to help understand what each of these mean. The detail of the measurement process can be found in Section 3.4.

1. **Forward hop count** is the number of hops taken to a destination in one direction only and a different number of hops may be used on the return path in cases where the routing protocol supports asymmetrical links. This is measured with the ping tool over a period of 10 seconds with the last established forward hop count being reported.
2. **Route changes** depicts the average number of route changes for all the node pairs that were measured, for example, if one pair had 0 route changes and another pair had one route change, the average number of route changes would be 0.5. This is measured with the ping tool over a period of 10 seconds.
3. **Packet loss** describes the average number of packets that were lost for all node pairs during the measurement period. This is reported by the ping tool and was measured over a period of 10 seconds.
4. **Delay** describes the average round trip time taken by an 84-byte ICMP packet for all node pairs tested using the ping tool over a period of 10 seconds.
5. **Throughput** describes the average TCP best effort throughput in an unloaded network between all node pairs over a period of 10 seconds using the Iperf tool. If a link cannot be established, the throughput is 0 and this is still included in the average calculation.
6. **No link** describes the percentage of links out of the total number of possible node pairs that couldn't be established when using the ping tool.

5.4.1 RESULTS FOR A STRING OF PEARLS 7 NODES LONG

This is the simplest multi-hop environment that can be created. Complexity is kept to a minimum and very few multiple equivalent routes are possible. Table 5.1 summarizes the results for all 42 possible pairs in a 7-node string of pearls topology.

Table 5.1: *Comparison of throughput, delay and packet loss for a 7-node string of pearls topology.*

	Forward hop count	Route changes	Packet loss (%)	Delay (ms)	Throughput (kbps)	No link (%)
AODV	1.33	0.43	11.19	37.24	2723.36	2.4
DYMO	1.52	0	9.52	3.65	2907.67	0
OLSR-ETX	1.43	0.1	8.57	27.56	2730.69	0
OLSR-RFC	1.67	0.76	2.14	5.35	2923.64	0

OLSR-RFC had the highest number of route changes and forward hops over the 10-second measurement period but had the best average throughput and the least amount of packet loss. The route changes were therefore constructive and converged the link towards a more optimal route. DYMO achieved the best performance in terms of delay. Only AODV had 1 case where the routing algorithm could not establish a link.

In order to understand the distribution of throughput for all the 42 pairs in the network, a cumulative distribution function is shown in Figure 5.8. The graphs are very similar except for the fact that AODV and OLSR-ETX have approximately 20% of their links unable to achieve any throughput in the 10 seconds that they were tested. There are also clearly noticeable discrete clusters of throughput categories around approximately 2100 kbps and 4200 kbps, which is due to discrete average achievable throughput at 1 and 2 hops respectively.

Overall there is not a large amount of noticeable difference between these routing protocols for small networks like this. From these results and others that are shown later, it is clear that although a ping packet may be possible between a node pair, this does not guarantee any usable throughput when testing a link. Throughput tests are far more taxing on link due to their higher buffer sizes (8k in this case) and during the 10-second throughput test with the IPerf tool, if the first large packet that is sent is not acknowledged, the throughput is recorded as 0.

More detailed graphs of performance are only shown for the next two sections where the grid complexity increases and the difference between the routing protocols becomes more marked.

5.4.2 RESULTS FOR 3X7 GRID (21 NODES)

The complexity is now increased somewhat and the routing algorithms can begin to choose between many alternative routes due a band of adjacent nodes on the line between the node pair being tested. Table 5.2 highlights the results for all 420 possible pairs.

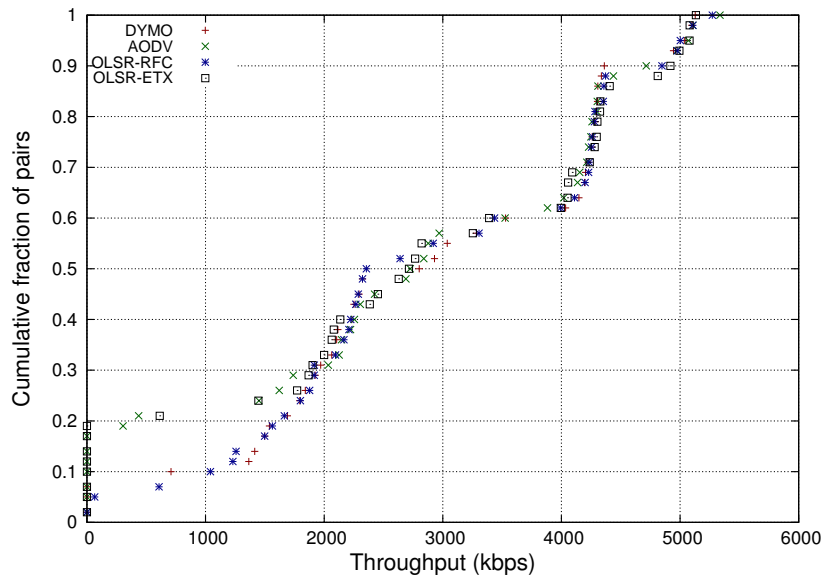


Figure 5.8: Throughput CDF for 7-node string of pearls.

Table 5.2: Comparison of throughput, delay and packet loss for 3x7 grid.

	Forward hop count	Route changes	Packet loss (%)	Delay (ms)	Throughput (kbps)	No link (%)
AODV	0.97	0.46	43.62	148.17	1245.23	30.0
DYMO	1.54	0.09	26.88	58.41	1701.69	13.3
OLSR-ETX	1.28	0.08	24.05	38.92	2899.34	16.2
OLSR-RFC	1.9	1.66	8.76	34.57	2113.12	4.7

AODV was clearly the worst performer in terms of number of failed links, average throughput and average delay. OLSR with ETX achieved the best average throughput with the lowest number of route changes, whereas OLSR-RFC achieved the best delay, lowest packet loss and least number of unsuccessful links with a relatively high number of route changes (1.66 changes in the 10-second test period).

Figure 5.9 shows a full set of performance metrics for the 21-node network as the distance between the nodes increase. There is a clear difference between the number of good readings for ping tests and the number of good readings for TCP throughput tests, As described before, throughput tests are far more taxing on a link due to their higher buffer sizes which can lead to timeouts due to the TCP window size become very large in poor links. OLSR-RFC showed the most resilience to distance in terms of maintaining a high percentage of good links.

Average throughput was remarkably similar amongst the various protocols as the distance increased, which is clearly deceptive judging by the actual averages, this means that there is an unbalanced distribution of data points at each of the distance classes. Average packet loss appears to increase fairly linearly with a wide amount of scatter as distance increases, but again AODV shows

the weakest performance here, with packet loss increasing very rapidly with distance, OLSR-RFC showed the lowest packet loss as distance increased.

A very clear relationship between route changes and distance is seen for the OLSR-RFC protocol, which increases fairly linearly and begins to level off after about 4 m. Route changes in DYMO and OLSR-ETX were almost impervious to distance. Delay increases linearly at a steady rate for all protocols other than AODV which shows a very rapid delay increase. Its average hop count is the lowest of all the routing protocols, which should normally lead to a low delay but as it has chosen very poor longer range links this has instead made its delay the highest among all the other protocols.

The cumulative distribution function shows that AODV had a 50% link failure rate when carrying out throughput tests. OLSR-RFC had the lowest link failure but most of the throughput was clustered in the lower (<2100 kbps) range, probably due to non-optimal high hop count. OLSR-ETX had a strong clustering pattern in the upper (>4000 kbps) region and DYMO had the highest peak in the 2100 kbps range due to its low hop count.

5.4.3 RESULTS FOR FULL 7X7 GRID (49 NODES)

Maximum network complexity is now used by activating nodes in the entire 7x7 grid. Table 5.3 highlights the results for all 2352 possible pairs.

Table 5.3: Comparison of throughput, delay and packet loss for full 7x7 grid.

	Forward hop count	Route changes	Packet loss (%)	Delay (ms)	Throughput (kbps)	No link (%)
AODV	1.36	0.53	71.22	117.87	773.33	60.6
DYMO	2.2	0.11	32.81	64.72	1165.66	17.6
OLSR-ETX	1.84	0.25	24.05	68.84	1187.57	19.2
OLSR-RFC	2.28	2.34	22.22	67.44	1330.05	16.2

AODV was clearly the weakest protocol in this scenario, with more than half the links achieving no route at all. All the other protocols performance metrics were very close. On the whole OLSR-RFC was marginally better than the rest, achieving the top average throughput rate of 1330 kbps.

Figure 5.10 shows a full set of performance metrics for the 49-node network as the distance between the nodes increases. The drop-off in percentage of good links is now even more marked than the case for 21 nodes. AODV falls off even more dramatically than the previous case reaching almost 0% good links after 4 m.

All the other graphs show very similar characteristics to the 21-node case other than the cumulative distribution graph. The CDF shows a far flatter throughput performance compared to the previous case but DYMO, OLSR-RFC and OLSR-ETX now exhibit very similar throughput distribution, all having about 40% link failure for throughput tests. AODV had close to 80% of its links unable to achieve any throughput.

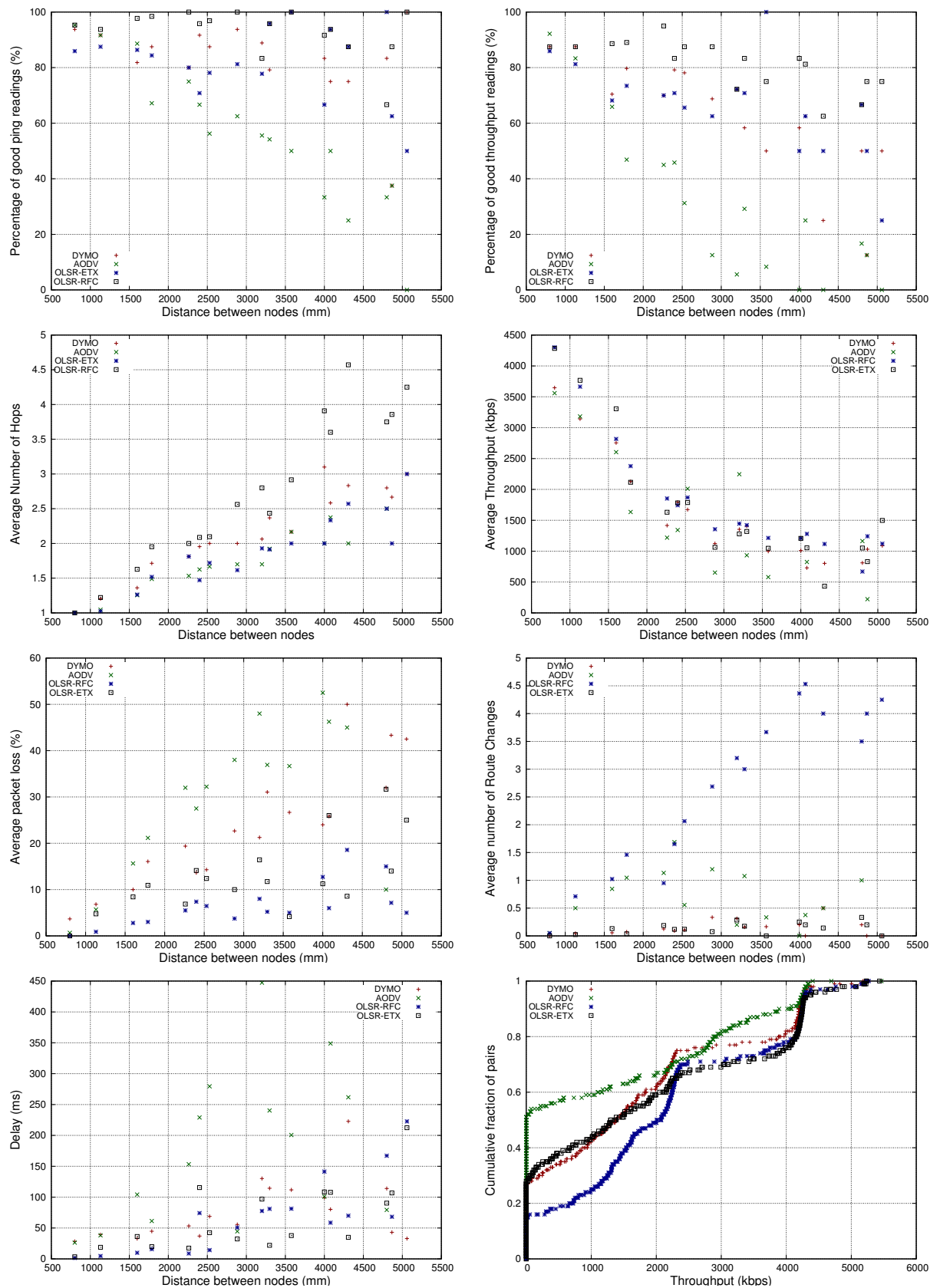


Figure 5.9: Performance metrics for routing protocols running in a 3x7 grid (see Appendix C for larger versions of these diagrams).

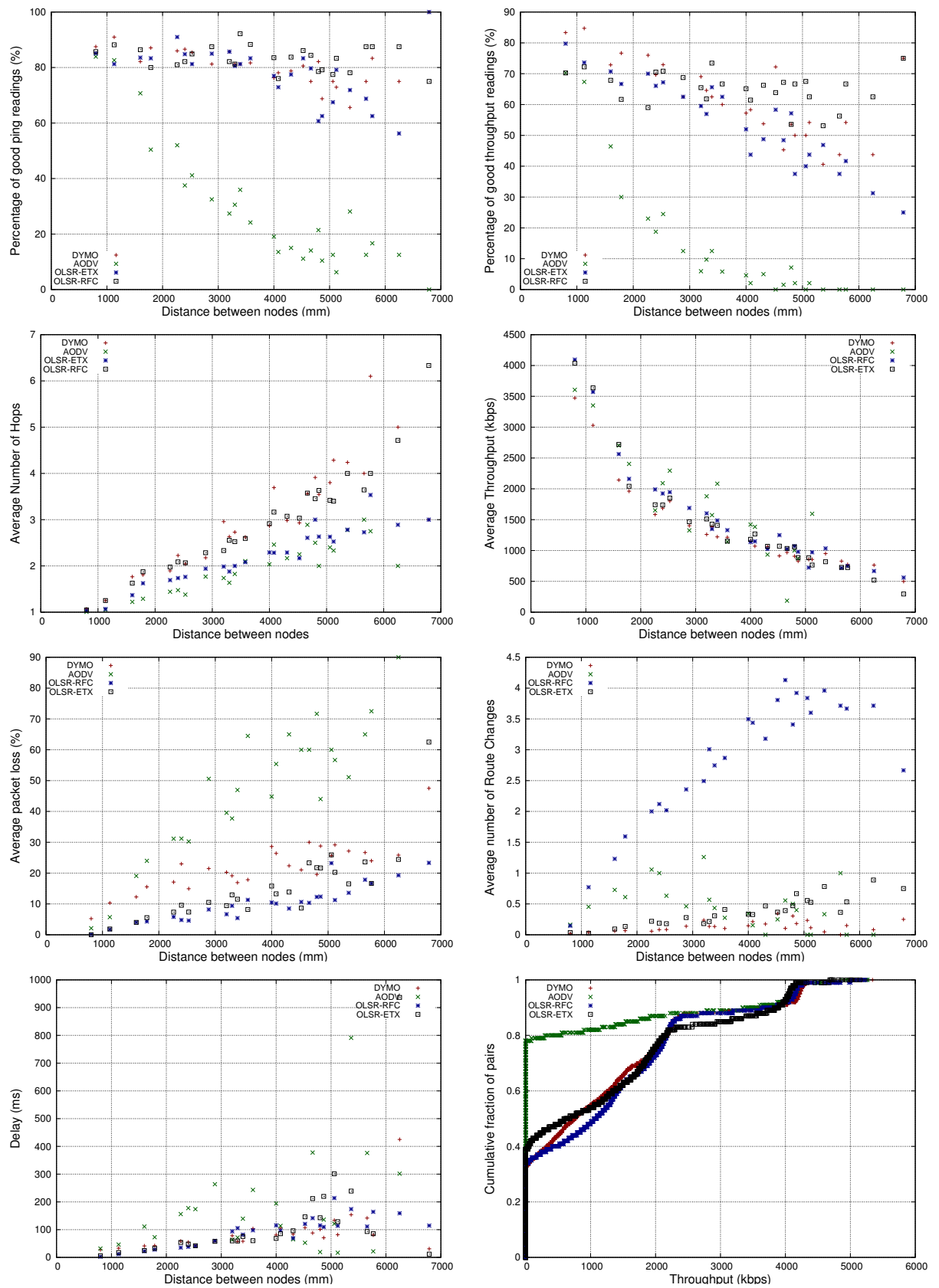


Figure 5.10: Performance metrics for routing protocols running in a 7x7 grid (see Appendix D for larger versions of these diagrams).

These results demonstrate how network performance quickly degrades for all routing protocols as the network size and complexity increases. AODV showed the most dramatic degradation as the number nodes and node density increased. As can be expected, as the network size increased and more possible routes were available in the grid and the amount of route flapping also increased which had a negative impact on throughput and packet loss except in the case of OLSR-RFC. OLSR-RFC using its hysteresis routing metric appeared to perform the best overall, especially as the network size increased. This was also experienced by Huhtonen [34], who observed that increasing node density favoured OLSR over AODV.

The ETX routing metric [16] was developed to improve the performance of routing in static wireless mesh networks where hop count was not suitable. However, OLSR-ETX appeared to perform worse than OLSR-RFC overall but this could be because hysteresis is better at quickly converging on more optimal routes in a highly dense mesh like this indoor wireless grid as its condition for considering a link established is stricter than the condition for dropping a link.

5.5 COMPARISON OF THROUGHPUT RESULTS AGAINST BASELINE

Finally Figure 5.11 shows the routing protocol's performance compared to the ideal multi-hop network that was set up in Section 4.3. AODV could not be compared due to 80% of the links failing to achieve any throughput.

The baseline presents the best possible throughput the routing protocols could achieve in the indoor wireless grid. OLSR-RFC reaches the baseline for the first 3 hops and then begins to drop off the target after 4 hops. DYMO comes 2nd at achieving the best throughput up to 3 hops with OLSR-ETX very close behind and overtaking DYMO after 4 hops. Gupta's indoor measurements are about 12% lower than any of the other protocols on this graph. This demonstrates that the conditions in the lab are far better than making use of offices to create a wireless testbed and relying on office walls to attenuate the signal.

5.6 A CHALLENGE TO THE ETX METRIC

The performance analysis that carried out so far has revealed that the ETX metric used with OLSR does not perform as well as using the standard hysteresis routing metric. This section will now revisit the ETX metric in real networks and calculate whether it accurately predicts whether a specific multi-hop path is optimal.

Consider a simple network shown in Figure 5.12.

ETX values were calculated based on Equations 5.1 and 5.2

$$ETX = \frac{1}{LQ \times NLQ} \quad (5.1)$$

$$ETX'_{AD} = ETX_{AB} + ETX_{BC} + ETX_{CD} \quad (5.2)$$

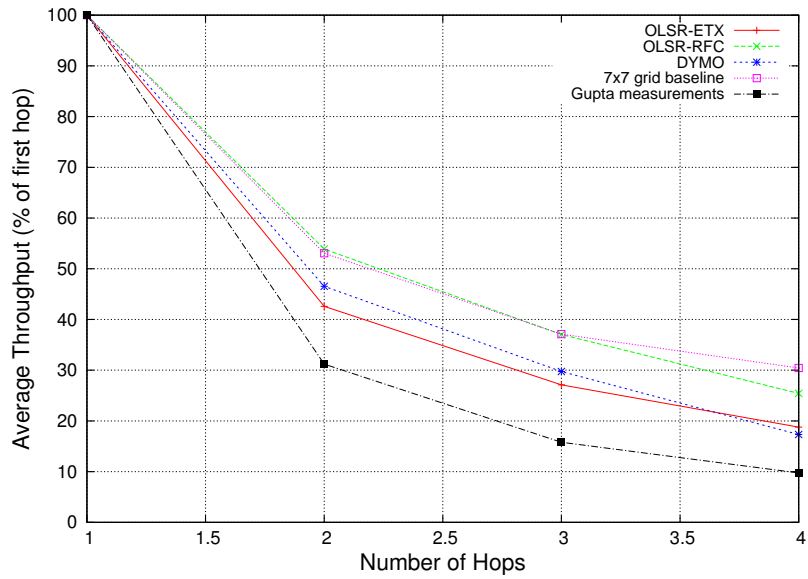


Figure 5.11: Comparison of routing protocol throughput to baseline.

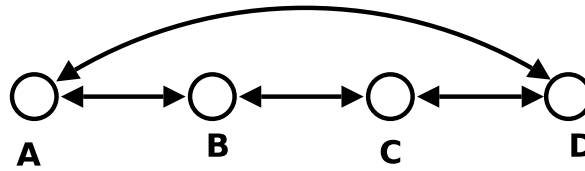


Figure 5.12: Simple 4-node string of pearls topology with 1 hop and 3 hop routes.

Two routes are possible in this graph between A and D; a single hop route denoted by ETX_{AD} and a 3-hop route denoted by ETX'_{AD} .

If the links were all perfectly symmetrical links with no packet losses then the following ETX values would be predicted for all the single-hop paths from A to D shown in Equations 5.3 to 5.6. The multi-hop ETX value for the path from A to D is shown in Equation 5.7.

$$ETX_{AB} = 1 \quad (5.3)$$

$$ETX_{BC} = 1 \quad (5.4)$$

$$ETX_{CD} = 1 \quad (5.5)$$

$$ETX_{AD} = 1 \quad (5.6)$$

$$ETX'_{AD} = 3 \quad (5.7)$$

Since ETX is a prediction of the average number of packet transmissions required for a successful packet to arrive at its destination and vice versa, the throughput, in one direction, expressed as a fraction of the maximum achievable throughput, if all packets were successful, is the inverse square root of this.

$$\lambda'_{AD} = \frac{1}{\sqrt{ETX'_{AD}}} \quad (5.8)$$

Gupta's best case throughput prediction expressed as a fraction of the throughput of the first hop is given by Equation 5.9.

$$\lambda_{BEST}(n) = \frac{1}{\sqrt{n}} \quad (5.9)$$

For perfectly symmetrical links with no packet loss these equations become equivalent and the prediction for throughput as a fraction of the first hop throughput is given by Equation 5.10.

$$\lambda'_{AD} = \lambda_{BEST}(n) = \frac{1}{\sqrt{3}} = 0.58 \quad (5.10)$$

But a model developed in ideal conditions in the mesh lab reveals a model for throughput given by Equation 5.11:

$$\lambda_{LAB}(n) = \frac{1}{n^{0.98}} \quad (5.11)$$

Throughput expressed as a fraction of the first hop throughput after 3 hops in a live network with no losses is given by Equation 5.12:

$$\lambda_{LAB}(3) = \frac{1}{3^{0.98}} = 0.34 \quad (5.12)$$

This shows that the predicted losses using the ETX algorithm are out by a factor of almost 2 compared to the actual losses that will be experienced, even in ideal lab conditions for 802.11. Analysis of the results for this specific scenario shows that ETX will only calculate the correct routes with the following conditions: The percentage of successful packets for ETX_{AD} is less than 34%, in which case it will correctly choose the multi-hop route, ETX'_{AD} , the percentage of successful packets for ETX_{AD} is greater than 58%, in which case it will correctly choose the single-hop route, ETX_{AD} . Any value between 34% and 58% will result in ETX incorrectly choosing the multi-hop route, ETX'_{AD} .

If ETX was modified to correctly predict optimal routes in all circumstances, it would lead to routes with shorter hops being chosen. This seems counter intuitive, as OLSR with hysteresis performed better with a higher number of hops, but reveals that the optimal hop count search space consists of local maxima and there is not a single clear optimal average hop count.

In the future, a weighted ETX calculation could possibly be used which bases its weights on live network measurements to more accurately predict optimal paths over multi-hop links.

CHAPTER SIX

CASE STUDY OF A RURAL MESH NETWORK PILOT

Nothing is more satisfying than moving from the discovery of new knowledge to using that knowledge to make the world a better place to live in.

6.1 INTRODUCTION

Once it was established that Optimized Link State Routing (OLSR) was a good choice of protocol for static wireless mesh networks, it was then used as the routing protocol of choice for building a rural wireless mesh network pilot. The ETX routing metric was used as it showed the best performance for medium sized networks and it allows one to graphically inspect the quality of the links.

This pilot network was used to learn if a network such as this could feasibly provide Internet access and local services such as VoIP to a rural community. It was also used to learn about the practical and social issues that are encountered when building a network of this nature.

Community wireless networks in rural areas are starting to emerge in developing regions around the globe. Some examples of these networks are: the Dharamsala Community Wireless Mesh Network [44], mesh networks being set up by CUWin in Ghana [45] and long distance wireless networks being set up in Rwanda, Ghana and Guinea Bissau by the TIER group at University of California, Berkeley [46]. Some of the key issues that make rural wireless networks unique are long distances between nodes, single, low bandwidth gateways to the Internet, high cost of Internet connectivity, lack of reliable power and low technical skill levels of people in the area who need to maintain the network. Often what might not be an acceptable level of service in an urban area is considered a good level of service in a rural area.

There are currently two approaches to the construction of community wireless networks. The first consists of a highly planned network with some nodes having multiple radios, carefully chosen antenna configurations and IP addressing structures to engineer high-quality links with good throughput.

The second approach makes use of single radio nodes, omni-directional and directional antennas and flat IP addressing schemes. The first approach is what one commonly finds occurring in urban areas where there is a high degree of ownership and skill level at each installation. The second approach is more ideally suited to rural areas where simplicity and cost take precedence over service quality.

This Section evaluates the performance of a simple single-radio mesh network running the OLSR protocol consisting of 9 nodes in a rural area of approximately 15 square kilometers in South Africa.

6.2 PEBBLES VALLEY MESH DESIGN

The Peebles valley mesh network is deployed over an area of about 15 square kilometers in a rural area near the Kruger National Park in South Africa. The network was built to explore a least cost 802.11 network to supply Internet connectivity, being supplied to an Aids clinic. This connects to surrounding schools, homes, farms and other clinic infrastructure through the mesh network. The Aids clinic, which is a non-governmental organisation (NGO) funded by a pharmaceutical company social grant, has brought hope to over 700 patients in the area over the 4 years it has been running. The VSAT Internet connectivity, which is provided free of charge by a sponsor, is usually underutilized every month, with clinic users only using approximately 60% of the available bandwidth each month.

The satellite link provides 2GB per month at a download rate of 256 kbps and an upload rate of 64 kbps. Once the 2GB capacity limit is reached the Internet connection is cut off until the beginning of the following month and no spare capacity can be carried over to the following month. This spare capacity is shared to users in the mesh network free of charge, but has to be carefully managed by a firewall to ensure that their usage does not effect the clinic's Internet availability.

Figure 6.1 is a map showing the Peebles valley mesh. The area is mountainous and line of site is not always easy to achieve unless you have some good elevation. For example, no link is achievable between D and E due to the mountainous terrain. A valley runs down the centre of the map which divides wealthier farming land on the left from a poorer tribal community on the right. Line of sight is usually possible across the valley and links tend to zig-zag between elevated points on either side of this valley. The dotted lines between the installations show the routes that the OLSR routing protocol has configured. A scale on the map is shown on the bottom left to give an idea of the distances involved. Each solid dot represents a wireless node and an empty dot represents a close cluster of nodes shown in the circles.

6.2.1 HARDWARE

The key decision criteria when choosing hardware for the project was cost. The cheapest off the shelf items that were available at the time were the Linksys WRT54G wireless routers. These are single radio 802.11 b/g routers which are capable of being re-flashed with a completely new operating system. They have a 200MHz CPU on board and use flash based memory with no fans or other moving parts. These devices are designed for indoor use and the first issue was to re-package the

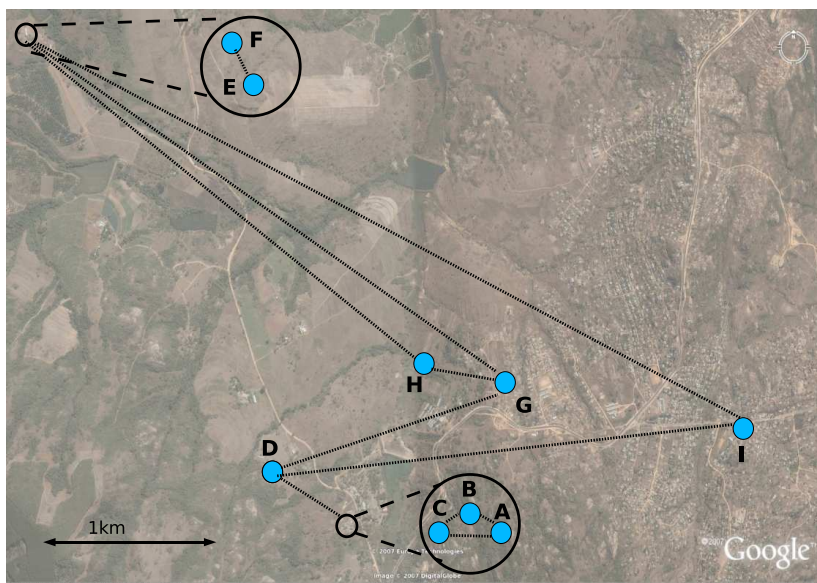


Figure 6.1: A map of the Peebles valley mesh. Each solid dot represents a wireless node. An empty dot represents a close cluster of nodes shown in the circles. The area on the left is wealthy farm land and the area on the right is poorer tribal land.

electronics so that it can be mounted on an outside mast.

An open enclosure is shown in Figure 6.2 mounted on a house on one of the farms. Power was injected over the Ethernet cable using a Power over Ethernet (POE) injector device. This helped simplify the installation, as only a single cable needed to be run between the outdoor unit and the power source and PC which are normally located in the same place. The type of outdoor antenna that was used depended on the range and radiation pattern needed to reach other nodes in the mesh. A Cantenna installation was also tested in the mesh at one of the house installations, this is also shown in Figure 6.2. Cantennas are low cost antennas which use tin cans as a waveguide to boost the antenna gain. Table 6.1 gives some detail about the features of each node which includes their antenna characteristics, whether they were indoor or outdoor nodes and the paths they typically use to get to the gateway node.

6.2.2 SOFTWARE

A standard Linksys WRT54G does not come with any mesh functionality. In order to turn the device into a mesh router, a new operating system and the mesh routing software needs to be installed on the unit. Freifunk, a group of open source wireless developers in Berlin, have developed a piece of firmware which packages a tiny version of Linux called OpenWRT, the OLSR routing protocol and some web based user interfaces. This firmware was used in the project with some modifications to enable remote traffic monitoring and bandwidth management.

Table 6.1: *Description of features of each mesh node. The node labels correspond with those on the map. The Hops column shows the number of hops to the Internet gateway and the “Path length to GW” column describes the total path distance along the OLSR selected route to the GW.*

N	Description	Type	Antenna	Hops	Path length to GW	OLSR Route to GW
A	ACTS Clinic (GW)	Outdoor	12dBi Yagi	0	50m	-
B	ACTS Accommodation	Indoor	2.14dBi Dipoles	1	50m	BA
C	ACTS Flats	Outdoor	8dBi Omni	1	90m	CA
D	USAID Farm	Outdoor	8dBi Flat Panel	1	620m	DA
E	Nut Farm	Outdoor	24dBi Grid	3	7.66km	EGDA
F	Nut Farm office	Indoor	2.14dBi Dipoles	4	7.76km	FEGDA
G	SAKHILE School	Outdoor	8dBi Flat panel	2	3.02km	GDA
H	Nurse Home	Outdoor	Cantenna	3	3.33km	HGDA
I	ACTS Hospice	Outdoor	24dBi Grid	2	3.94km	IDA

6.2.3 GATEWAY

The mesh node which acts as a gateway to the Internet needs to be able to control the amount of bandwidth each user on the mesh is allowed to use. To fulfil this function some byte counting functionality was installed on this node using some scripting and standard Linux Iptables rules. Each user was allocated a set amount of bandwidth per month and once this was used up they needed to wait until the beginning of the following month before they could access the Internet again. The clinic agreed to make 400MB available to the mesh network and this was then shared between all 10 nodes in the mesh network, giving each user about 40 MB per month on average. A default route to the VSAT Internet link was advertised to the entire network using the OLSR protocol’s dynamic gateway feature.

6.2.4 SERVICES

In order to make a rural mesh network a rich user experience, a wide array of local services were installed on a server in the mesh. As Internet traffic is expensive and limited, creating a high degree of localised traffic is a key strategy for any rural mesh network designer. Here are some of the services that were made available:

1. *DNS Server:* In order to make finding nodes on the mesh simpler, a DNS server was installed and each mesh node was given a host name. In the future a distributed DNS service could be explored which can potentially run on each mesh router and can start up when parts of the mesh are isolated due to link failures.
2. *Proxy server:* There are a number of reasons to run a proxy server. Firstly saving on expensive Internet traffic is vital, secondly there are a number of automated updates that run on Windows



Figure 6.2: Outdoor mesh node with repackaged Linksys WRT54G electronics in a waterproof aluminium case. The picture on the left shows an installation at node D is using a commercial 8dBi flat panel, the picture on the right shows an installation at node H which is using a home made Cantenna.

machines in particular and these can quickly use up a user's bandwidth quota without their awareness. A proxy can also be used to block these automated updates. The proxy was set up in transparent proxy mode so that all port 80 traffic was automatically routed to the server and the user didn't need to enter any proxy settings on their web browser.

3. *Local Ubuntu Linux repository:* Updating Linux-based machines or installing new applications over the Internet is a bandwidth-costly exercise. The latest release of Ubuntu Linux is mirrored on the server every 6 months by manually bringing a copy on a hard drive to the site and copying it over to the server.
4. *Asterisk server:* VoIP is a key applications on rural mesh networks which can save a large amount of money due to the high cost of mobile phone calls. Asterisk, which is a open source/free software implementation of a telephone private branch exchange (PBX), was installed and two VoIP phones were installed to connect the clinic and the hospice. In the future any user on the network can use a software/hardware based VoIP phone anywhere on the mesh to communicate with each other for free.
5. *Samba server:* Samba is a useful service to allow users to share files amongst each other. For example, if someone downloads a particular service pack they can put it on the samba file server for other users to access and avoid duplicating the download.
6. *Local school Wikipedia:* Wikipedia has become an invaluable reference tool for finding basic information on topics of interest. The school can use this as a resource for their teachers and

learners. This is particularly vital for them, as school learners often don't have access to proper text books or reference books. A local sanitised Wikipedia which has content aimed at school learners was installed on the server for this purpose.

6.2.5 CONFIGURATION

6.2.5.1 ADDRESSING

All the nodes in the mesh network were given static IP addresses, in the private IP range, for their Wireless and LAN ports. The following scheme was followed: Wireless IP addresses were 10.1.1.x and the LAN IP addresses were 10.2.x.1. A DHCP server is run on each node which hands out a block of addresses to clients connecting to the mesh node. All wireless nodes and client devices are reachable from anywhere on the mesh due to OLSR's Host Network Address (HNA) advertising mechanism which adds the LAN side IP address block in the routing table of all other nodes.

6.2.5.2 802.11 AND OLSR SETTINGS

The Linksys WRT54G's are capable of 802.11b or 802.11g mode of operation. The nodes were all set to auto select between b/g mode based on the signal quality available. The signal strength varied greatly in the mesh which meant that some nodes were switching down to 802.11b 2 Mbps and others were using 802.11g mode at 24 Mbps data rates. Signal strength was set to 100 mW, which is the legal limit in South Africa in the 2.4 GHz ISM band although the legal Effective Isotropic Radiated Power (EIRP) limit, which is also 100 mW, is broken to establish long range links with directional antennas. The OLSR routing protocol was set to use RFC recommended values other than the routing metric which was set to ETX.

6.3 EVALUATION

The results that will be presented were derived from a set of various measurement processes that are outlined here, the methodology used being strongly based on work done by MIT Roofnet [30].

1. The TCP throughput is the result of one-way bulk transfers of 100 source buffers of 8192 bytes each being sent between each pair of nodes in the mesh. A standard Linux tool called `ttcp` was used for this test and throughput is measured as the number of bytes that were delivered to the receiving node. This process is repeated 3 times and an average is finally recorded.
2. The latency is established by sending 84-byte pings once per second and the average round-trip time is recorded.
3. All tests are done with RTS/CTS disabled as this did not improve the performance of the mesh. Other researchers have reported similar findings [40].
4. Hop count was recorded by examining the routing tables generated by OLSR on each node.

5. All radios were set to auto-select 802.11b or 802.11g mode as well as the data rate being used. This will be dependent on the signal strength being reported by the radio.
6. The Peebles valley mesh normally provides Internet access to users and this was not disabled during these experiments. However, as will be discussed later, the throughput of the satellite link compared to the throughput of the links in the mesh is significantly lower and so even if there was some Internet traffic, it would have had a small effect on the results.

6.3.1 THROUGHPUT AND DELAY PERFORMANCE

Figure 6.3 shows the distribution of TCP throughput among all pairs of nodes in the mesh. The average throughput is 2324 kbps and the median is 1276 kbps. The distribution of throughput can be understood by hop count between pairs as well as other environmental factors such as distance or obstacles such as trees or buildings. Hop count plays the largest role in determining a drop in throughput and Table 6.2 illustrates this. Figure 6.4 shows the throughput with its standard deviation as the number of hops increase. The high degree of standard deviation is due to different data rates being selected, based on signal quality between links and the wide range of distances as well as obstacles, such as trees, between nodes.

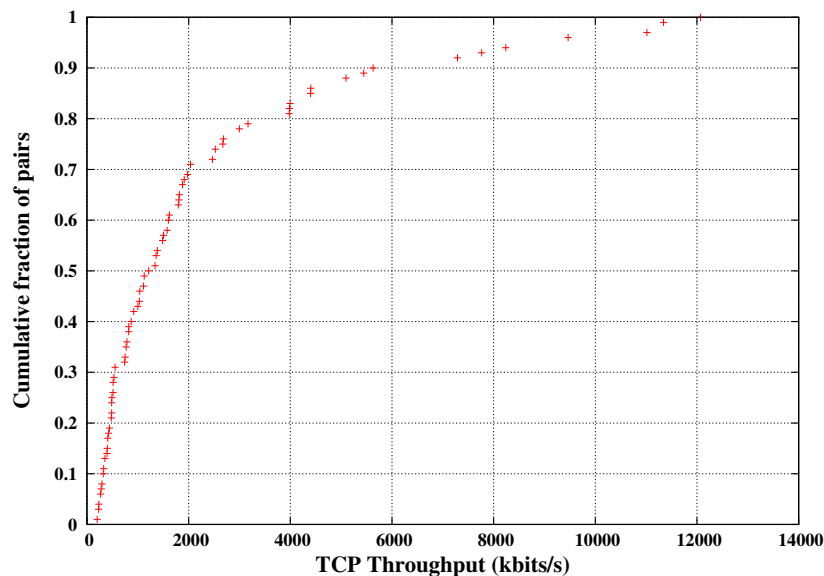


Figure 6.3: *Cumulative distribution function.*

The performance of the Peebles valley mesh can now be compared to those of the indoor testbed and previous measurements carried out by Gupta. All these results are presented together in Figure 6.5.

The Peebles valley results are almost identical to those that Gupta experienced when carrying out multi-hop experiments with laptops between offices. This shows that the multi-hop throughput exponent index, shown in Equation 6.1 is dependent on the link budget between nodes. This link

Table 6.2: Average TCP throughput and round-trip ping latency between each pair in the network, arranged by the number of hops in route chosen by OLSR.

Hops	Pairs	Throughput (kbps)	Latency (ms)
1	23	4867	4.69
2	24	1593	4.98
3	14	812	5.78
4	9	571	5.8
5	2	336	7.3
Avg: 2.21	Total: 72	Avg: 2324	Avg: 5.71

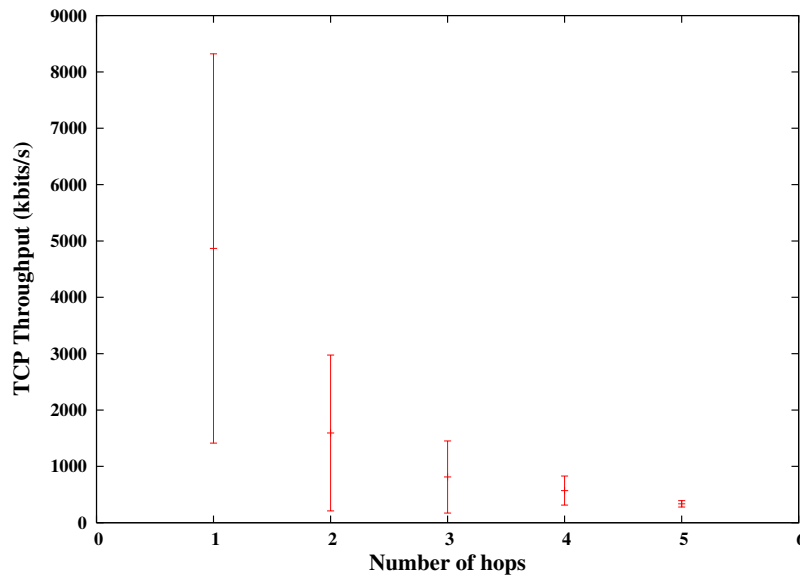


Figure 6.4: Effect of number of hops on throughput.

budget can be low because of distances between nodes, obstacles or because of lower gain antennas being employed. The 7x7 grid results, using ideal conditions, shows better performance due to no packet losses being present in the network.

A linear regression on the log of the x and y axis for the throughput in Peebles Valley was carried out using a least mean squares fit. This reveals a slope of 1.62 which is close to 1.68 discovered by Gupta in his indoor trials. The predicted throughput for this network is thus shown by Equation 6.1.

$$\lambda_{PEEBLES}(n) = \frac{W}{n^{1.62}} \quad (6.1)$$

This formula can now be used to extrapolate how many hops result in an average throughput which is less than the 256 kbps VSAT satellite link being used. If the average baseline throughput for one a single hop (W) is set to 4867, the predicted average throughput is 267 kbps after 6 hops and 208 kbps after 7 hops. The bottleneck to the Internet in this unloaded network being caused by the

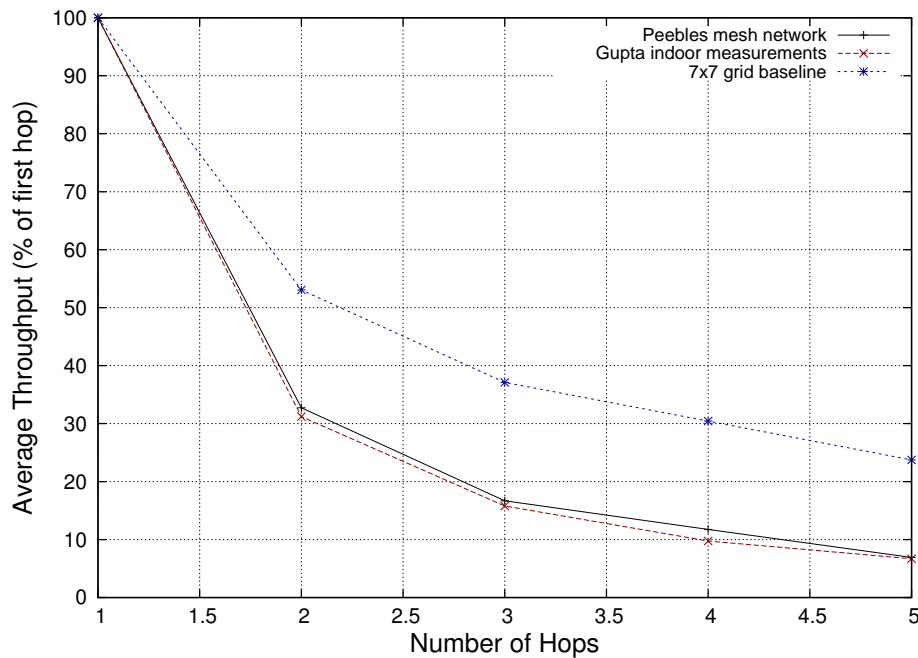


Figure 6.5: Comparison of theoretical, indoor and outdoor throughput.

mesh network occurs only after 7 hops.

Tables 6.2 also shows round-trip latencies for 84-byte ping packets to estimate the delay on an idle network. Interactive latency is acceptable when there is a single user on the network. The average user will experience 5.71 ms of latency between any pair of nodes. A VoIP phone has been set up at point A (ACTS clinic) and point I (ACTS Hospice) and no noticeable delay is experienced in this two hop link even when there is some Internet activity. Figure 6.6 shows the amount of delay with standard deviation as the number of hops increases. What is noticeable is that each hop only introduces an average 0.5 ms increase in latency whereas the application and the kernel stack appear to add about another 4 ms of delay overhead. In a loaded network these figures would rise significantly due to queuing and interference in the network.

6.3.2 INTERNET USAGE PATTERNS

As described earlier, a small portion of Internet bandwidth was allocated each user and once this is used up it is was not available again until the following month. Users could, however, request to be allocated additional bandwidth and if the ACTS clinic usage was fairly low that particular month, more bandwidth could be allocated on a case by case basis by an administrator.

The cumulative bandwidth used at each node is shown in Figure 6.7. Users who had never been exposed to the Internet, such as the nurse's house and Sakhile school, found it difficult to understand how to control their bandwidth usage. More training is needed on how to use bandwidth sparingly; for example, you will notice that the 40 MB allocated to Sakhile school was used within 4 days.

The nurse's house makes use of a cantenna installation as shown in Figure 6.2. Her first daughter

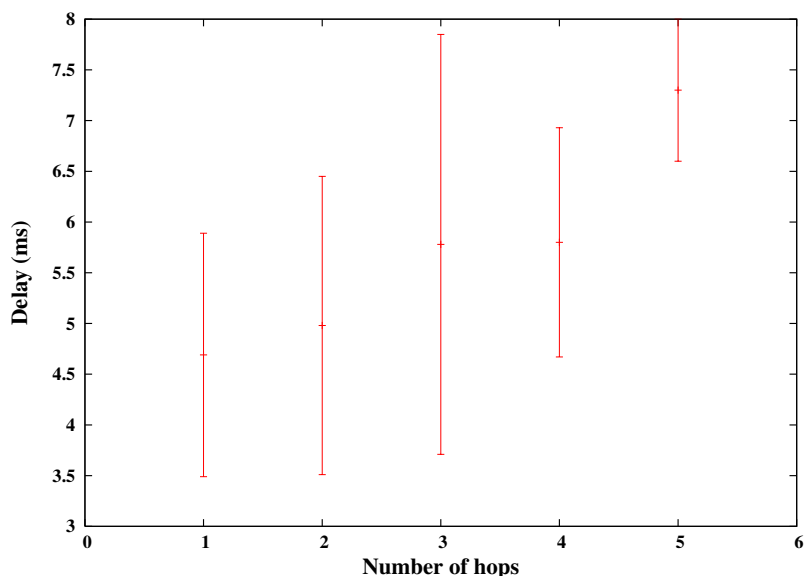


Figure 6.6: *Effect of number of hops on delay.*

lives at home looking after her baby and doesn't have a job. As a result she is one of the most prolific users of the Internet. One of her other daughters used the Internet, supplied by this project, to find a job and is now part of the formal economy in another part of the country. Her first daughter uses the Internet for social networking, growing her IT skills and looking for jobs. As this site belongs to a staff member of the clinic, extra bandwidth has been allocated if spare capacity was available. You will notice the graph plateaus at some points and then ramps up again; this was usually when extra bandwidth was requested and there was a delay of a few days before it was actually allocated.

Some of the reasons for the lack of activity of other users is the availability of 3G in the area to the wealthier farmers such as the nut farm (node E and F) and USAID (node D). Convenience is a priority over cost for these users and the process of reconfiguring their computer to connect to the mesh is seen as a burden even though it can give them some free bandwidth. The sites are, however, important for connectivity to other areas in the mesh. Guests who visit the nut farm and USAID tend to be the main users and one of the business partners on the nut farm, who doesn't have a 3G account, is an occasional user of the network.

Another useful usage pattern to observe is the amount of outbound versus the amount of inbound traffic from the Internet. Table 6.3 shows these statistics for a months usage as well as the percentage of the total traffic which was inbound. A high percentage of inbound traffic, as is the case at Sakhile school, shows a typical asymmetric web usage pattern. When this approaches 50 percent, as is the case with ACTS accommodation, the nurse's home and USAID, it reveals a higher degree of social networking being carried out with applications like instant messaging and peer-to-peer VoIP. This correlates well with the type of users in question; for example, the ACTS accommodation block is used by overseas visitors to the AIDS clinic and they use the network to correspond with friends back home. The nurse's first daughter, as described earlier, uses the network to correspond with friends

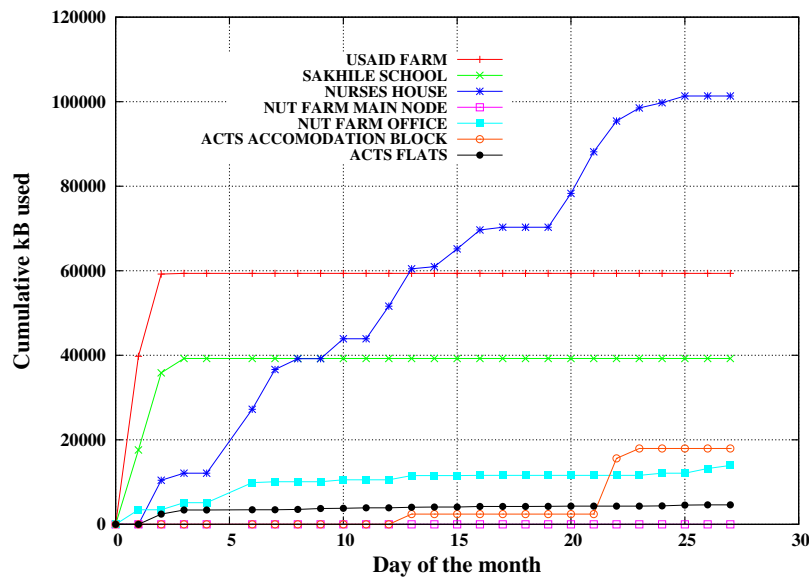


Figure 6.7: Internet usage pattern.

around the country. The hospice node only has a VoIP phone to make internal calls to the clinic and so no Internet traffic was observed there. The nut farm main node is simply used as a repeater to the office node, so all Internet traffic is only observed coming from the office node's IP address, which is why no traffic is observed there either.

Table 6.3: Internet usage pattern of users during the month of August 2007.

N	Description	Inbound (KB)	Outbound (KB)	Total (KB)	% In
B	ACTS Accommodation	9945	7997	17942	55
C	ACTS Flats	3447	1171	4618	75
D	USAID Farm	26073	33308	59381	44
E	Nut farm	0	0	0	0
F	Nut farm office	10853	3074	13927	78
G	Sakhile School	37491	1765	39256	96
H	Nurses Home	52123	49238	101361	51
I	Hospice	0	0	0	0

Windows machines connecting to the mesh network would often launch automatic updates without the user's awareness. The transparent proxy service installed on the network allowed a rule to be configured on the proxy which blocked all access to these updates. Other updates that need to be blocked were virus update programs which also run without the user's awareness. A better approach to automated updates, in bandwidth constrained environments, is to place all these service packs and virus updates on the shared server to prevent users duplicating common downloads.

6.3.3 BEHAVIOURAL PATTERNS OF USERS

Exposing the Internet for the first time to users, brings with it a certain amount of responsibility. Although the Internet brings people a wealth of information, it also brings with it many potentially harmful aspects. Keeping a community-based mesh network running also requires a good level of stewardship by the users. Some of the key behavioural patterns we have observed are:

- First-time Internet users were easily fooled into believing they had won huge sums of money by Internet scams which typically manifest themselves as pop up screens. Pop-up blockers can partly prevent these kinds of problems but more importantly, educating users on not believing everything that the Internet presents to them is vital.
- Personal information, such as mobile phone numbers, was freely shared over the Internet. Identity theft and banking phishing schemes are rife on the Internet and users need to be made aware of these dangers.
- There was little conceptual understanding of what type of Internet usage consumes large amounts of bandwidth. A graph was available from a web site which showed what percentage they had consumed but wasn't viewed by users due their lack of understanding of graphs. A more tangible mechanism is needed on a PC which has a visible decreasing counter when bandwidth is consumed.
- Up-time in the network was often severely hampered by users unplugging their equipment. Plugging mesh nodes into a wall socket might not always be the best solution as these might sometimes be needed for other electrical devices when the Internet is not being used.
- Viruses were very common on Windows machines and these machines often needed to be formatted and Windows reinstalled. Using Linux based systems minimizes the risk of virus attacks as well as being free. But users, such as teachers at the school, were afraid to embrace an unknown operating system as they saw this as an extra hurdle to an already difficult task of becoming IT literate in Windows.
- Instant messaging tools such as Skype have proved to be a very valuable helpline for inexperienced users in the network. Users would often message more experienced users in the cities to find out how to fix a computer problem or set up a new application. It was even possible to remotely log into the mesh network and fix a problem on a PC while messaging a user. The social networking revolution that is taking place on the Internet at the moment could be the key solution to creating support structures for users in rural networks.

6.3.4 ENVIRONMENTAL OBSERVATIONS

Placing sensitive electronic equipment outdoors and exposing it to the elements brings with it its own set of challenges. Here are some of the environmental issues we have observed:

- lightning in the area is very severe and the granite rocky outcrops tend to attract lightning particularly at the farms and clinic. Over the 2 years that the project has been running, 4 hubs, 2 PC Ethernet ports and 2 wireless router Ethernet ports were damaged by lightning. No wireless routers have been completely destroyed by lightning even though they are mounted on rooftops. The Wireless routers are supplied with 5 Ethernet ports and when one is damaged by lightning, it was found that another one could be used and the router would continue to function normally. A long length of Ethernet tends to be the main cause of problems, with the Electromagnetic Field (EMF) from lightning being induced in the copper and damaging equipment to which it is attached. At the clinic, Ethernet between building was replaced with fibre optic cable and this removed the problem completely. Ethernet from the wireless routers is kept as short as possible and is now routed through lightning protectors built into many UPS's and this has also removed the problem.
- The Peebles valley area has a subtropical climate with an average daily maximum temperature of 27°C and an average daily minimum temperature of 13°C . The average yearly rainfall is 767 mm with an average of 100 days having more than 1 mm of rain. The aluminium outdoor enclosures that were used have proved to handle the elements very well and after 2 years no visible material fatigue was observed in the cases. The seals have also showed no signs of wear and the electronics inside the cases has been kept dry. The antenna was severely rusted after 2 years but this has had no effect on its performance. The standard CAT5 Ethernet cable that is run from the outdoor unit down into the building has started to show signs of hardening and cracking where it is exposed to the sun. In the future a higher grade UV resistant CAT5 cable will be used in sections which are exposed to the sun.

6.4 CONCLUSION

This trial rural mesh network has illustrated that single radio mesh networks based on low-cost commodity wireless equipment is a viable means to provide Internet connectivity to an area with limited broadband connectivity. The mesh network provides a satisfactory grade of service for Internet access based on a best effort shared VSAT satellite Internet resource. Average throughput speeds of 2324 kbps and an average delay of 5.7ms was achieved between any two nodes on the unloaded mesh network with an average hop count of 2.21.

Training first time users of the Internet on how to use Internet and local server resources effectively is a difficult challenge. Installing voice and instant messaging applications to allow them to contact more experienced users in the city has helped at least create a lifeline when they need advice. Users also need to understand that each of their nodes forms a crucial point in the mesh network and the network depends on their node staying on all the time. There needs to be more awareness of what type of usage behaviour results in large amounts of bandwidth being consumed since a simple usage graph available on the local server hasn't been effective. Some innovation around a bandwidth usage

application which uses graphical and audible alerts is needed.

6.5 FUTURE CONSIDERATIONS

Ideally, before first time users of the Internet visit their first web page, training programs should be given on the dangers of the Internet, such as scams, viruses, and protection of personal information. If training programs are not possible, a portal page which is always displayed before visiting the Internet could warn users of these dangers with up to date information on the latest scams.

Once local services such as video conferencing for Tele-health or Tele-education and local bandwidth-intensive repositories are used, the single radio mesh network will be pushed to its technical limits and far more congestion will be observed. If these usage patterns begin emerging, some improvement to the mesh infrastructure might become necessary with multiple radio nodes being installed at strategic points.

Further analysis is also required on understanding the performance of these networks under severe load conditions which will help answer basic questions like how many VoIP calls can be supported for a mesh network with a specific average hop count.

CHAPTER SEVEN

CONCLUSIONS

Life is the art of drawing sufficient conclusions from insufficient premises

Samuel Butler

This thesis was able to demonstrate that a scaled indoor wireless testbed based on a grid structure can be constructed in a single room and yet still yield good multi-hop characteristics that one would find in typical outdoor networks. Performance characteristics of 3 MANET protocols, OLSR, AODV and DYMO, were extracted from running these on the indoor wireless testbed. This helped clarify each of the strengths and weaknesses of these protocols under different network conditions. An outdoor wireless mesh network was then constructed in a rural area using OLSR, the best performing routing protocol in the indoor testbed, and this showed that a very satisfactory broadband service can be supplied to a rural community using mesh networking technology.

7.1 SUMMARY OF CONTRIBUTION

The specific contributions made in the course of this research are the following:

- A summary of the development of ad hoc networking over the past few decades was presented including currently available testbed networks, previous work on routing protocol comparisons and limitations of mathematical modelling and simulation. Only 2 other testbed networks that are based on a regular grid structure were discovered, these being the ORBIT lab at Rutgers University and the MINT lab at Ohio state University.
- A scaled indoor wireless grid was developed and modelled which yields multi-hop characteristics of up to 5 hops in the full 7x7 grid when the power is set to 0 dBm with 30 dB attenuators.

A very powerful experimental platform was created, which allows a mesh node to boot off a central server thus allowing a new experiment to run on all 49 nodes within a matter of minutes. Challenges encountered when constructing the lab were highlighted to help other researchers when they wish to build a similar facility. For example, communication grey zones need to be mitigated by locking the broadcast rate to the data rate.

- The electromagnetic environment of the lab was characterized and this revealed that pure free space loss is not achievable and Fresnel zone clearance, multipath fading, antenna coupling, radio mode and data rate all effect the reported signal strength of nodes in the grid. Signal levels diverged by as much as 10 dB from free space loss predictions, with divergence increasing as the distance between communicating points increased.
- The complexity of the wireless grid was analyzed and it was found that a large number of alternative routes are available between distant points in the grid. This results in a very challenging environment for routing protocols to operate in. In the special case, where a node is only within range of its adjacent node along the perpendicular axis, a total of 924 equivalent hop routes are possible in the full 7x7 grid between the two furthest point on the grid. There are 170277 possible routes through the grid if the radius is increased to the diagonal between two adjacent nodes.
- Detailed analysis of AODV, DYMO and OLSR using two routing metrics was carried out [47]. This set of protocols have never been benchmarked on a large scale live testbed and present new results and insights into their performance in a static mesh network environment. The AODV protocol showed the weakest performance in the grid with close to 60% of possible link pairs achieving no route for the full 7x7 grid. However it did present the least amount of routing overhead compared with other routing protocols. DYMO showed good results for its low routing overhead with the least amount of delay for the full 7x7 grid and the 2nd best throughput performance in a simple string of pearls topology. The RFC version of OLSR using the hysteresis routing metric had the best overall performance in a full 7x7 grid, in terms of throughput and successful routes but OLSR with the ETX extension performed better, in terms of throughput, in medium size networks of about 21 nodes.
- Route flapping for all three routing protocols was also analysed in order to understand its effect on throughput performance. As highlighted already, the grid contains a very large number of alternative routes and convergence is challenging for a routing protocol. Route flapping in the grid ranged from an average of 0.5 route changes in 10 seconds for AODV to 2.3 route changes for OLSR with hysteresis. However, OLSR, which is a proactive protocol making use of a metric which is sensitive to packet loss, performed well in spite of the high degree of route flapping. AODV on the other hand, which is a reactive protocol making use of a count based metric performed poorly with its relatively high degree of route flapping. Clearly, whenever

AODV changed to a new route it was converging on a less optimal route whereas OLSR was converging on more optimal routes.

- The ETX routing metric was analysed for real networks and it was discovered that ETX only predicts optimal multi-hop network paths in theoretically ideal network conditions. It was calculated that if 802.11-based links are used with the ETX metric, the predicted losses are out by a factor of almost 2 compared to the actual losses that will be experienced, even in ideal lab conditions with no packet loss between adjacent nodes.
- A trial rural mesh network pilot was built and this has illustrated that single radio mesh networks based on low cost commodity wireless equipment are a viable means to provide Internet connectivity to an area with limited broadband connectivity [48]. Mesh networking based on OLSR provides a satisfactory grade of service for Internet access based on a best effort shared VSAT satellite Internet resource. In the network consisting of 9 nodes, covering an area of about 15 square kilometers, average throughput speeds of 2324 kbps and an average delay of 5.7ms were achieved between any two nodes on the unloaded mesh network with an average hop count of 2.21.
- A comparison of the throughput versus number of hops was made between this pilot rural network and the indoor testbed over 4 hops using the OLSR-ETX protocol. The multi-hop losses were far more severe in the case of the rural mesh network with 2nd and 3rd hop throughput ratio to 1st hop throughput being 20% lower than the 2nd and 3rd hop throughput ratio of the indoor network for a similar size network. But this was mostly due to some of the long distance links switching to a lower data rate due to increased packet loss, whereas the data rate was kept constant in the indoor lab.

7.2 FUTURE WORK

The current thesis forms a good baseline for future experimental research where the performance of new or improved ad hoc networking protocols on the indoor wireless testbed or rural outdoor testbed can be analysed. Future work can be divided into three main categories of research related to (1) the improvement of testbed lab conditions, (2) refinement of experimental parameters and (3) the refinement of ad hoc networking routing protocols to make them more suitable to static mesh networks and real network conditions.

7.2.1 IMPROVEMENTS TO THE INDOOR TESTBED LAB CONDITIONS

- Clear the Fresnel zone by increasing the antenna installation height (above floor and PC cases)
 - install antennas on pedestals made of non-conducting material.
- Make use of microwave absorbing materials on the walls to mitigate multipath effects in the lab and approach the realism of an outdoor wireless network.

- Migrate the entire lab to the 5 GHz ISM band to avoid current interference issues in the 2.4 GHz ISM band.
- Try to minimize parasitic RF coupling between nodes by utilising additional screening and/or absorbing material, or placing the PC inside a screening box/cabinet,
- Develop the lab software framework to a point where other researchers from anywhere in the world can schedule experimental time on the testbed, similar to what is done at Emulab and ORBIT.
- Some degree of node mobility is necessary to emulate mesh networks where there may be a number of mobile users roaming between wireless routers. This can initially be done using virtual node mobility, similar to that being used by ORBIT, where various nodes in the grid assume the character of a single mobile node. Eventually, a number of mobile robots making use of a positioning system, with wireless routers mounted on them, would be an ideal platform for these sort of experiments

7.2.2 REFINEMENT OF EXPERIMENTAL PARAMETERS

- All these performance tests were carried out using suggested configuration parameters that are published in MANET RFCs and Internet drafts. In the future it will be interesting to see how performance can be tweaked for specific topologies by changing parameters such as HELLO intervals.
- These experiments were performed using a single data flow through the network between a pair of nodes being tested. In the future, the effect of multiple data flows on the routing, throughput or delay performance would be vital to establishing a complete picture of the network performance of routing protocols in a mesh network.
- It is difficult to compare pro-active and reactive routing protocols as they achieve very different outcomes, with pro-active protocols establishing a complete picture of all possible routes through the network and reactive protocols only establishing routes that are required. More work is needed on establishing a fair comparison metric which looks at, for example, the “routing overhead” to “established routes” ratio.
- A mesh network making use of multiple gateways is another interesting area of future research. These gateways can be chosen based on offered throughput, delay performance or even monetary cost. The indoor mesh lab could be used to emulate multiple gateways at various points around the grid.

7.2.3 REFINEMENT OF AD HOC ROUTING PROTOCOLS

- What has emerged out of this work is that simulation-based results and results from real wireless networks are often very different. Further work on refining routing algorithms and routing metrics to adapt to live network conditions is now required. For example, this thesis highlighted that the ETX routing metric does not realistically predict the best multi-hop route through a network.
- There are many instances in mesh networks where most traffic is only interested in reaching a gateway point to the Internet. In cases like this, a reactive protocol such as DYMO or AODV may be sufficient to only establish these routes and then cache them until the link is broken. These algorithms could be refined for this specific class of networks.
- There are routing instances where delay and throughput tend to be mutually exclusive. This was noticed when comparing DYMO to OLSR-RFC where DYMO established routes with the least delay and OLSR-RFC established routes with the best throughput. Application directed routing could be a new area of protocol refinement in which routing protocols adapt to the needs of the application, whether this be least delay or highest throughput.

Some further work is also needed to compare simulation results to results from the indoor lab. This can be done fairly easily in cases where the same source code is available for ns2 simulations and for real hardware. This will help quantify the extent to which simulations are limited in their ability to emulate the physical layer. Integrating ns2 with the lab's experimental framework, in which ns2 simulation scripts are used to run actual real network experiments on the indoor lab, will also greatly simplify the current process of setting up an experiment which involves complex Perl scripting.

7.3 CONCLUSION

Wireless mesh networking has enormous potential to redefine connectivity paradigms in the developing world from a centralized operator based approach to a decentralized community-based approach. Wireless testbeds such as the ones developed in this thesis will undoubtedly play a significant role in accelerating the research, development and uptake of these technologies in disadvantaged communities who are isolated from the global information society. It is hoped that this work will catalyse more interest in refining routing algorithms to work more effectively in realistic wireless mesh networks with eventual widespread deployments across Africa and the rest of the developing world.

REFERENCES

- [1] O. Purbo, “Self-Finance Sustainable ICT for Development: Strengthening the Grassroots,” Tech. Rep., IDRC, 2004.
- [2] V. Naik, E. Ertin, H. Zhang, and A. Arora, “Wireless Testbed Bonsai,” *Proc. 2nd Intl Workshop Wireless Network Measurement*, April 2006.
- [3] S. Ganu, H. Kremo, R. Howard, and I. Seskar, “Addressing repeatability in wireless experiments using the orbit testbed,” in *Proc. of IEEE Tridentcom*, Trento, Italy, February 2005.
- [4] G. Dodig-Crnkovic, “Shifting the Paradigm of Philosophy of Science: Philosophy of Information and a New Renaissance,” *Minds and Machines*, vol. 13, no. 4, pp. 521–536, 2003.
- [5] R.E. Bellman, *On a Routing Problem*, Rand Corp, 1956.
- [6] EW Dijkstra, “A note on two problems in connexion with graphs,” *Numerische Mathematik*, vol. 1, no. 1, pp. 269–271, 1959.
- [7] J. McQuillan, G. Falf, and I. Richer, “A review of the development and performance of the arpanet routing algorithm,” *IEEE Transactions on Communications*, vol. C-26, no. 12, pp. 1802–1811, 1978.
- [8] Y. Afek, E. Gafni, and M. Ricklin, “Upper and lower bounds for routing schemes in dynamic networks,” in *IEEE Annual Symposium on Foundations of Computer Science (FOCS)*, October 1989.
- [9] J. Moy, “Ospf version 2,” Tech. Rep., IETF, 1998.
- [10] “IETF Mobile Ad-Hoc Networks (MANET) Working Group,” 1 August 2007, <http://www.ietf.org/html.charters/manet-charter.html>.
- [11] IEEE, *Draft Standard for Information Technology - Telecommunications and Information Exchange Between Systems - LAN/MAN Specific Requirements - Part 11: Wireless Medium Access Control (MAC) and physical layer (PHY) specifications: Amendment: ESS Mesh Networking*, IEEE, New York, NY, USA, March 2007, P802.11s/D1.02.

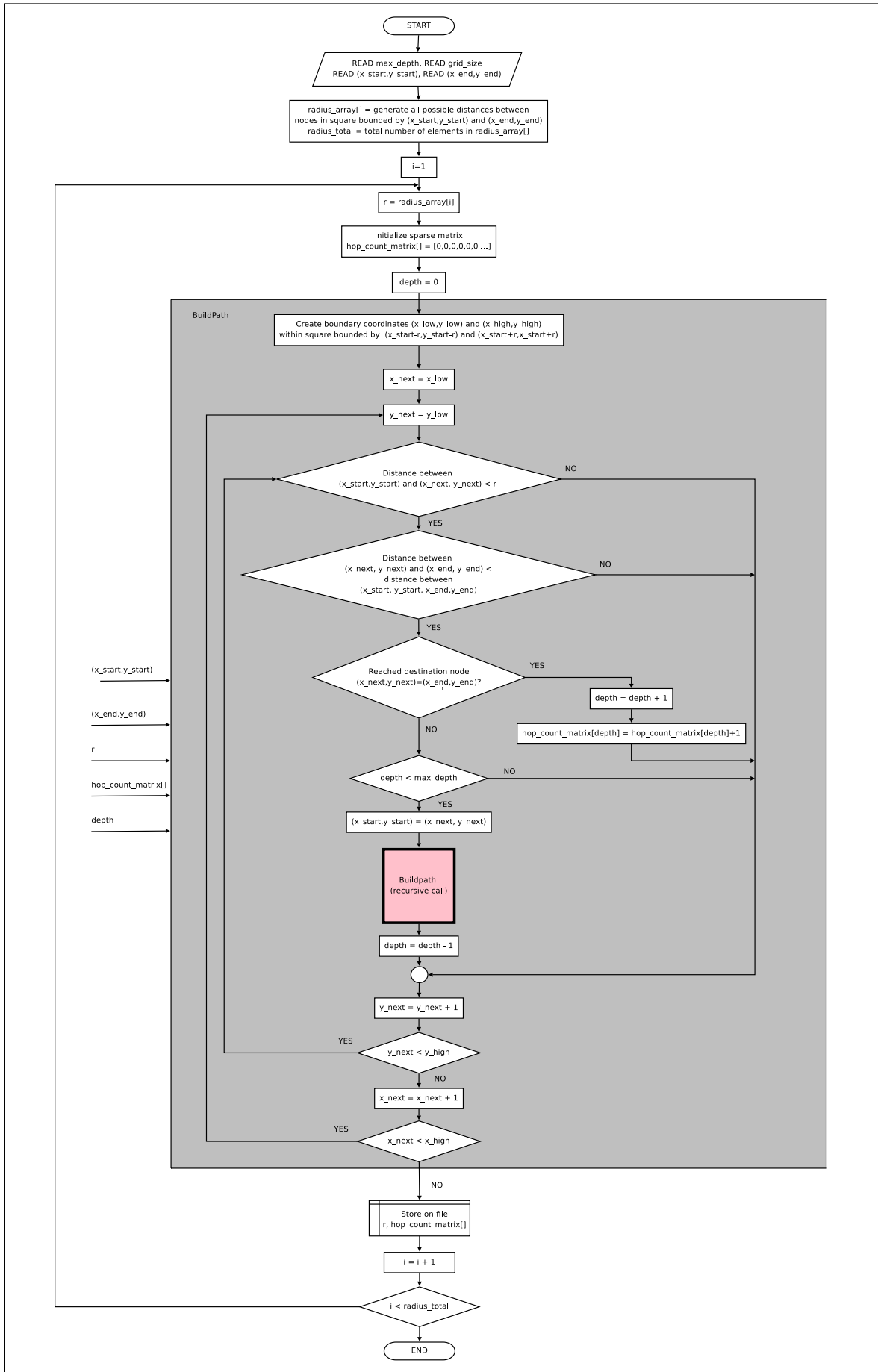
- [12] C.E. Perkins and E.M. Royer, “Ad-hoc on-demand distance vector routing,” *Proceedings of the 2nd IEEE Workshop on Mobile Computing Systems and Applications*, vol. 2, pp. 90–100, 1999.
- [13] I. Chakeres, E. Belding-Royer, and C. Perkins, “Dynamic MANET On-demand (DYMO) Routing,” *draft-ietf-manet-dymo-10.txt, Internet Draft (work in progress), July, 2007.*
- [14] P. Jacquet, P. Muhlethaler, T. Clausen, A. Laouiti, A. Qayyum, and L. Viennot, “Optimized link state routing protocol for ad hoc networks,” *Multi Topic Conference. IEEE INMIC 2001. Technology for the 21st Century. Proc. IEEE International*, pp. 62–68, 2001.
- [15] D.B. Johnson and D.A. Maltz, “Dynamic source routing in ad hoc wireless networks,” *Mobile Computing*, vol. 353, pp. 153–181, 1996.
- [16] D.S.J.D. Couto, D. Aguayo, J. Bicket, and R. Morris, “a high-throughput path metric for multi-hop wireless routing,” *Wireless Networks*, vol. 11, no. 4, pp. 419–434, 2005.
- [17] T. Clausen and C. Dearlove, “MANET Neighborhood Discovery Protocol (NHDP),” *draft-ietf-manet-nhdp-04 (work in progress), June, 2007.*
- [18] A Tonnesen, “Implementing and extending the optimized link state routing protocol,” M.S. thesis, University of Oslo, Norway, 2004.
- [19] “Uppsala university aodv-uu website,” 1 August 2007, <http://core.it.uu.se/core/index.php/AODV-UU>.
- [20] “University of murcia dymoum website,” 1 August 2007, <http://masimum.dif.um.es/?Software:DYMOUM>.
- [21] “Nsf workshop on network research testbeds, chicago, il,” October 2002, http://www.net.cs.umass.edu/testbed_workshop/.
- [22] B. White, J. Lepreau, L. Stoller, R. Ricci, S. Guruprasad, M. Hibler, C. Barb, and A. Joglekar, “An integrated experimental environment for distributed systems and networks,” *ACM SIGOPS Operating Systems Review*, vol. 36, pp. 255–270, 2002.
- [23] D. Johnson, T. Stack, R. Fish, D.M. Flickinger, L. Stoller, R. Ricci, and J. Lepreau, “Mobile Emulab: A Robotic Wireless and Sensor Network Testbed,” *IEEE Infocom*, 2006.
- [24] G. Judd and P. Steenkiste, “Repeatable and Realistic Wireless Experimentation through Physical Emulation,” *Proc. of Hotnets*, 2003.
- [25] R Draves, J Padhye, and B Zill, “Comparison of routing metrics for static multi-hop wireless networks,” in *Proceedings of Special Interest Group on Data Communications (SIGCOMM)*, Portland, Oregon, August 2004.

- [26] S. Sanghani, TX Brown, S. Bhandare, and S. Doshi, "EWANT: the emulated wireless ad hoc network testbed," *Wireless Communications and Networking. IEEE WCNC 2003.*, vol. 3, 2003.
- [27] D.A. Maltz, J.G. Broch, and D.B. Johnson, *Experiences Designing and Building a Multi-hop Wireless Ad Hoc Network Testbed*, School of Computer Science, Carnegie Mellon University, 1999.
- [28] H. Lundgren, D. Lundberg, J. Nielsen, E. Nordstrom, and C. Tschudin, "A large-scale testbed for reproducible ad hoc protocol evaluations," *Wireless Communications and Networking Conference. IEEE WCNC 2002.*, vol. 1, 2002.
- [29] P. De, A. Raniwala, S. Sharma, and T. Chiueh, "MiNT: A Miniaturized Network Testbed for Mobile Wireless Research," *Proc. of Infocom 2005. Miami, FL*, 2005.
- [30] J. Bicket, D. Aguayo, S. Biswas, and R. Morris, "Architecture and evaluation of an unplanned 802.11 b mesh network," *Proc. of the 11th Annual International Conference on Mobile Computing and Networking*, pp. 31–42, 2005.
- [31] P. Bhagwat, B. Raman, and D. Sanghi, "Turning 802.11 inside-out," *ACM SIGCOMM Computer Communication Review*, vol. 34, no. 1, pp. 33–38, 2004.
- [32] J. Broch, D.A. Maltz, D.B. Johnson, Y.C. Hu, and J. Jetcheva, "A performance comparison of multi-hop wireless ad hoc network routing protocols," *Proceedings of the 4th Annual ACM/IEEE International Conference on Mobile Computing and Networking*, pp. 85–97, 1998.
- [33] S.R. Das, C.E. Perkins, and E.M. Royer, "Performance comparison of two on-demand routing protocols for adhoc networks," *INFOCOM 2000. Proc. of the Nineteenth Annual Joint Conference of the IEEE Computer and Communications Societies. IEEE*, vol. 1, 2000.
- [34] A. Huhtonen, "Comparing AODV and OLSR Routing Protocols," *Telecommunications Software and Multimedia*, 2004.
- [35] J. Hsu, S. Bhatia, M. Takai, R. Bagrodia, and M.J. Acriche, "Performance of mobile ad hoc networking routing protocols in realistic scenarios," *Military Communications Conference. MILCOM 2003. IEEE*, vol. 2, 2003.
- [36] P. Gupta and P.R. Kumar, "The capacity of wireless networks," *IEEE Transactions on Information Theory*, vol. 46, no. 2, pp. 288–404, March 2000.
- [37] L. Kleinrock and J. Silvester, "Optimum transmission radii for packet radio networks or why six is a magic number," *Proceedings of the IEEE National Telecommunications Conference*, vol. 4, pp. 1–4, 1978.
- [38] T.R. Andel and A. Yasinac, "On the credibility of manet simulations," *Computer*, vol. 39, no. 7, pp. 48–54, July 2006.

- [39] H. Lundgren, E. Nordström, and C. Tschudin, “Coping with communication gray zones in IEEE 802.11 b based ad hoc networks,” *Proceedings of the 5th ACM International Workshop on Wireless Mobile Multimedia. WOWMOM 2002*, pp. 49–55, 2002.
- [40] K. Xu, M. Gerla, and S. Bae, “Effectiveness of RTS/CTS handshake in IEEE 802.11 based ad hoc networks,” *Ad Hoc Network Journal*, vol. 1, no. 1, pp. 107–123, 2003.
- [41] C.A. Balanis, *Antenna Theory: Analysis and Design*, Wiley, 1997.
- [42] P. Gupta and R. Drag, “An experimental scaling law for ad-hoc networks,” Tech. Rep., Bell Laboratories, 2006.
- [43] K. Ramachandran, I. Sheriff, E. Belding-Royer, and K. Almeroth, “Routing stability in static wireless mesh networks,” *Passive and Active Network Measurement*, vol. 4427, pp. 73–82, June 2007.
- [44] “The Dharamsala Community Wireless Mesh Network,” 1 August 2007, <http://drupal.airjaldi.com/node/56>.
- [45] “Community Wireless Solutions (CUWIN),” 1 August 2007, <http://www.cuwin.org/>.
- [46] “Technology and Infrastructure for Emerging Regions (TIER),” 1 August 2007, <http://tier.cs.berkeley.edu/wiki/>.
- [47] D.L. Johnson and A. Lysko, “Overview of the Meraka wireless grid test bed for evaluation of ad-hoc routing protocols,” in *Southern African Telecommunication Networks and Applications Conference (SATNAC’07)*, September 2007.
- [48] D.L. Johnson, “Evaluation of a single radio mesh network in south africa,” in *ICTD07: International Conference on Information and Communication Technologies and Development*, Bangalore, India, December 2007.

APPENDIX A

PATH SEARCH CODE TO FIND ROUTES THROUGH GRID



APPENDIX B

LOG-NORMAL SHADOWING MODEL

The log-normal shadowing model is used to represent large scale fading in a radio network. It helps to predict the average and expected variation of the radio signal.

Equation B.1 shows the most common representation of the log-normal shadowing model

$$R(d) = R(d_0) - 10n \log \frac{d}{d_0} + N_\sigma \quad (\text{B.1})$$

where :

- d is the distance to the antenna.
- $R(d)$ is the component of the received signal strength which is proportional to distance.
- d_0 is a reference distance in the far-field of the transmitting antenna.
- $R(d_0)$ is the reference received power level at distance d_0 from the antenna.
- n is the free space path loss exponent
 - In buildings with clear line of sight $n = 1.5$
 - In buildings with obstructed paths $n = 3.0$
- N_σ is the zero-mean normally distributed random variable with standard deviation σ
 - σ describes the amount of scatter in the environment and can range from 3 to 9

APPENDIX C

LARGE FORMAT DIAGRAMS FOR PERFORMANCE ANALYSIS IN 3X7 GRID

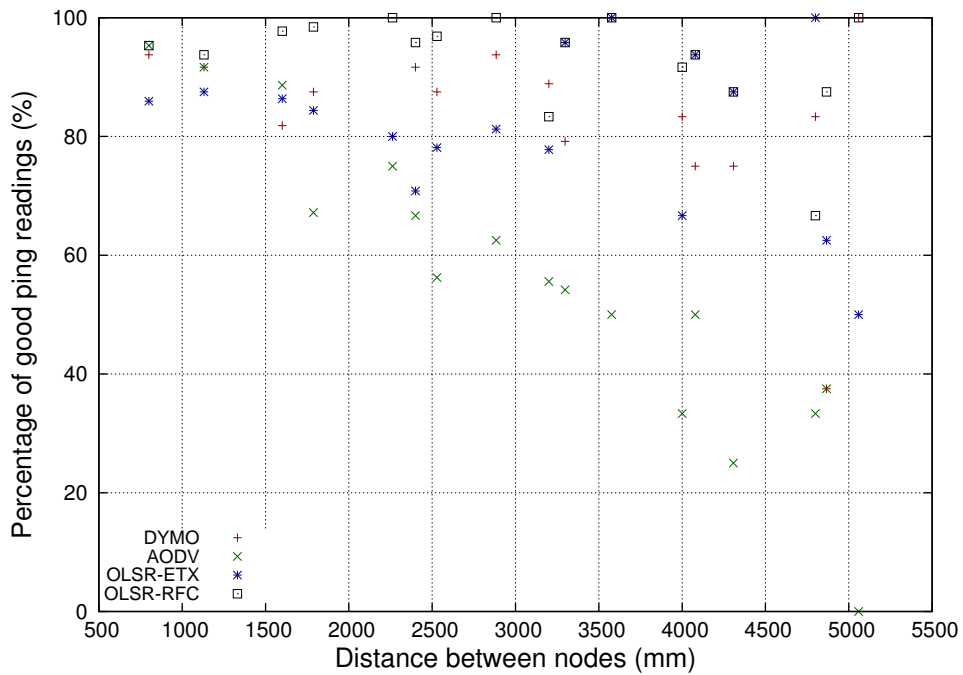


Figure C.1: Percentage of good readings vs distance for ping tests between nodes in 3x7 grid.

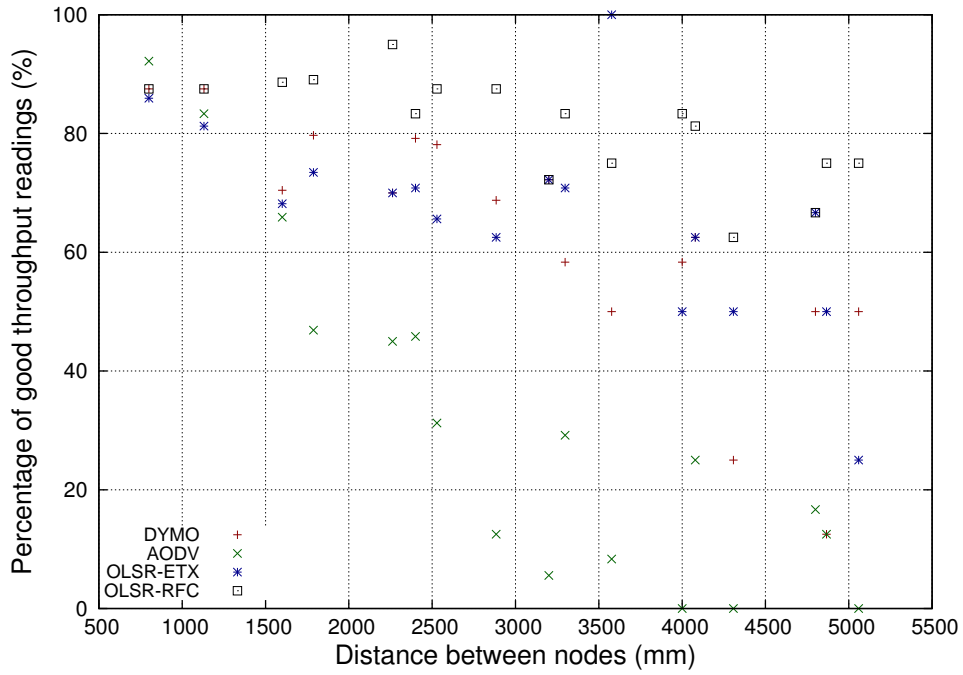


Figure C.2: Percentage of good readings vs distance for throughput tests between nodes in 3x7 grid.

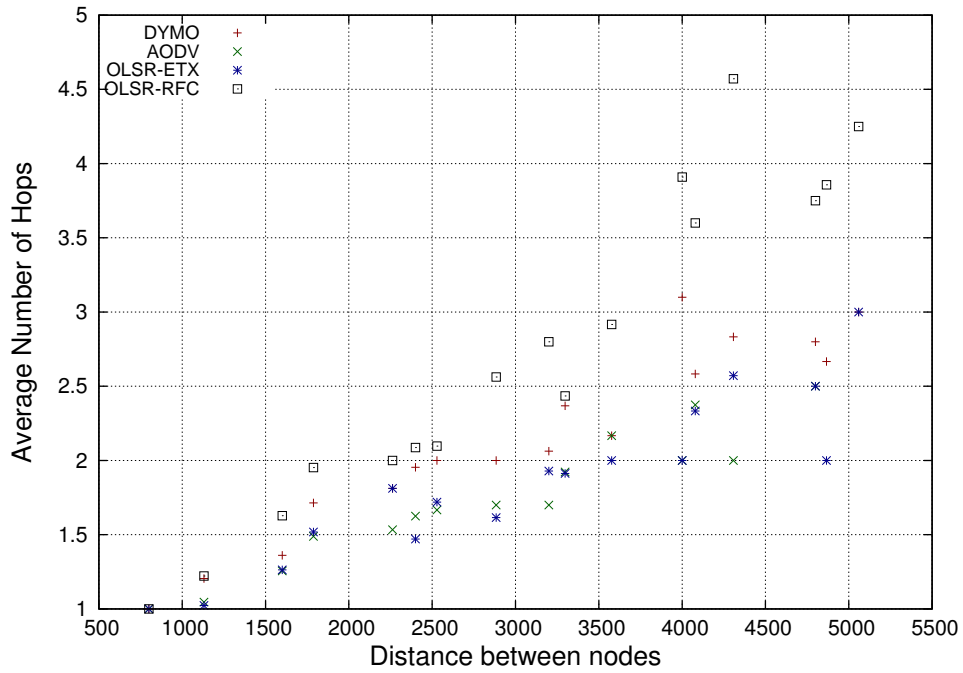


Figure C.3: Average hop count vs distance for ping tests between nodes in 3x7 grid.

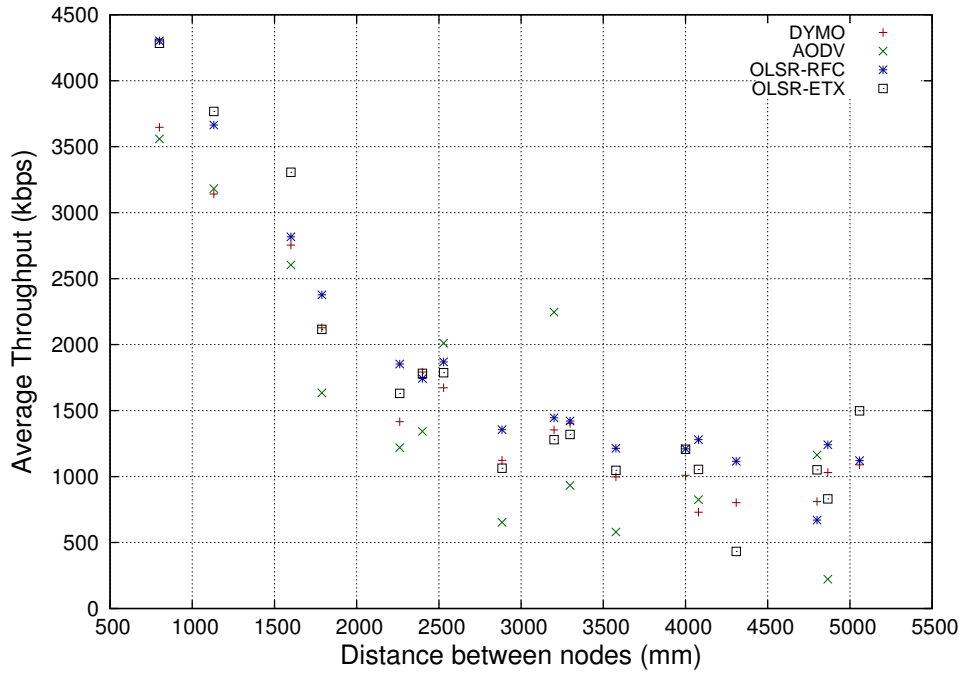


Figure C.4: Average throughput vs distance in 3x7 grid.

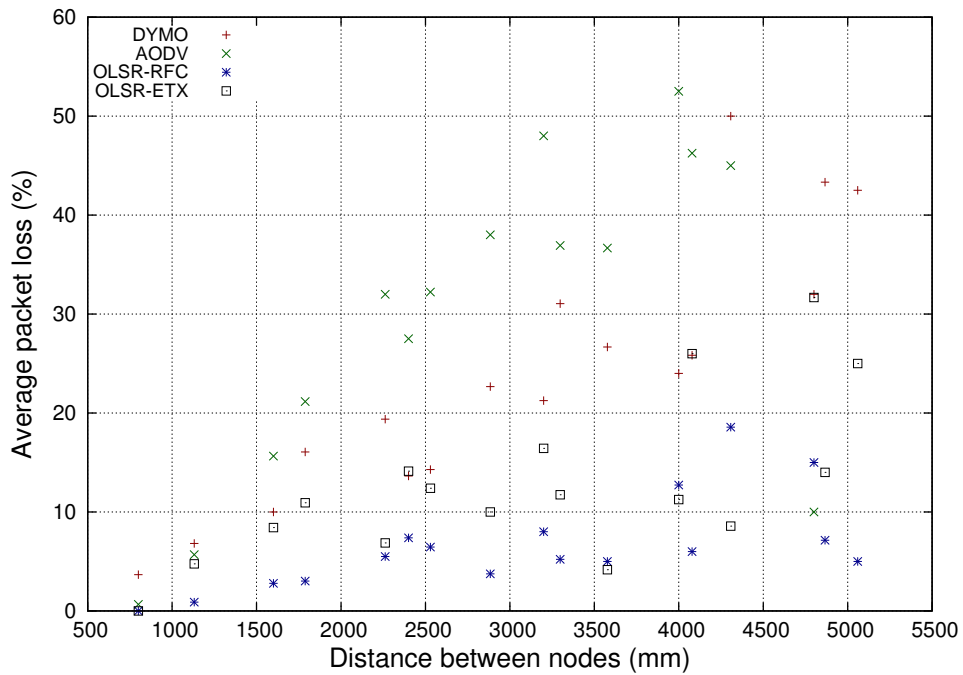


Figure C.5: Average packet loss vs distance for ping tests between nodes in 3x7 grid.

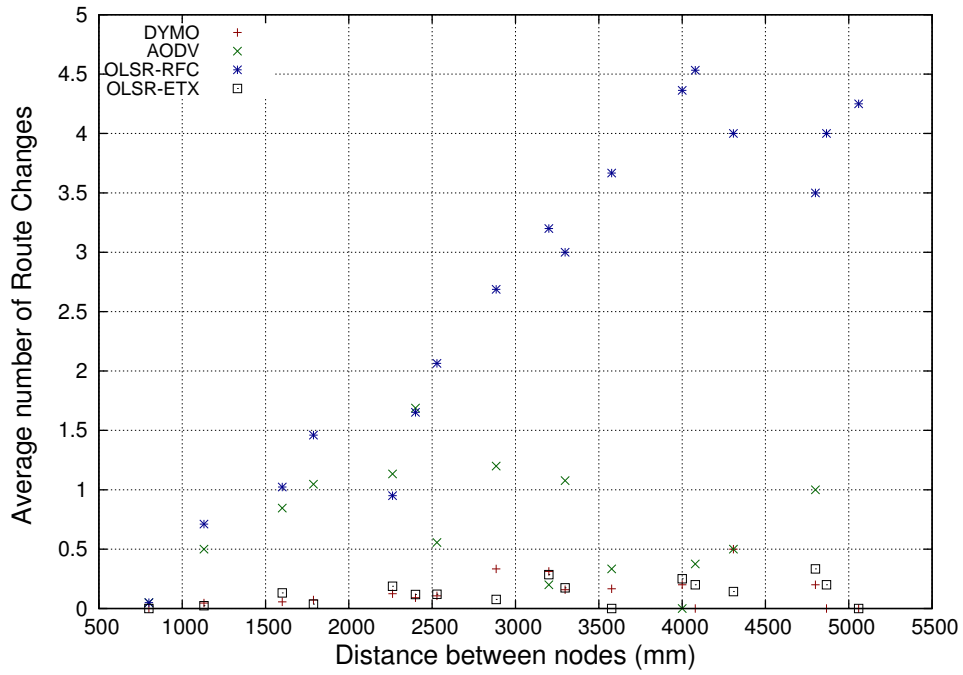


Figure C.6: Average number of route change vs distance for ping tests between nodes in 3x7 grid

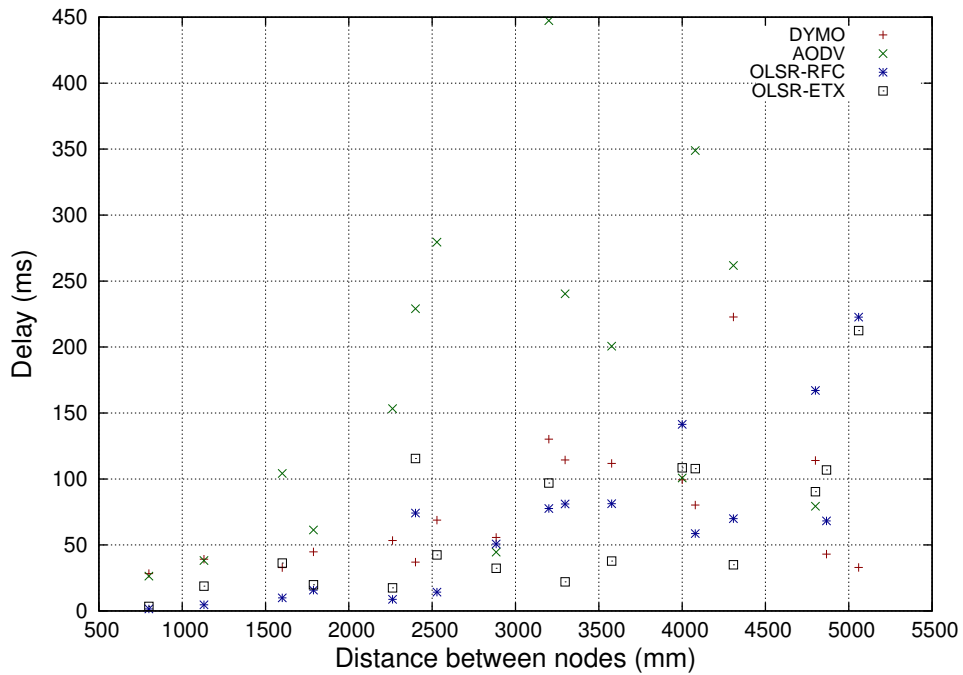


Figure C.7: Average round trip delay vs distance for ping tests between nodes in 3x7 grid.

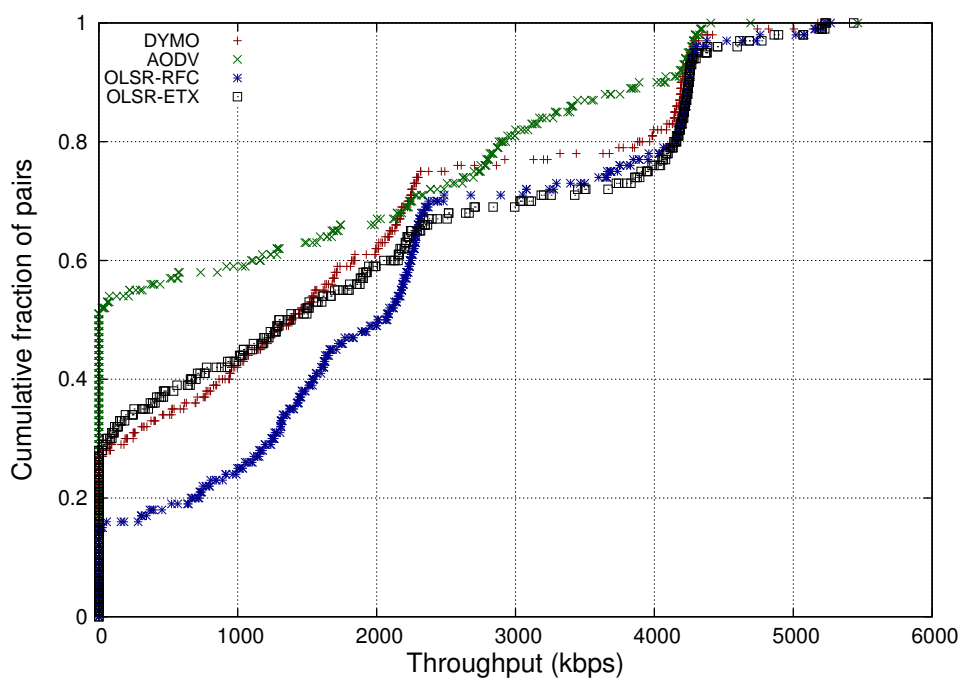


Figure C.8: *Cummulative distribution function for throughput tests between nodes in 3x7 grid*

APPENDIX D

LARGE FORMAT DIAGRAMS FOR PERFORMANCE ANALYSIS IN 7X7 GRID

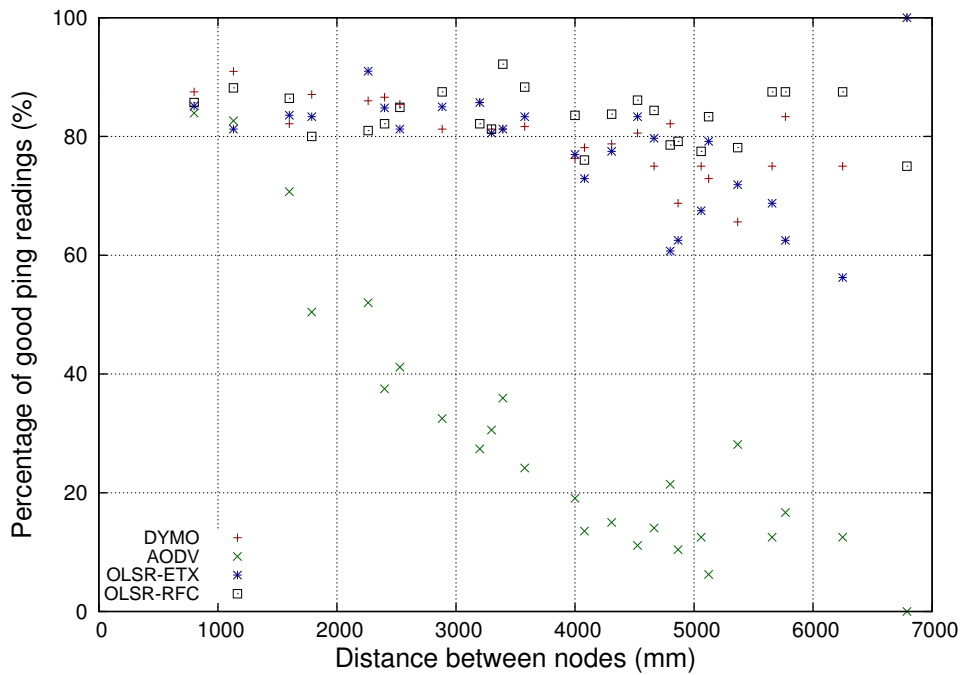


Figure D.1: Percentage of good readings vs distance for ping tests between nodes in 7x7 grid.

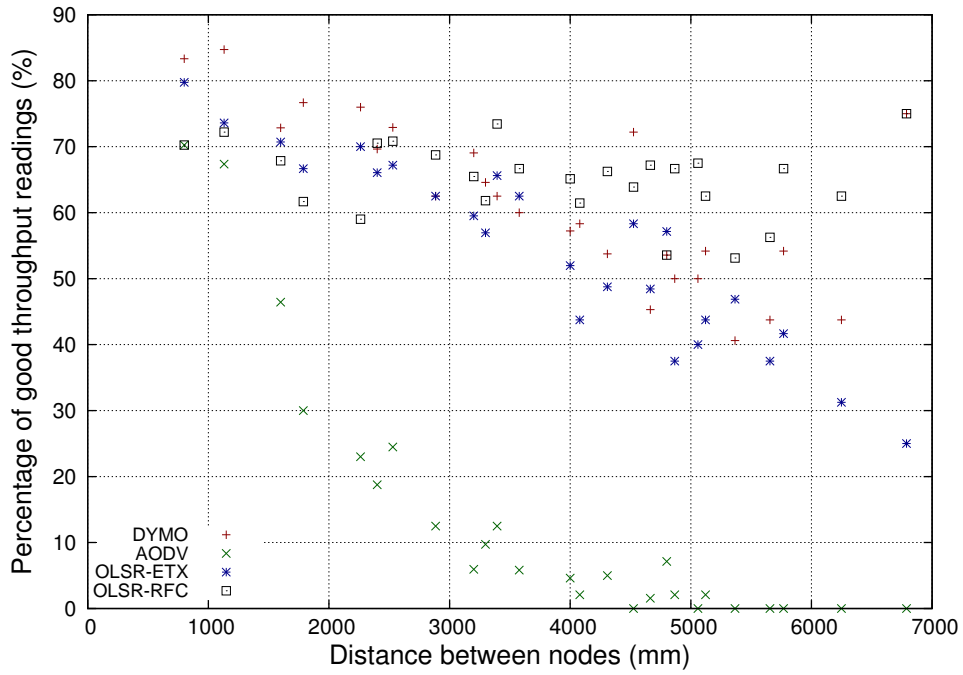


Figure D.2: Percentage of good readings vs distance for throughput tests between nodes in 7x7 grid.

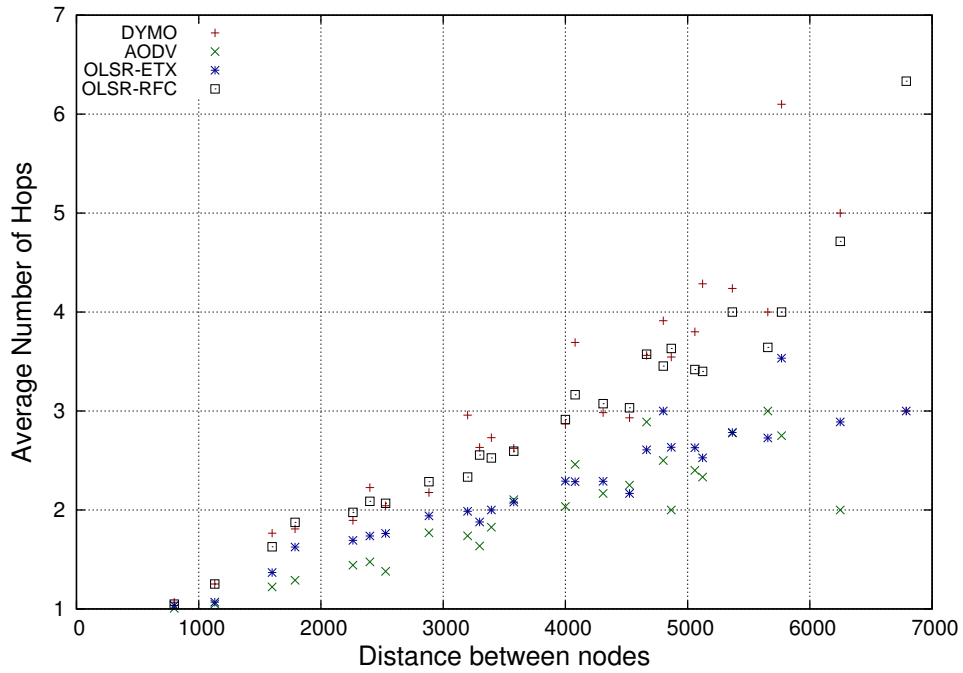


Figure D.3: Average hop count vs distance for ping tests between nodes in 7x7 grid.

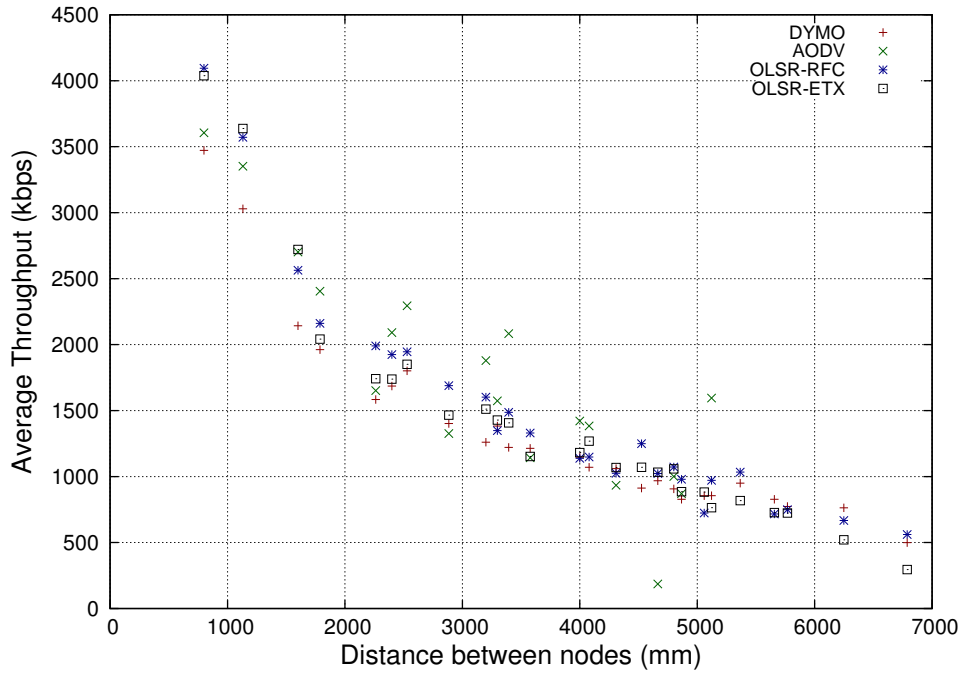


Figure D.4: Average throughput vs distance in 7x7 grid.

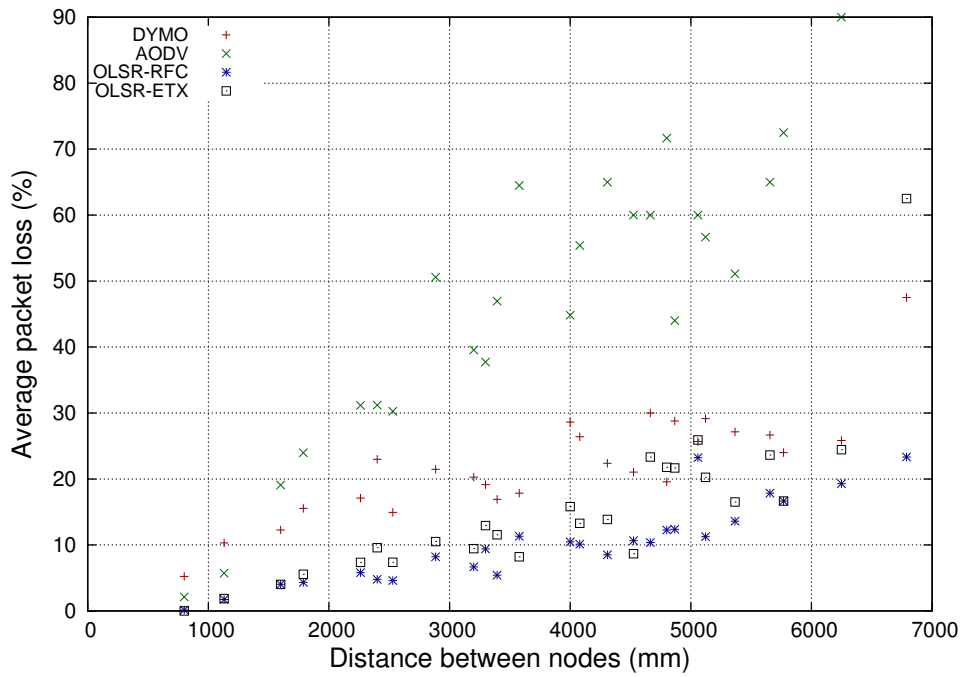


Figure D.5: Average packet loss vs distance for ping tests between nodes in 7x7 grid.

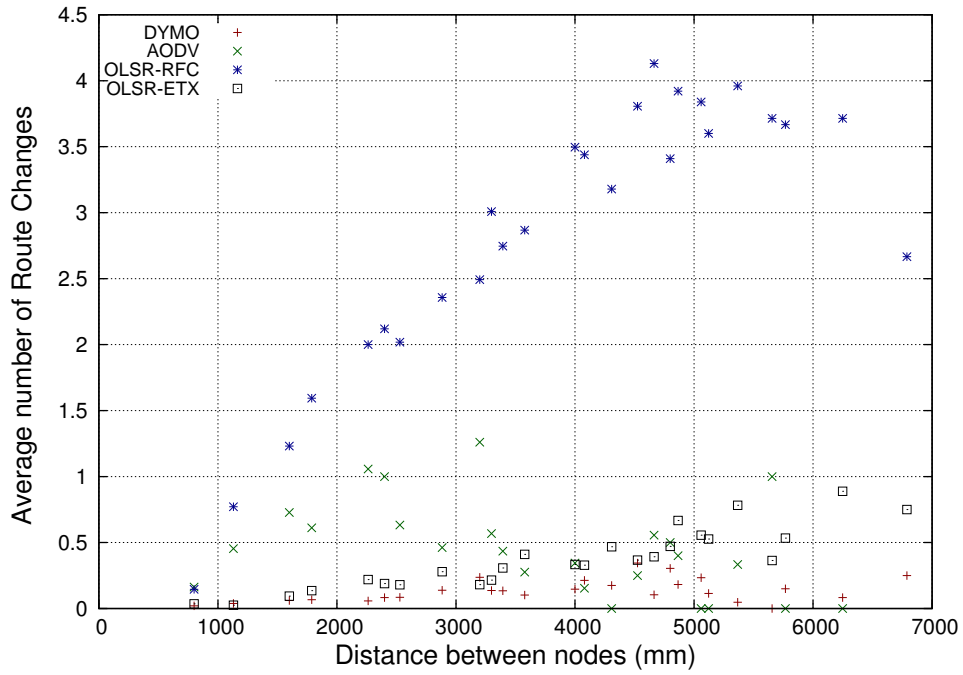


Figure D.6: Average number of route change vs distance for ping tests between nodes in 7x7 grid

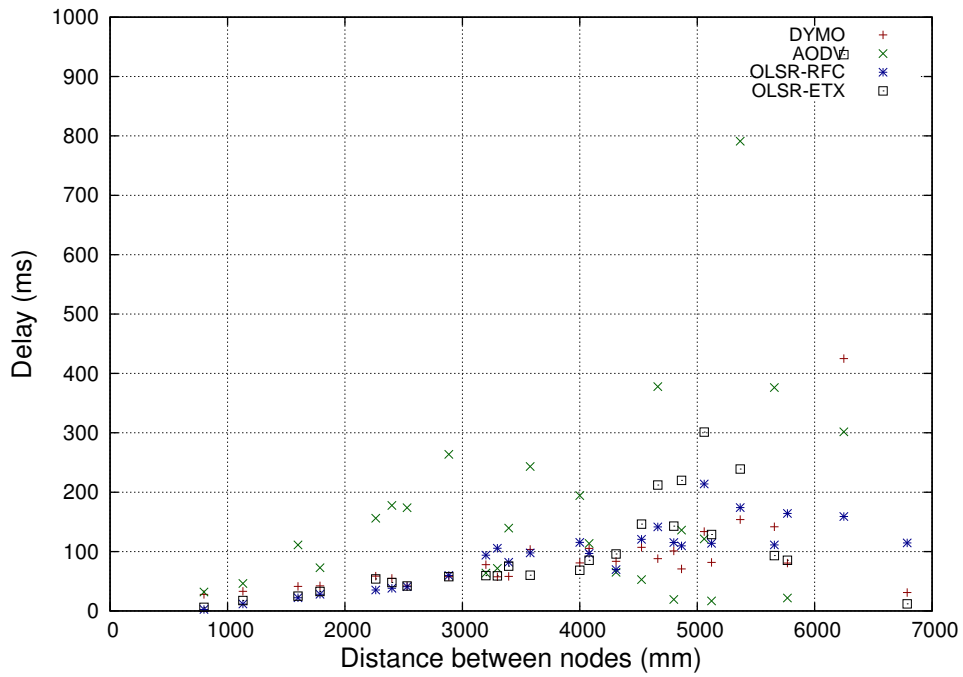


Figure D.7: Average round trip delay vs distance for ping tests between nodes in 7x7 grid.

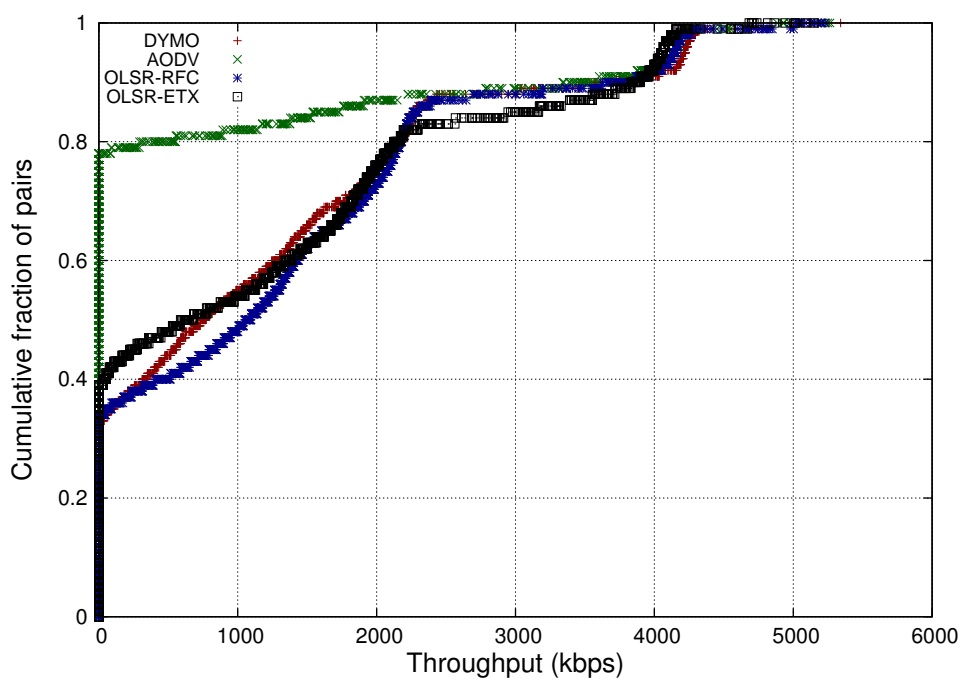


Figure D.8: *Cummulative distribution function for throughput tests between nodes in 7x7 grid*